Wavelet Frames And Orthonormal Wavelets With Compact Support For Sparse Decompositions

Harmonic Analysis

Project Report

Peter Løfqvist Henriksen

9-10th Semester, 2019-2020

Aalborg University
Mathematics

Mathematics
Aalborg University
http://www.aau.dk

AALBORG UNIVERSITY
STUDENT REPORT

Title:
Wavelet Frames And Orthonormal Wavelets With Compact Support For Sparse Decompositions

Theme:
Harmonic Analysis

Project Period:
Spring Semester 2019 - Autumn Semester 2020

Project Group:
5.220

Participant(s):
Peter Løfqvist Henriksen

Supervisor(s):
Morten Nielsen

Copies: 2

Page Numbers: 91

Date of Completion:
June 2, 2020

Abstract:

In this project, frames will be defined as well at the wavelet frame transformation and how to construct them by the use of the oblique extension principle.

From this construction, the discrete wavelet frame transformation will be stated along side the discrete orthonormal wavelet transformation.

The two transformations will then be compared by showing examples of noise reduction.

Contents

Preface **VII**

1 Introduction **1**

2 Wavelets With Compact Support **3**

3 Frames **7**

4 Wavelet frames **19**
4.1 The Unitary extension principle 22
4.2 The oblique extension principle 36

5 Wavelet Transformation **43**
5.1 Wavelet Transformation Algorithm 49
5.2 Wavelet Frame Transformation 52

6 Discussion **59**
6.1 Overview 59
6.1.1 Orthonormal Wavelet 59
6.1.2 Wavelet Frames 59
6.2 Accessibility 60
6.2.1 Orthonormal Wavelet 60
6.2.2 Wavelet Frames 60
6.3 Comparison 61
6.4 Examples of Algorithm 62
6.4.1 Noise Reduction 62
6.4.2 Results 84

7 Conclusion **89**

Bibliography **91**

Preface

This project is written in the ninth and tenth semester mathematics at Aalborg University during the spring semester of 2019 and autumn semester of 2020. The theme of this project is *harmonic analysis* with focus on the theory of wavelets frames and the discrete wavelet frame and orthonormal wavelet transformation. The prerequisite knowledge required to read this project is mathematical knowledge corresponding to having completed a bachelor in mathematics and understand the concept of orthonormal wavelets and its construction. References are denoted by numbers (e.g. [1]) corresponding to numbers in the bibliography. Definitions, theorems, propositions, corollaries, and lemmas are numbered consecutively according to the corresponding chapter, section and subsection.

Aalborg University, June 2, 2020

Peter Løfqvist Henriksen
<plhe15@student.aau.dk>

Chapter 1

Introduction

The orthonormal wavelet transformation is a tool used in applicable harmonic analysis to create decompositions of signals, such as sound or images. In contrast to the Fourier transformation, the orthonormal wavelet transformation is effective in finding localized transient phenomena. Constructing such wavelets can be quite troublesome and taxing, thus a less troublesome and taxing method for decomposing will be researched in this project and compared to the orthonormal wavelet transformation. This method is called the wavelet frame transformation, or framelet transformation, and is based on a generalisation of basis called frames. This project is a continuation of the project *Wavelets* [6] which explore the design of compactly supported wavelets and how to construct them. First some important information from *Wavelets* will be stated, followed by the definition of Frames. Frames are then used to construct wavelets frames and from these constructions, the respectively discrete transformation will be defined. A discussion then follows to determine the pros, cons and performance at noise reduction between the orthonormal wavelet transformation and wavelet frame transformation.

Chapter 2

Wavelets With Compact Support

In this chapter, orthonormal wavelets with compact support will be summarized from *Wavelets* [6].

Orthonormal wavelets are generally constructed from a multiresolution analysis (MRA). An MRA is defined as follows:

Definition 2.1 (Multiresolution analysis)
A *multiresolution analysis* (MRA) is a sequence of closed subspaces $V_j \subset L^2(\mathbb{R})$ for $j \in \mathbb{Z}$ satisfying

(i) $V_j \subset V_{j+1}$ for all $j \in \mathbb{Z}$,

(ii) $f \in V_j$, if and only if, $f(2(\cdot)) \in V_{j+1}$ for all $j \in \mathbb{Z}$,

(iii) $\bigcap_{j\in\mathbb{Z}} V_j = \{0\}$,

(iv) $\overline{\bigcup_{j\in\mathbb{Z}} V_j} = L^2(\mathbb{R})$,

(v) There exist a function $\varphi \in V_0$ such that $\{\varphi(\cdot - k) \mid k \in \mathbb{Z}\}$ is an orthonormal basis for V_0.

The function φ in Definition 2.1 (v) is called a *scaling function* of the given MRA. It is possible, using the structure of the MRA, to construct a set of disjointed orthogonal closed subspaces of $L^2(\mathbb{R})$, W_j for $j \in \mathbb{Z}$, such that

$$L^2(\mathbb{R}) = \bigoplus_{j=-\infty}^{\infty} W_j$$

where W_j is the orthogonal complement of V_j in V_{j+1}. If there exist a function $\psi \in W_0$ such that $\{\psi(\cdot - k) \mid k \in \mathbb{Z}\}$ is an orthonormal basis for W_0, then ψ is called an orthonormal wavelet and $\{2^{\frac{j}{2}}\psi\left(2^j\left(\cdot\right)-k\right) \mid j,k\in\mathbb{Z}\}$ forms an orthonormal basis for $L^2\left(\mathbb{R}\right)$. It has been shown, in [6], that any $\psi\in W_0$ is an orthonormal wavelet for $L^2\left(\mathbb{R}\right)$, if and only if,

$$\hat{\psi}\left(2\omega\right)=e^{i\omega}\nu\left(2\omega\right)\overline{m_0\left(\omega+\pi\right)}\hat{\varphi}\left(\omega\right)$$

for almost every $\omega\in\mathbb{R}$ and some 2π-periodic measurable function ν such that

$$\left|\nu\left(\omega\right)\right|=1$$

almost everywere on $(-\pi,\pi)$. The function m_0 is defined as

$$m_0\left(\omega\right)=\sum_{k\in\mathbb{Z}}a_k e^{-ik\omega} \tag{2.1}$$

where $a_k=\frac{1}{2}\left\langle\varphi\left(\frac{1}{2}x\right),\varphi\left(x-k\right)\right\rangle$ and φ is a scaling function of the corresponding MRA. Since $W_0\subseteq V_1$, $\psi\in W_0$ can be described as a countable linear combination of translates of $\varphi\left(2x\right)$ such that

$$\psi\left(x\right)=2\sum_{k\in\mathbb{Z}}\left(-1\right)^k\overline{a_{-k}}\varphi\left(2x-\left(k-1\right)\right). \tag{2.2}$$

This means that the wavelet ψ have compact support if the corresponding scaling function φ has compact support. If it is possible to construct a scaling function with compact support, then it is possible to directly construct wavelets with compact support. By assuming that m_0 is a trigonometric polynomial satisfying

$$\begin{aligned}&m_0\in C^1\left(-\pi,\pi\right)\ \text{ is a }2\pi\text{-periodic function,}\\&\left|m_0\left(\omega\right)\right|^2+\left|m_0\left(\omega+\pi\right)\right|^2=1,\\&\left|m_0\left(0\right)\right|=1.\end{aligned} \tag{2.3}$$

and

$$m_0\left(\omega\right)\neq0\quad\text{for}\quad\omega\in\left[-\frac{1}{2}\pi,\frac{1}{2}\pi\right], \tag{2.4}$$

φ is constructed by letting

$$\hat{\varphi}\left(\omega\right)=\prod_{j=1}^{\infty}m_0\left(2^{-j}\omega\right). \tag{2.5}$$

Then φ is a scaling function with compact support for a MRA. The question is now, does there exist such a m_0 function? The answer is yes and can be constructed by finding a function g such that $g\left(\omega\right)=\left|m_0\left(\omega\right)\right|^2$. This function must be a non-negative trigonometric polynomial satisfying

$$\begin{aligned}&\text{(i)}\quad g(\omega)+g(\omega+\pi)=1\text{ for all }\omega\in\left(-\pi,\pi\right),\\&\text{(ii)}\quad g(0)=1,\\&\text{(iii)}\quad g(\omega)>0\text{ for }\omega\in\left[-\frac{1}{2}\pi,\frac{1}{2}\pi\right].\end{aligned} \tag{2.6}$$

A function satisfying this is

$$g_k(\omega) = 1 - c_k \int_0^{\omega} (\sin(t))^{2k+1} \, dt$$

where

$$c_k = \int_0^{\pi} (\sin(t))^{2k+1} \, dt.$$

The Haar wavelet, Example 3.4 from [6], can be constructed from this function by letting $k = 0$ such that $g_0(\omega) = \frac{1}{2}(1 + \cos\omega)$ and thus

$$\frac{1}{2}\left(1 + e^{i\omega}\right) \frac{1}{2}\left(1 + e^{-i\omega}\right) = \frac{1}{2}(1 + \cos(\omega)).$$

This gives $m_0 = \frac{1}{2}\left(1 + e^{i\omega}\right)$ which constructs the scaling function $\varphi(x) = 1_{[-1,0)}(x)$ and thus constructs the Haar wavelet

$$\begin{aligned} \psi(x) &= \varphi(2x+1) - \varphi(2x) \\ &= 1_{\left[-1,-\frac{1}{2}\right)} - 1_{\left[-\frac{1}{2},0\right)}. \end{aligned}$$

Chapter 3

Frames

In this chapter, the theory of frames will be described such that construction of wavelet frames is possible. This chapter is based on [3].

For this chapter, $\mathcal{H}$ denotes a separable Hilbert space such that $\mathcal{H} \neq \{0\}$. Every element $f \in \mathcal{H}$ can be described as a linear combination of elements f_k and unique coefficients $c_k(f)$ such that

$$f = \sum_{k=1}^{\infty} c_k(f) f_k, \tag{3.1}$$

where $\{f_k\}_{k=1}^{\infty}$ is a basis for $\mathcal{H}$. *Frames* have a similar structure as the basis for $\mathcal{H}$. A frame is also a sequence of elements $\{f_k\}_{k=1}^{\infty}$ in $\mathcal{H}$ such that every $f \in \mathcal{H}$ can be described as in Equation (3.1), but the coefficients $c_k(f)$ are not necessarily unique.

Definition 3.1 (Frame)
A sequence $\{f_k\}_{k=1}^{\infty}$ in $\mathcal{H}$ is a frame for $\mathcal{H}$ if there exist constants $A, B > 0$ such that

$$A \|f\|_{\mathcal{H}}^2 \leq \sum_{k=1}^{\infty} |\langle f, f_k \rangle|^2 \leq B \|f\|_{\mathcal{H}}^2, \quad \forall f \in \mathcal{H}. \tag{3.2}$$

The constants A and B are called *frame bounds*. It is trivial to see that the frame bounds are not unique, but there exist thus so-called optimal frame bounds. These are called the *optimal upper frame bound* and *optimal lower frame bound* and are, respectively, the infimum over all upper frame bounds and the supremum over all lower frame bounds. When these optimal frame bounds coincide, the frame is called a *tight frame*.

Definition 3.2
A sequence $\{f_k\}_{k=1}^{\infty}$ in $\mathcal{H}$ is a tight frame if there exists a constant $A > 0$ such that

$$\sum_{k=1}^{\infty} |\langle f, f_k \rangle|^2 = A \|f\|_{\mathcal{H}}^2, \quad \forall f \in \mathcal{H}. \tag{3.3}$$

The constant A is called the frame bound.

Testing if a sequence is a frame can be taxing, since Equation (3.2) needs to be satisfied for all $f \in \mathcal{H}$. The following lemma states that it is only necessary to check Equation 3.2 over a dense subset of $\mathcal{H}$ instead of all of $\mathcal{H}$.

Lemma 3.3
Let $\{f_k\}_{k=1}^{\infty}$ be a sequence of elements in $\mathcal{H}$ and let $A, B > 0$ exist such that

$$A \|f\|_{\mathcal{H}}^2 \leq \sum_{k=1}^{\infty} |\langle f, f_k \rangle|^2 \leq B \|f\|_{\mathcal{H}}^2, \quad \forall f \in V \tag{3.4}$$

where V is a dense subset of $\mathcal{H}$. Then $\{f_k\}_{k=1}^{\infty}$ is a frame for $\mathcal{H}$ with frame bounds A, B.

Proof
Since V is a dense subset of $\mathcal{H}$, for every $f \in \mathcal{H}$, there exists a sequence of functions $f_n \in V$ where

$$\exists N \in \mathbb{Z} \forall n \geq N : \|f_n - f\|_{\mathcal{H}} < \frac{1}{n}.$$

This gives that $\{f_n\}_{n=1}^{\infty}$ converges to f. Using this fact, Fatou's lemma and Equation (3.4)

$$\begin{aligned}
A \|f\|_{\mathcal{H}}^2 &= \lim_{n\to\infty} \left(A \|f_n\|_{\mathcal{H}}^2 \right) \\
&\leq \lim_{n\to\infty} \sum_{k=1}^{\infty} |\langle f_n, f_k \rangle|^2 \\
&\leq \sum_{k=1}^{\infty} \lim_{n\to\infty} |\langle f_n, f_k \rangle|^2 \\
&= \sum_{k=1}^{\infty} |\langle f, f_k \rangle|^2.
\end{aligned}$$

The same arguments can be used to achieve

$$\sum_{k=1}^{\infty} |\langle f, f_k \rangle|^2 \leq B \|f\|_{\mathcal{H}}^2 .$$

■

A sequence $\{f_k\}_{k=1}^{\infty}$ is called a complete sequence if $\overline{\text{span}}\{f_k\}_{k=1}^{\infty} = \mathcal{H}$. This implies that a frame $\{f_k\}_{k=1}^{\infty}$ is complete. Sequences $\{f_k\}_{k=1}^{\infty}$ that are not complete in $\mathcal{H}$ can, therefore, not form frames for $\mathcal{H}$, but it is still possible that it forms a frame for the closed linear span of $\{f_k\}_{k=1}^{\infty}$. This gives a general definition for every sequence.

Definition 3.4
Let $\{f_k\}_{k=1}^{\infty}$ be a sequence of elements in $\mathcal{H}$. Then $\{f_k\}_{k=1}^{\infty}$ is called a *frame sequence* if it is a frame for $\overline{\text{span}}\{f_k\}_{k=1}^{\infty}$.

Let us examine what happens with $\overline{\text{span}}\{f_k\}_{k=1}^{\infty}$ if $\{f_k\}_{k=1}^{\infty}$ is a frame for $\mathcal{H}$. In that case,

$$\overline{\text{span}}\{f_k\}_{k=1}^{\infty} = \mathcal{H}.$$

This is due to the fact that $\mathcal{H}$ can be split into a direct sum of orthogonal spaces

$$\mathcal{H} = U \oplus U^{\perp}.$$

Now we define $U = \overline{\text{span}}\{f_k\}_{k=1}^{\infty}$. If $f \in \mathcal{H}$ is chosen to be orthogonal to all f_k, $k \in \mathbb{N}$, then

$$0 = \sum_{k=1}^{\infty} |\langle f, f_k \rangle|^2 \geq A \|f\|^2 \geq 0$$

which implies that $f = 0$. This gives that $U^{\perp} = \{0\}$ which gives the wished result. It is then trivial that every frame of $\mathcal{H}$ is also a frame sequence of $\mathcal{H}$. From Definition 3.1, it is clear that a frame $\{f_k\}_{k=1}^{\infty}$ is a bessel sequence, defined in Definition 3.1.2 from [3], with a Bessel bound equal to the upper frame bound of $\{f_k\}_{k=1}^{\infty}$. The operator

$$T : \ell^2 (\mathbb{N}) \to \mathcal{H}$$

defined as

$$T\left(\{c_k\}_{k=1}^{\infty}\right) = \sum_{k=1}^{\infty} c_k f_k \tag{3.5}$$

is then a bounded operator by Theorem 3.1.3 from [3]. Corollary 3.1.5 from [3] states that for all $\{c_k\}_{k=1}^{\infty} \in \ell^2(\mathbb{N})$, $\sum_{k=1}^{\infty} c_k f_k$ converges unconditionally. This means that the order of elements in the sum does not matter. Using Lemma 3.1.1 from [3], the adjoint operator of T

$$T^* : \mathcal{H} \to \ell^2(\mathbb{N})$$

is given by

$$T^*(f) = \{\langle f, f_k \rangle\}_{k=1}^{\infty}. \tag{3.6}$$

The operator T is called the *pre-frame operator* or the *synthesis operator*, and the adjoint operator T^* is called the *analysis operator*. These operators are used to prove that every $f \in \mathcal{H}$ is actually able to be described be a infinite linear combination of elements in a frame of $\mathcal{H}$. Composing T and its adjoint operator T^*, the *frame operator* is obtained

$$S : \mathcal{H} \to \mathcal{H},$$

described by

$$\begin{aligned} S(f) &= TT^*(f) \\ &= \sum_{k=1}^{\infty} \langle f, f_k \rangle f_k. \end{aligned} \tag{3.7}$$

Since $\{f_k\}_{k=1}^{\infty}$ is a Bessel sequence in $\mathcal{H}$, $\sum_{k=1}^{\infty} \langle f, f_k \rangle f_k$ will converge unconditionally for all $\{c_k\}_{k=1}^{\infty} \in \ell^2(\mathbb{N})$. Some important properties of S will now be stated.

Lemma 3.5
Let $\{f_k\}_{k=1}^{\infty}$ be a frame of $\mathcal{H}$ with frame operator S and frame bounds A, B. Then the following statements are true:

(i) S is bounded, invertible, self-adjoint, and positive.

(ii) $\{S^{-1} f_k\}_{k=1}^{\infty}$ is a frame with frame operator S^{-1} and frame bounds B^{-1}, A^{-1}.

(iii) if A, B are optimal frame bounds for $\{f_k\}_{k=1}^{\infty}$, then the bounds B^{-1}, A^{-1} are optimal for $\{S^{-1} f_k\}_{k=1}^{\infty}$.

Proof
(i): Since T and T^* are bounded linear operators and $S = TT^*$

$$\begin{aligned} \|S\|_{\mathcal{H}} &= \|TT^*\|_{\mathcal{H}} \\ &\le \|T\|_{\mathcal{H}} \|T^*\|_{\mathcal{H}} \\ &= \|T\|_{\mathcal{H}}^2 \le B \end{aligned}$$

and thus makes S bounded. It is trivial that S is Self-adjoint since

$$S^* = (TT^*)^* = TT^* = S.$$

Equation (3.2) can be rewritten as

$$A\langle f, f\rangle \leq \langle S(f), f\rangle \leq B\langle f, f\rangle, \quad \forall f \in \mathcal{H}. \tag{3.8}$$

This can further be rewritten as

$$\begin{aligned} 0 &\leq B\langle f, f\rangle - \langle S(f), f\rangle \leq B\langle f, f\rangle - A\langle f, f\rangle \\ 0 &\leq \left\langle \left(I - B^{-1}S\right) f, f\right\rangle \leq \left\langle \frac{B-A}{B} f, f\right\rangle. \end{aligned}$$

Theorem 2.2.3 from [3] states that if S is bounded and $\|I - S\|_{\mathcal{H}} < 1$, then S is invertible. Since

$$\begin{aligned} \left\|I - B^{-1}S\right\| &= \sup_{\|f\|_{\mathcal{H}}=1} \left|\left\langle \left(I - B^{-1}S\right) f, f\right\rangle\right| \\ &\leq \sup_{\|f\|_{\mathcal{H}}=1} \left|\left\langle \frac{B-A}{B} f, f\right\rangle\right| \\ &= \frac{B-A}{B} < 1, \end{aligned}$$

it is concluded that S is invertible. This also shows that S is positive since

$$0 \leq A\,\|f\|^2_{\mathcal{H}} \leq \langle S(f), f\rangle$$

for all $f \in \mathcal{H}$. (ii): Since the operator S is self-adjoint, S^{-1} is also self-adjoint. This means that for all $f \in \mathcal{H}$,

$$\begin{aligned} \sum_{k=1}^{\infty} \left|\left\langle f, S^{-1}f_k\right\rangle\right|^2 &= \sum_{k=1}^{\infty} \left|\left\langle S^{-1}f, f_k\right\rangle\right|^2 \\ &\leq B\left\|S^{-1}f\right\|^2_{\mathcal{H}} \\ &\leq B\left\|S^{-1}\right\|^2_{\mathcal{H}} \|f\|^2_{\mathcal{H}}, \end{aligned}$$

since $\{f_k\}_{k=1}^{\infty}$ is a Bessel sequence. Furthermore follows that $\{S^{-1}f_k\}_{k=1}^{\infty}$ is a Bessel sequence. The frame operator can be found by following the logic of Equation (3.7) as

$$\begin{aligned} \sum_{k=1}^{\infty} \left\langle f, S^{-1}f_k\right\rangle S^{-1}f_k &= S^{-1}\sum_{k=1}^{\infty} \left\langle S^{-1}f, f_k\right\rangle f_k \\ &= S^{-1}SS^{-1}f = S^{-1}f. \end{aligned}$$

This makes S^{-1} the frame operator for $\{S^{-1}f_k\}_{k=1}^{\infty}$. It is trivial that S^{-1} commutes with S and I. Using Theorem 2.4.2 from [3], which states that if this is the case, then $IS^{-1} \leq SS^{-1}$ and $SS^{-1} \leq IS^{-1}$ in the sense of positive definite operators. Using this fact on Equation (3.8) results in

$$\begin{aligned} A\left\langle S^{-1}f,f\right\rangle &\leq \left\langle SS^{-1}f,f\right\rangle \leq B\left\langle S^{-1}f,f\right\rangle \\ A\left\langle S^{-1}f,f\right\rangle &\leq \|f\|_{\mathcal{H}}^2 \leq B\left\langle S^{-1}f,f\right\rangle. \end{aligned}$$

This gives

$$B^{-1}\|f\|_{\mathcal{H}}^2 \leq \left\langle S^{-1}f,f\right\rangle \leq A^{-1}\|f\|_{\mathcal{H}}^2, \quad \forall f \in \mathcal{H}.$$

By inserting $S^{-1}f = \sum_{k=1}^{\infty}\langle f, S^{-1}f_k\rangle S^{-1}f_k$, the following is obtained:

$$B^{-1}\|f\|_{\mathcal{H}}^2 \leq \sum_{k=1}^{\infty}\left|\left\langle f,S^{-1}f_k\right\rangle\right|^2 \leq A^{-1}\|f\|_{\mathcal{H}}^2, \quad \forall f \in \mathcal{H}. \tag{3.9}$$

This makes B^{-1} and A^{-1} frame bounds of $\{S^{-1}f_k\}_{k=1}^{\infty}$. (iii): Let A be the optimal lower bound for $\{f_k\}_{k=1}^{\infty}$ and assume that $C < A^{-1}$ is the optimal upper bound for $\{S^{-1}f_k\}_{k=1}^{\infty}$. Then $\{\left(S^{-1}\right)^{-1}S^{-1}f_k\}_{k=1}^{\infty} = \{f_k\}_{k=1}^{\infty}$, the lower bound $C^{-1} > A$. This is a contradiction since A is the optimal lower bound. Thus $C = A^{-1}$ which makes A^{-1} the optimal upper bound for $\{S^{-1}f_k\}_{k=1}^{\infty}$. Similar arguments can be made for B and B^{-1} be optimal bounds.

■

The frame $\{S^{-1}f_k\}_{k=1}^{\infty}$ is called the *canonical dual frame* of $\{f_k\}_{k=1}^{\infty}$. The following theorem contains the most important frame result. It states that if $\{f_k\}_{k=1}^{\infty}$ is a frame for $\mathcal{H}$, then every element of $\mathcal{H}$ can be described as an infinite linear combination of $\{f_k\}_{k=1}^{\infty}$. This theorem is why frames can be seen as a kind of generalized basis.

Theorem 3.6
Let $\{f_k\}_{k=1}^{\infty}$ be a frame with frame operator S. Then

$$f = \sum_{k=1}^{\infty}\langle f, S^{-1}f_k\rangle f_k, \quad \forall f \in \mathcal{H} \tag{3.10}$$

and

$$f = \sum_{k=1}^{\infty}\langle f, f_k\rangle S^{-1}f_k, \quad \forall f \in \mathcal{H}. \tag{3.11}$$

Both series converge unconditionally for all $f \in \mathcal{H}$.

Proof
Let $f \in \mathcal{H}$, and let $\{f_k\}_{k=1}^{\infty}$ be a frame with frame operator S. Using the properties from Lemma 3.5,

$$\begin{aligned} f &= SS^{-1}f \\ &= \sum_{k=1}^{\infty} \left\langle S^{-1}f, f_k \right\rangle f_k \\ &= \sum_{k=1}^{\infty} \left\langle f, S^{-1}f_k \right\rangle f_k. \end{aligned}$$

This sum converges unconditionally, since $\{f_k\}_{k=1}^{\infty}$ is a Bessel sequence and $\{\langle f, S^{-1}f_k \rangle\}_{k=1}^{\infty} \in \ell^2(\mathbb{N})$, hence Corollary 3.1.4 from [3]. The expantion

$$f = \sum_{k=1}^{\infty} \langle f, f_k \rangle S^{-1} f_k$$

is obtained by the same arguments but using $f = S^{-1}Sf$.

∎

The constants $\langle f, S^{-1}f_k \rangle$ are called *frame coefficients*, and the above theorem states that all the information of a function $f \in \mathcal{H}$ can be described by the sequence $\{\langle f, S^{-1}f_k \rangle\}_{k=1}^{\infty}$. Also this describes one of the main challenges in frame theory. To be able to find the frame coefficients, it is necessary to know the inverse frame operator for the frame or at least the canonical dual frame. One way to get around this problem is to only consider tight frames.

Corollary 3.7
If $\{f_k\}_{k=1}^{\infty}$ is a tight frame with frame bound A, then the canonical dual frame is $\{A^{-1}f_k\}_{k=1}^{\infty}$ and

$$f = \frac{1}{A} \sum_{k=1}^{\infty} \langle f, f_k \rangle f_k, \quad \forall f \in \mathcal{H}. \tag{3.12}$$

Proof
Since $\{f_k\}_{k=1}^{\infty}$ is a tight frame,

$$\begin{aligned} \langle Sf, f \rangle &= \sum_{k=1}^{\infty} |\langle f, f_k \rangle|^2 \\ &= A \|f\|_{\mathcal{H}}^2 = \langle Af, f \rangle, \quad \forall f \in \mathcal{H}, \end{aligned}$$

which gives that

$$\langle (S - AI) f, f \rangle = 0, \quad \forall f \in \mathcal{H}.$$

Lemma 2.4.3 from [3] states that if $S - AI$ is a self-adjoint operator. Then $S - AI = 0$, and thus $S = AI$, which gives that S^{-1} acts by multiplication of A^{-1}. Theorem 3.6 then states that

$$\begin{aligned} f &= \sum_{k=1}^{\infty} \langle f, S^{-1} f_k \rangle f_k \\ &= \frac{1}{A} \sum_{k=1}^{\infty} \langle f, f_k \rangle f_k, \quad \forall f \in \mathcal{H}. \end{aligned}$$

■

By scaling the elements $\{f_k\}_{k=1}^{\infty}$ in a tight frame, it is possible to obtain frame bound $A = 1$. Equation (3.12) thus have the same representation as an orthonormal basis. Another advantage for tight frames is that the structure of the canonical dual frame is the same as the frame itself, since $f_k = \frac{1}{A} f_k$ for all $k \in \mathbb{N}$. For example, if the frame has wavelet structure, the canonical dual frame will have wavelet structure as well. In contrast, for non-tight frames, the canonical dual frame of a wavelet frame might not have wavelet structure. For non-tight frames, it is necessary to find another way to avoid the problem of inverting the frame operator. In fact, for a frame $\{f_k\}_{k=1}^{\infty}$ that is not also a basis, it will be proven that there exist another frame $\{g_k\}_{k=1}^{\infty}$ such that

$$f = \sum_{k=1}^{\infty} \langle f, g_k \rangle f_k, \quad \forall f \in \mathcal{H}. \tag{3.13}$$

These frames $\{g_k\}_{k=1}^{\infty}$ are called the *dual frame* of $\{f_k\}_{k=1}^{\infty}$. Since the canonical dual frame of $\{f_k\}_{k=1}^{\infty}$ can be difficult to find, there will exist other dual frames that can be much easier to find. Before showing this is the case, the similarity between the canonical dual frame and the dual Riesz basis will be stated.

Theorem 3.8
Let $\{f_k\}_{k=1}^{\infty}$ be a Riesz basis for $\mathcal{H}$. Then $\{f_k\}_{k=1}^{\infty}$ is a frame for $\mathcal{H}$ with frame bounds equal to the Riesz basis bounds. The dual Riesz basis is in this case equal to the canonical dual frame $\{S^{-1} f_k\}_{k=1}^{\infty}$.

Proof
This proof is similar to the proof of Theorem 5.2.1 on page 106 [3].

■

Frames $\{f_k\}_{k=1}^{\infty}$ that are not a Riesz basis are said to be *overcomplete* and called a *redundant frame*. This is the case, since for such a frame, there exist $\{c_k\}_{k=1}^{\infty} \in \ell^2(\mathbb{N}) \setminus \{0\}$ such that

$$\sum_{k=1}^{\infty} c_k f_k = 0. \tag{3.14}$$

This means that there exist some dependency between the frame elements.

Theorem 3.9
Let $\{f_k\}_{k=1}^{\infty}$ be a frame in $\mathcal{H}$. The the following statements are equivalent:

(i) $\{f_k\}_{k=1}^{\infty}$ is a Riesz basis for $\mathcal{H}$.

(ii) If $\sum_{k=1}^{\infty} c_k f_k = 0$ for some $\{c_k\}_{k=1}^{\infty} \in \ell^2(\mathbb{N})$, then $c_k = 0$ for all $k \in \mathbb{N}$.

Proof
Let $\{f_k\}_{k=1}^{\infty}$ be a frame for $\mathcal{H}$. Assume first (i) and that $\sum_{k=1}^{\infty} c_k f_k = 0$ for a sequence $\{c_k\}_{k=1}^{\infty} \in \ell^2(\mathbb{N})$. Since $\{f_k\}_{k=1}^{\infty}$ is a Riesz basis, there will exist a bounded bijective operator U and a orthonormal basis, $\{e_k\}_{k=1}^{\infty}$, such that $\{f_k\}_{k=1}^{\infty} = \{Ue_k\}_{k=1}^{\infty}$. This gives that

$$U \sum_{k=1}^{\infty} c_k e_k = 0$$

which implies that

$$\sum_{k=1}^{\infty} c_k e_k = 0.$$

Since U is injective and $\{e_k\}_{k=1}^{\infty}$ is an orthonormal basis, we have $c_k = 0$ for all $k \in \mathbb{N}$. Assume now (ii) and choose $\{c_k\}_{k=1}^{\infty}$ to be the canonical orthonormal basis for $\ell^2(\mathbb{N})$. Then the assumtion in (ii) makes the pre-frame operator, T, associated with the frame $\{f_k\}_{k=1}^{\infty}$ to be injective. T is surjective, since $\{f_k\}_{k=1}^{\infty}$ is a frame. Definition 3.3.1 in [3] thus gives that $\{f_k\}_{k=1}^{\infty}$ is a Riesz basis since $Tc_k = f_k$ for all $k \in \mathbb{N}$.

■

For overcomplete frames, it is easy to see that $f \in \mathcal{H}$ has many representations in terms of the frame elements in a given frame $\{f_k\}_{k=1}^{\infty}$ for $\mathcal{H}$. This is the result of the following equality:

$$f = \sum_{k=1}^{\infty} \langle f, S^{-1} f_k \rangle f_k \tag{3.15}$$

$$= \sum_{k=1}^{\infty} \left(\langle f, S^{-1} f_k \rangle + c_k \right) f_k \tag{3.16}$$

for any $\{c_k\}_{k=1}^{\infty} \in \ell^2(\mathbb{N}) \setminus \{0\}$ satisfying Equation (3.14). The question becomes, does there exist a frame $\{g_k\}_{k=1}^{\infty}$ such that $\langle f, S^{-1}f_k\rangle + c_k = \langle f, g_k\rangle$ for all $k \in \mathbb{N}$? This question is answered as a result of the following theorem.

Theorem 3.10
Let $\{f_k\}_{k=1}^{\infty}$ be an overcomplete frame. Then there exist frames $\{g_k\}_{k=1}^{\infty}$ such that $\{g_k\}_{k=1}^{\infty} \neq \{S^{-1}f_k\}_{k=1}^{\infty}$ and

$$f = \sum_{k=1}^{\infty} \langle f, g_k\rangle f_k \tag{3.17}$$

for all $f \in \mathcal{H}$.

Proof
Assume first for some $\ell \in \mathbb{N}$ that $f_\ell = 0$, which makes $S^{-1}f_\ell = 0$. Construct $\{g_k\}_{k=1}^{\infty}$ by letting $g_k = S^{-1}f_k$ for all $k \in \mathbb{N}$ where $k \neq \ell$ and choose g_ℓ to be an arbitrary non-zero element in $\mathcal{H}$. This gives that $\{g_k\}_{k=1}^{\infty} \neq \{S^{-1}f_k\}_{k=1}^{\infty}$, since $g_\ell \neq S^{-1}f_\ell$ and, from the frame decomposition, it follows that

$$\begin{aligned} f &= \sum_{k=1}^{\infty} \langle f, S^{-1}f_k\rangle f_k \\ &= \sum_{k=1}^{\infty} \langle f, g_k\rangle f_k. \end{aligned}$$

This is given using $\langle f, g_\ell\rangle f_\ell = \langle f, S^{-1}f_\ell\rangle f_\ell = 0$. Assume now that $f_k \neq 0$ for all $k \in \mathbb{N}$. Since $\{f_k\}_{k=1}^{\infty}$ is an overcomplete frame, Theorem 3.9 states that there exist a sequence $\{c_k\}_{k=1}^{\infty} \in \ell^2(\mathbb{N}) \setminus \{0\}$ such that

$$\sum_{k=1}^{\infty} c_k f_k = 0.$$

This means that there exist an $\ell \in \mathbb{N}$ such that $c_\ell \neq 0$ which we can write as

$$f_\ell = \frac{-1}{c_\ell} \sum_{k \neq \ell} c_k f_k.$$

By proving that $\{f_k\}_{k\neq\ell}$ is a frame for $\mathcal{H}$, its canonical dual frame can be defined to be $\{g_k\}_{k\neq\ell}$ and, by letting $g_\ell = 0$, a frame can be found for which Equation (3.17) is true. $\{g_k\}_{k=1}^{\infty}$ is different from $\{S^{-1}f_k\}_{k=1}^{\infty}$, since $S^{-1}f_\ell \neq 0$. Given $\{f_k\}_{k\neq\ell}$, which is a Bessel sequence, it is only necessary to prove that the lower frame bound exists.

Let $f \in \mathcal{H}$, then using Cauchy-Schwarz inequality gives

$$\begin{aligned}
|\langle f, f_\ell \rangle|^2 &= \left| \left\langle f, \frac{-1}{c_\ell} \sum_{k \neq \ell} c_k f_k \right\rangle \right|^2 \\
&\leq \frac{1}{|c_\ell|^2} \sum_{k \neq \ell} |c_k|^2 \sum_{k \neq \ell} |\langle f, f_k \rangle|^2 \\
&= C \sum_{k \neq \ell} |\langle f, f_k \rangle|^2
\end{aligned}$$

where $C = \frac{1}{|c_\ell|^2} \sum_{k \neq \ell} |c_k|^2$. Letting A denote the lower frame bound for $\{f_k\}_{k*=1}^{\infty}$,

$$\begin{aligned}
A \|f\|^2 &\leq \sum_{k=1}^{\infty} |\langle f, f_k \rangle|^2 \\
&= \sum_{k \neq \ell} |\langle f, f_k \rangle|^2 + |\langle f, f_\ell \rangle|^2 \\
&\leq (1 + C) \sum_{k \neq \ell} |\langle f, f_k \rangle|^2 .
\end{aligned}$$

Thus the lower bound for $\{f_k\}_{k \neq \ell}$ is $\frac{A}{1+C}$.

■

Since $\{f_k\}_{k=1}^{\infty}$ and $\{g_k\}_{k=1}^{\infty}$ are dual frames,

$$f = \sum_{k=1}^{\infty} \langle f, f_k \rangle g_k.$$

The following lemma proves this claim:

Lemma 3.11
Let $\{f_k\}_{k=1}^{\infty}$ and $\{g_k\}_{k=1}^{\infty}$ be Bessel sequences in $\mathcal{H}$. Then the following statements are equivalent:

(i) $f = \sum_{k=1}^{\infty} \langle f, g_k \rangle f_k, \quad \forall f \in \mathcal{H}$

(ii) $f = \sum_{k=1}^{\infty} \langle f, f_k \rangle g_k, \quad \forall f \in \mathcal{H}$

(iii) $\langle f, g \rangle = \sum_{k=1}^{\infty} \langle f, f_k \rangle \langle g, g_k \rangle, \quad \forall f, g \in \mathcal{H}.$

In the case one of the conditions are satisfied, $\{f_k\}_{k=1}^{\infty}$ and $\{g_k\}_{k=1}^{\infty}$ are dual frames for $\mathcal{H}$. If B denotes the upper frame bound for $\{f_k\}_{k=1}^{\infty}$, then B^{-1} is a lower frame bound for $\{g_k\}_{k=1}^{\infty}$.

Proof
The pre-frame operators for the sequences $\{f_k\}_{k=1}^{\infty}$ and $\{g_k\}_{k=1}^{\infty}$ defined, respectively, as T and U. Then (i) can be written as

$$f = I(f) = TU^*(f).$$

Since I is an self-adjoint operator, this will be equivalent to

$$f = I(f) = UT^*(f)$$

which is the statement in (ii). It is clear that (ii) implies (iii), but the other way around, a little more arguments is needed. Assume (iii) and fix $f \in \mathcal{H}$. Then $\sum_{k=1}^{\infty}\langle f, f_k\rangle g_k$ will be a well defined element in $\mathcal{H}$, since $\{f_k\}_{k=1}^{\infty}$ and $\{g_k\}_{k=1}^{\infty}$ are Bessel sequences. This makes $\{\langle f, f_k\rangle\}_{k=1}^{\infty} \in \ell^2(\mathbb{N})$, and thus $\sum_{k=1}^{\infty}\langle f, f_k\rangle f_k$ convergent. Consider now the following:

$$\begin{aligned}\left\langle f - \sum_{k=1}^{\infty}\langle f, f_k\rangle g_k, g\right\rangle &= \langle f, g\rangle - \left\langle \sum_{k=1}^{\infty}\langle f, f_k\rangle g_k, g\right\rangle \\ &= \langle f, g\rangle - \sum_{k=1}^{\infty}\langle f, f_k\rangle \langle g_k, g\rangle = 0, \quad \forall g \in \mathcal{H}.\end{aligned}$$

This shows (iii) implies (ii). In the case where the equivalent conditions are satisfied, we can write

$$\|f\|_{\mathcal{H}}^2 = \langle f, f\rangle = \sum_{k=1}^{\infty}\langle f, g_k\rangle \langle f_k, f\rangle, \quad \forall f \in \mathcal{H}.$$

Assuming that one of the families $\{g_k\}_{k=1}^{\infty}$ or $\{f_k\}_{k=1}^{\infty}$ are Bessel sequences, the other family will satisfy the lower frame condition with a lower frame bound equal to the Bessel bound of the first family. Since $\|f\| > 0$, Cauchy-Schwarz inequality can be used such that

$$\left|\sum_{k=1}^{\infty}\langle f, g_k\rangle \langle f_k, f\rangle\right| \le \left(\sum_{k=1}^{\infty}|\langle f, g_k\rangle|^2\right)^{\frac{1}{2}} \left(\sum_{k=1}^{\infty}|\langle f_k, f\rangle|^2\right)^{\frac{1}{2}}.$$

Assuming that $\{f_k\}_{k=1}^{\infty}$ is a Bessel sequence,

$$\left(\sum_{k=1}^{\infty}|\langle f, g_k\rangle|^2\right)^{\frac{1}{2}} \left(\sum_{k=1}^{\infty}|\langle f_k, f\rangle|^2\right)^{\frac{1}{2}} \le \left(\sum_{k=1}^{\infty}|\langle f, g_k\rangle|^2\right)^{\frac{1}{2}} \|f\|_{\mathcal{H}} B^{\frac{1}{2}}.$$

This gives

$$\frac{1}{B}\|f\|_{\mathcal{H}} \le \sum_{k=1}^{\infty}|\langle f, g_k\rangle|^2$$

which concludes this proof.

■

Chapter 4

Wavelet frames

In this chapter the construction of wavelet frames will be discussed. This chapter is based upon [3], unless other is specified.

As seen in Chapter 2, the base wavelet ψ is a function in W_0, a closed subspace of $L^2(\mathbb{R})$, where $\{2^{\frac{j}{2}}\psi\left(2^j(\cdot)-k\right) \mid j,k \in \mathbb{Z}\}$ forms an orthonormal basis for $L^2(\mathbb{R})$. But constructing such a function can be troublesome, since Equation (2.2) is a potential infinite sum which is impossible to calculate exact in practice. We are interested in creating a frame with the same wavelet structure from a more simple function then the wavelet function ψ. Some notation will be defined to simplify equations in this chapter.

$$T_k : L^2(\mathbb{R}) \to L^2(\mathbb{R})\,;\, T_b(f)(x) = f(x-k) \tag{4.1}$$

$$D^j : L^2(\mathbb{R}) \to L^2(\mathbb{R})\,;\, D^j(f)(x) = 2^{\frac{j}{2}} f\left(2^j x\right) \tag{4.2}$$

Definition 4.1
Let $\psi \in L^2(\mathbb{R})$. A frame of the form $\{D^j T_k \psi\}_{j,k\in\mathbb{Z}}$ in $L^2(\mathbb{R})$ is called a *dyadic wavelet frame*.

Choosing $\psi \in L^2(\mathbb{R})$ to be the wavelet constructed from Chapter 2, the series of functions $\{D^j T_k \psi\}_{j,k\in\mathbb{Z}}$ is exactly the orthonormal wavelet basis for $L^2(\mathbb{R})$. It then make sense to define wavelet frames this way. The associated frame operator to the frame $\{D^j T_k \psi\}_{j,k\in\mathbb{Z}}$ is given by

$$S : L^2(\mathbb{R}) \to L^2(\mathbb{R})\,;\, S(f) = \sum_{j,k\in\mathbb{Z}} \left\langle f, D^j T_k \psi \right\rangle D^j T_k \psi. \tag{4.3}$$

From Theorem 3.6, the frame decomposition will then be

$$f = \sum_{j,k\in\mathbb{Z}} \left\langle f, S^{-1}D^jT_k\psi \right\rangle D^jT_k\psi, \quad \forall f \in L^2(\mathbb{R}). \tag{4.4}$$

The frame decomposition coefficients $\langle f, S^{-1}D^jT_k\psi\rangle$ can be very inconvenient to calculate since it is nessesary to calculate the action of the inverse frame operator on $D^jT_k\psi$ for all $j,k \in \mathbb{Z}$. Thus a more simple way to calculate frame decomposition coefficients is needed. As stated in Chapter 3 there are two ways to avoid the canonical dual frame, by looking at tight frames or overcomplete frames and look for dual frames that are easier to calculate. For this to work the frame and dual frame must have wavelet structure. Since we want the frame to have wavelet structure it is only natural to assume some of the same things for the generator of the frame as is assumed for the generator of an orthonormal wavelet. Doing this leads to a very convenient algorithmic structure. A specific assumption comes in the form the generating wavelet function takes, as stated in Equation (2.2) and can be rewritten as

$$\psi(x) = \sum_{k\in\mathbb{Z}} c_k DT_k\varphi(x) \tag{4.5}$$

where φ is the scaling function satisfying an equation of the form

$$\hat{\varphi}(2\omega) = H_0(\omega)\,\hat{\varphi}(\omega)$$

for some 2π-periodic function $H_0 \in L^2(-\pi,\pi)$. This structure should not only be desirable for a single wavelet frame, but also for its dual wavelet frames. This means that the generator, for these dual wavelet frames, is wised to be of the form of Equation (4.5). For practical use it is desirable that the sum in Equation (4.5) is a finite sum, thus the choice of φ becomes a lot more restrictive to functions with compact support. An obvious candidate for the function φ in this case is the B-spline functions B_m. B-spline functions are piecewise polynomials supported on compact subintervals of the positive real axis. B-splines are defined inductively. The first order of B-spline is defined as

$$B_1(x) = 1_{[0,1]}(x).$$

This function is also known as the Haar scaling function. The n-th order B-spline is defined as, assuming the $n-1$ order B-spline has been defined,

$$\begin{aligned} B_n(x) &= B_{n-1} * B_1(x) \\ &= \int_0^1 B_{n-1}(x-t)\, dt. \end{aligned}$$

Using B-splines as φ, the sum in Equation (4.5) will become finite. It is not possible to obtain a construction that gives a pair of finite dual wavelet frames using B-splines this way.

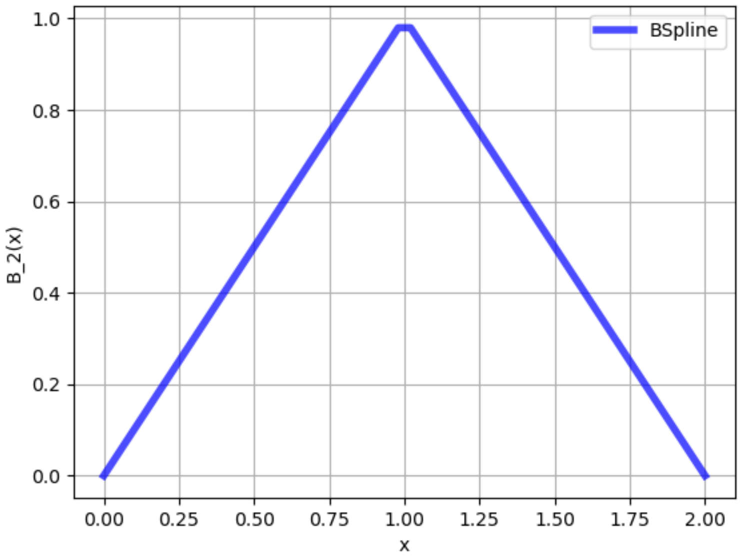

Figure 4.1: 1a

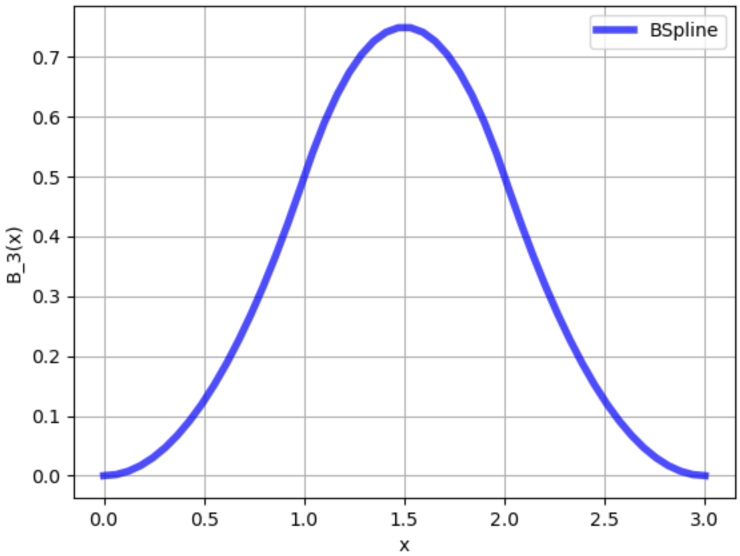

Figure 4.2: 1b

Figure 4.3: Plots of B-splines of different orders. 1a is of degree two and 1.b is of order three.

Theorem 4.2
Let B_m denote the m-th order B-spline for some $m > 1$. Then there does not exist pairs of dual wavelet frames $\{D^j T_k \psi\}_{j,k\in\mathbb{Z}}$ and $\{D^j T_k \widetilde{\psi}\}_{j,k\in\mathbb{Z}}$ for which ψ and $\widetilde{\psi}$ are finite linear combinations of functions $D^j T_k B_m$ where $j, k \in \mathbb{Z}$.

Proof
This theory is proven by [1] and [2]. ■

A solution to this problem does exist. By considering wavelet frames generated by a sequence of functions of the wavelet type, extra freedom is gained.

Definition 4.3
For two sequences of functions

$$\psi_1, \psi_2, \ldots, \psi_n \in L^2(\mathbb{R}) \text{ and } \widetilde{\psi}_1, \widetilde{\psi}_2, \ldots, \widetilde{\psi}_n \in L^2(\mathbb{R}).$$

the sequences $\{D^j T_k \psi_\ell\}_{j,k\in\mathbb{Z},\ell=1,\ldots,n}$ and $\{D^j T_k \widetilde{\psi}_\ell\}_{j,k\in\mathbb{Z},\ell=1,\ldots,n}$ are called a pair of dual *multiwavelet frames* if they both are Bessel sequences and

$$f = \sum_{\ell=1}^{n} \sum_{j,k\in\mathbb{Z}} \left\langle f, D^j T_k \psi_\ell \right\rangle D^j T_k \widetilde{\psi}_\ell, \quad \forall f \in L^2(\mathbb{R}). \tag{4.6}$$

From Lemma 3.11 it follows that the Bessel sequences $\{D^j T_k \psi_\ell\}_{j,k\in\mathbb{Z},\ell=1,\ldots,n}$ and $\{D^j T_k \widetilde{\psi}_\ell\}_{j,k\in\mathbb{Z},\ell=1,\ldots,n}$ form a pair of dual frames. A pair of dual multiwavelet frames is called *sibling frames* or *bi-frames*. The frame $\{D^j T_k \psi_\ell\}_{j,k\in\mathbb{Z},\ell=1,\ldots,n}$ itself is called a *multiwavelet frame*.

4.1 The Unitary extension principle

In this section the unitary extension principle will be proven. This principle enables us to construct tight frames for $L^2(\mathbb{R})$ of the form $\{D^j T_k \psi_\ell\}_{j,k\in\mathbb{Z},\ell=1,\ldots,n}$. The sequence $\psi_1, \psi_2, \ldots, \psi_n \in L^2(\mathbb{R})$ will be constructed on the basis of a function that satisfy an equation similar to Equation (3.2) from [6]. This function will play the same role as the scaling function does for orthonormal wavelets. Denote this function as ψ_0. The general setup will now explain what conditions that falls upon ψ_0.

General setup: Let $\psi_0 \in L^2(\mathbb{R})$, $\mathbb{T} = (-\pi, \pi)$ and assume that

(i) there exist a function $H_0 \in L^\infty(\mathbb{T})$ such that

$$\hat{\psi}_0(2\omega) = H_0(\omega)\, \hat{\psi}_0(\omega). \tag{4.7}$$

(ii) $\lim_{\omega\to 0}\hat{\psi}_0(\omega) = 1$.

Let now $H_1, \ldots, H_n \in L^\infty(\mathbb{T})$ and define $\psi_1, \psi_2, \ldots, \psi_n \in L^2(\mathbb{R})$ by

$$\hat{\psi}_\ell(2\omega) = H_\ell(\omega)\,\hat{\psi}_0(\omega), \quad \ell = 0, \ldots, n. \tag{4.8}$$

Last, let H be the $(n+1)\times 2$ matrix-valued function defined by

$$H(\omega) = \begin{pmatrix} H_0(\omega) & T_\pi H_0(\omega) \\ H_1(\omega) & T_\pi H_1(\omega) \\ \vdots & \vdots \\ H_n(\omega) & T_\pi H_n(\omega) \end{pmatrix}, \ \omega \in \mathbb{R}. \tag{4.9}$$

With this setup in mind the purpose is to find the conditions on $H_1, \ldots, H_n$ such that $\psi_1, \psi_2, \ldots, \psi_n$ defined by Equation (4.8) generates a multiwavelet frame for $L^2(\mathbb{R})$. Note that if H_ℓ is known then ψ_ℓ can be explicit expressed. Expanding H_ℓ in a Fourier series, $H_\ell(\omega) = \sum_{k\in\mathbb{Z}} c_{k,\ell} e^{-ik\omega}$. Using the inverse Fourier transformation on Equation (4.8), we obtain

$$\frac{1}{2}\psi_\ell\left(\frac{x}{2}\right) = \sum_{k\in\mathbb{Z}} c_{k,\ell}\psi_0(x-k)$$

which can be rewritten as

$$\psi_\ell(x) = 2\sum_{k\in\mathbb{Z}} c_{k,\ell}\psi_0(2x-k). \tag{4.10}$$

Since we want the same wavelet structure as an orthonormal wavelet with compact support, it is prefered that H_ℓ are trigonometric polynomials. This implies that ψ_ℓ have compact support if ψ_0 has compact support and the sum in Equation (4.10) is finite. Note that setting up in this way preserves the algorithmic structure of a multiresolution. This is shown in Theorem 3.6.6 form [3] by defining

$$V_j = \overline{\text{span}}\{D^j T_k \psi_0\},\ j \in \mathbb{Z}.$$

The theorem states that if $\psi_0 \in L^2(\mathbb{R})$, $|\hat{\psi}_0| > 0$ in a neighberhood of 0 and there exist a bounded 2π-periodic function H_0 such that Equation (4.7) is true, then all the conditions for a multiresolution analysis in Definition 2.1 except for condition (v) is satisfied. Also since ψ_ℓ is constructed from Equation (4.10) then $\psi_\ell \in V_1$ for $\ell = 1, \ldots n$.

Now that the general setup is complete, a few lemmas will be stated before the unitary extension principle can be proven. One of the main tools used is the *periodization* of a function formally defined by

$$\mathcal{P}f(\omega) = \sum_{n\in\mathbb{Z}} f(\omega + 2\pi n),\ \omega \in \mathbb{R} \quad \text{where} \quad f : \mathbb{R} \to \mathbb{C}.$$

This definition will now be shown to be well defined for $f \in L^1(\mathbb{R})$.

Lemma 4.4
If $f \in L^1(\mathbb{R})$, then $\sum_{n\in\mathbb{Z}} f(\omega + 2\pi n)$ converges absolutely for almost every $\omega \in \mathbb{R}$ and $\mathcal{P}f \in L^1(\mathbb{T})$. Furthermore,

$$\int_{\infty}^{\infty} f(\omega)\, d\omega = \int_{-\pi}^{\pi} \mathcal{P}f(\omega)\, d\omega. \tag{4.11}$$

Proof
Assume $f \in L^1(\mathbb{R})$, then using a special case of Tonelli's theorem

$$\begin{aligned}\int_{-\pi}^{\pi} \sum_{n\in\mathbb{Z}} |f(\omega + 2\pi n)|\, d\omega &= \sum_{n\in\mathbb{Z}} \int_{-\pi}^{\pi} |f(\omega + 2\pi n)|\, d\omega \\ &= \int_{-\infty}^{\infty} |f(\omega)|\, d\omega < \infty.\end{aligned}$$

This shows that $\sum_{n\in\mathbb{Z}} f(\omega + 2\pi n)$ is absolutly convergent for almost every $\omega \in \mathbb{R}$ and thus $\mathcal{P}f \in L^1(\mathbb{T})$ since

$$|\mathcal{P}f(\omega)| \leq \sum_{n\in\mathbb{Z}} |f(\omega + 2\pi n)|, \quad \text{a.e. } \omega \in \mathbb{R}.$$

Equation (4.11) now follows from Lebesgue's dominated convergence theorem. ∎

Periodization is used in the following lemmas.

Lemma 4.5
let $g, \psi_0 \in L^2(\mathbb{R})$ and assume that $\mathcal{P}\left(g\overline{\hat{\psi}_0}\right) \in L^2(\mathbb{T})$, then

$$\mathcal{P}\left(g\overline{\hat{\psi}_0}\right) = \sum_{k\in\mathbb{Z}} \frac{1}{2\pi} \left\langle g, \hat{\psi}_0 e^{ik\omega} \right\rangle e^{ik\omega} \tag{4.12}$$

and

$$\int_{-\pi}^{\pi} \left|\mathcal{P}\left(g\overline{\hat{\psi}_0}\right)\right|^2 = \sum_{k\in\mathbb{Z}} \left| \frac{1}{2\pi} \left\langle g, \hat{\psi}_0 e^{ik\omega} \right\rangle \right|^2. \tag{4.13}$$

Proof
Since $g, \psi_0 \in L^2(\mathbb{R})$ we have $g\overline{\hat{\psi}_0} \in L^1(\mathbb{R})$. From Lemma 4.4 the function

$$\mathcal{P}\left(g\overline{\hat{\psi}_0}\right)(\omega) = \sum_{n\in\mathbb{Z}} g(\omega + 2\pi n)\, \overline{\hat{\psi}_0(\omega + 2\pi n)}$$

is well defined. Using Equation (4.11)

$$\begin{aligned}\left\langle g, \hat{\psi}_0 e^{ik\cdot} \right\rangle &= \int_{-\infty}^{\infty} g(\omega)\, \overline{\hat{\psi}_0(\omega) e^{-ik\omega}} d\omega \\ &= \int_{-\pi}^{\pi} \sum_{n\in\mathbb{Z}} \left(g(\omega+2\pi n)\, \overline{\hat{\psi}_0(\omega+2\pi n) e^{-ik(\omega+2\pi n)}} \right) d\omega \\ &= \int_{-\pi}^{\pi} \sum_{n\in\mathbb{Z}} \left(g(\omega+2\pi n)\, \overline{\hat{\psi}_0(\omega+2\pi n)} \right) e^{-ik\omega} d\omega.\end{aligned}$$

This makes $\frac{1}{2\pi}\left\langle g, \hat{\psi}_0 e^{ik\cdot} \right\rangle$ the k-th Fourier coefficient for the 2π-periodic function $\mathcal{P}\left(g\overline{\hat{\psi}_0}\right)(\omega)$. Since $\mathcal{P}\left(g\overline{\hat{\psi}_0}\right)(\omega) \in L^2(\mathbb{T})$ by assumption, the lemma follows: Equation (4.12) is the Fourier expansion of $\mathcal{P}\left(g\overline{\hat{\psi}_0}\right)$ in a Fourier series, and Equation (4.13) comes from Parseval's equation.

■

Because of Lemma 3.4, it is enough to prove the unitary extension principle on a dense subspace of $L^2(\mathbb{R})$. The dense subspace that will be used is the set of functions, f, for which the Fourier transform, $\hat{f}$, is continuous and has compact support. Denote this space

$$\mathcal{D} = \left\{ f \in L^2(\mathbb{R}) \mid \hat{f} \in C_c(\mathbb{R}) \right\}. \tag{4.14}$$

In the following lemmas this dense subspace will be used.

Lemma 4.6
Let $\psi_0 \in L^2(\mathbb{R})$, $f \in \mathcal{D}$ and assume that $\lim_{\omega\to 0} \hat{\psi}_0(\omega) = 1$. Then for any $\epsilon > 0$ there exists $J \in \mathbb{Z}$ such that

$$(1-\epsilon)\, 2\pi \|f\|_2^2 \leq \sum_{k\in\mathbb{Z}} \left| \left\langle f, D^j T_k \psi_0 \right\rangle \right|^2 \leq (1+\epsilon)\, 2\pi \|f\|_2^2, \text{ for all } j \geq J.$$

Proof
Let $j \in \mathbb{Z}$ and $f \in \mathcal{D}$. The product function $\left(D^j \hat{f}\right) \overline{\hat{\psi}_0}$ belongs to $L^1(\mathbb{R})$. Lemma 4.4 states that $\mathcal{P}\left(\left(D^j \hat{f}\right) \overline{\hat{\psi}_0}\right)$ is well defined. First it must be proven that $\mathcal{P}\left(\left(D^j \hat{f}\right) \overline{\hat{\psi}_0}\right) \in L^2(\mathbb{T})$. Since $f \in \mathcal{D}$, $D^j \hat{f}$ will have compact support, say, in the interval $[-N, N]$.

Then for $\omega \in \mathbb{T}$,

$$\begin{aligned}\left|\mathcal{P}\left(\left(D^j\hat{f}\right)\overline{\hat{\psi}_0}\right)\right| &= \left|\sum_{n\in\mathbb{Z}}\left(D^j\hat{f}\right)(\omega+2\pi n)\,\overline{\hat{\psi}_0(\omega+2\pi n)}\right| \\ &= \left|\sum_{n=-N}^{N}\left(D^j\hat{f}\right)(\omega+2\pi n)\,\overline{\hat{\psi}_0(\omega+2\pi n)}\right| \\ &\leq \left\|D^j\hat{f}\right\|_\infty \sum_{n=-N}^{N}\left|\overline{\hat{\psi}_0(\omega+n)}\right|.\end{aligned}$$

Since $\sum_{n=-N}^{N}\left|\overline{\hat{\psi}_0(\omega+n)}\right|$ is a finite linear combination of translates of a function in $L^2(\mathbb{R})$, $\mathcal{P}\left(\left(D^j\hat{f}\right)\overline{\hat{\psi}_0}\right) \in L^2(\mathbb{T})$. Using Plancherel's theorem and that $\langle f, D^j g\rangle = \langle D^{-j}f, g\rangle$ we have

$$\left\langle f, D^j T_k \psi_0\right\rangle = \frac{1}{2\pi}\left\langle D^j\hat{f}, \hat{\psi}_0 e^{-ik\cdot}\right\rangle.$$

Consider

$$\sum_{k\in\mathbb{Z}}\left|\left\langle f, D^j T_k\psi_0\right\rangle\right|^2 = \sum_{k\in\mathbb{Z}}\left|\frac{1}{2\pi}\left\langle D^j\hat{f}, \hat{\psi}_0 e^{-ik\cdot}\right\rangle\right|^2.$$

Since $D^j\hat{f}$ have compact support, $\sum_{k\in\mathbb{Z}}\left|\frac{1}{2\pi}\left\langle D^j\hat{f}, \hat{\psi}_0 e^{-ik\cdot}\right\rangle\right|^2$ converges unconditionally. Using this and Lemma 4.5

$$\begin{aligned}\sum_{k\in\mathbb{Z}}\left|\left\langle f, D^j T_k\psi_0\right\rangle\right|^2 &= \sum_{k\in\mathbb{Z}}\left|\frac{1}{2\pi}\left\langle D^j\hat{f}, \hat{\psi}_0 e^{ik\cdot}\right\rangle\right|^2 \\ &= \int_{-\pi}^{\pi}\left|\mathcal{P}\left(\left(D^j\hat{f}\right)\overline{\hat{\psi}_0}\right)\right|^2 d\omega \\ &= \int_{-\pi}^{\pi}\left|\sum_{n\in\mathbb{Z}}\left(D^j\hat{f}\right)(\omega+2\pi n)\,\overline{\hat{\psi}_0(\omega+2\pi n)}\right|^2 d\omega.\end{aligned}$$

Let $\epsilon > 0$ be given. By assumption $\lim_{\omega\to 0}\hat{\psi}_0 = 1$, we can choose $b \in]0,\pi[$ such that $1-\epsilon \leq \left|\hat{\psi}_0(\omega)\right|^2 \leq 1+\epsilon$ whenever $|\omega| \leq b$. Choosing $J \in \mathbb{Z}$ such that $D^j\hat{f}$ have support in $[-b,b]$ for $j > J$,

$$\int_{-\pi}^{\pi}\left|\sum_{n\in\mathbb{Z}}\left(D^j\hat{f}\right)(\omega+2\pi n)\,\overline{\hat{\psi}_0(\omega+2\pi n)}\right|^2 d\omega = \int_{-\pi}^{\pi}\left|\left(D^j\hat{f}\right)(\omega)\,\hat{\psi}_0(\omega)\right|^2 d\omega$$

for all $j > J$. This implies

$$(1-\epsilon)\left\|D^j\hat{f}\right\|_2^2 \leq \sum_{k\in\mathbb{Z}}\left|\left\langle f, D^j T_k\psi_0\right\rangle\right|^2 \leq (1+\epsilon)\left\|D^j\hat{f}\right\|_2^2.$$

Since D^j is a unitary operator, and using Plancherel's theorem, we obtain

$$(1-\epsilon)\,2\pi\,\|f\|_2^2 \leq \sum_{k\in\mathbb{Z}} \left|\left\langle f, D^j T_k \psi_0 \right\rangle\right|^2 \leq (1+\epsilon)\,2\pi\,\|f\|_2^2 .$$

Thus the lemma follows from this.

■

Since $\psi_\ell \in L^2(\mathbb{R})$ for every $\ell = 1,\ldots,n$ the same calculations as in the proof of Lemma 4.6 can be modified such that

$$\sum_{k\in\mathbb{Z}} \left|\left\langle f, D^j T_k \psi_\ell \right\rangle\right|^2 = \int_{-\pi}^{\pi} \left| \sum_{n\in\mathbb{Z}} \left(D^j \hat{f}\right)(\omega+2\pi n)\,\overline{\hat{\psi}_\ell(\omega+2\pi n)} \right|^2 d\omega.$$

Since $\left(D^j \hat{f}\right)(\omega+2\pi n)\,\overline{\hat{\psi}_\ell(\omega+2\pi n)} \in L^1(\mathbb{R})$,

$$\sum_{n\in\mathbb{Z}} \left(D^j \hat{f}\right)(\omega+2\pi n)\,\overline{\hat{\psi}_\ell(\omega+2\pi n)} \in L^1(\mathbb{T})$$

will converge absolutely, hence Lemma 4.4. This implies that

$$\sum_{k\in\mathbb{Z}} \left|\left\langle f, D^j T_k \psi_\ell \right\rangle\right|^2 < \infty$$

which further implies that

$$\left\{\left\langle f, D^j T_k \psi_\ell \right\rangle\right\}_{k\in\mathbb{Z}} \in \ell^2(\mathbb{Z}) \tag{4.15}$$

for all $j \in \mathbb{Z}$ and all $\ell = 1,\ldots,n$. A family of functions $F_{j,\ell} \in L^2(\mathbb{T})$ can then be defined by the Fourier series

$$F_{j,\ell}(\omega) = \sum_{k\in\mathbb{Z}} \left\langle f, D^j T_k \psi_\ell \right\rangle e^{-ik\omega}. \tag{4.16}$$

The definition of $F_{j,\ell}$ is defined in terms of ψ_ℓ, which is defined by ψ_0 and H_ℓ. It is natural to assume that there exist an expression for $F_{j,\ell}$ in terms of $F_{j,0}$ and H_ℓ. This expression is proven in the following lemma.

Lemma 4.7
Let $\{\psi_\ell, H_\ell\}_{\ell=0}^n$ be as in the general setup. Then for all $j \in \mathbb{Z}, \ell = 0,1,\ldots,n$,

$$F_{j-1,\ell}(\omega) = 2^{-\frac{1}{2}} \left(\overline{H_\ell\left(\frac{\omega}{2}\right)} F_{j,0}\left(\frac{\omega}{2}\right) + \overline{T_\pi H_\ell\left(\frac{\omega}{2}\right)} T_\pi F_{j,0}\left(\frac{\omega}{2}\right) \right)$$

for almost every $\omega \in \mathbb{R}$.

Proof
Using the properties of D and Plancherel's theorem

$$\begin{aligned}\left\langle f, D^{j-1}T_k\psi_\ell\right\rangle &= \left\langle D^{-j}f, D^{-1}T_k\psi_\ell\right\rangle\\ &= \left\langle D^{-j}f, T_{2k}D^{-1}\psi_\ell\right\rangle\\ &= \frac{1}{2\pi}\left\langle D^j\hat{f}, e^{-i2k\cdot}D\hat{\psi}_\ell\right\rangle.\end{aligned}$$

Equation (4.8) and Lemma 4.4 then gives

$$\begin{aligned}\left\langle f, D^{j-1}T_k\psi_\ell\right\rangle &= \frac{1}{2\pi}\left\langle D^j\hat{f}, e^{-i2k\cdot}\sqrt{2}H_\ell\hat{\psi}_0\right\rangle\\ &= \frac{1}{\sqrt{2}\pi}\int_{-\infty}^{\infty}\left(D^j\hat{f}\right)(\omega)\,\overline{H_\ell(\omega)\,\hat{\psi}_0(\omega)}e^{i2k\omega}d\omega\\ &= \frac{1}{\sqrt{2}\pi}\int_{-\pi}^{\pi}\mathcal{P}\left(\left(D^j\hat{f}\right)(\omega)\,\overline{H_\ell(\omega)\,\hat{\psi}_0(\omega)}\right)e^{i2k\omega}d\omega\\ &= \frac{1}{\sqrt{2}\pi}\left(\int_0^{\pi}\mathcal{P}\left(\left(D^j\hat{f}\right)(\omega)\,\overline{H_\ell(\omega)\,\hat{\psi}_0(\omega)}\right)e^{i2k\omega}d\omega+\right.\\ &\qquad\left.\int_0^{\pi}T_\pi\mathcal{P}\left(\left(D^j\hat{f}\right)(\omega)\,\overline{H_\ell(\omega)\,\hat{\psi}_0(\omega)}\right)e^{i2k\omega}d\omega\right)\\ &= \frac{1}{\sqrt{2}\pi}\int_0^{\pi}\left(\mathcal{P}\left(\left(D^j\hat{f}\right)(\omega)\,\overline{H_\ell(\omega)\,\hat{\psi}_0(\omega)}\right)+\right.\\ &\qquad\left.T_\pi\mathcal{P}\left(\left(D^j\hat{f}\right)(\omega)\,\overline{H_\ell(\omega)\,\hat{\psi}_0(\omega)}\right)\right)e^{i2k\omega}d\omega.\end{aligned}$$

This makes $\sqrt{2}\left\langle f, D^{j-1}T_k\psi_\ell\right\rangle$ the $(-k)$-th coefficient in the Fourier series expansion for the π-periodic function

$$\mathcal{P}\left(\left(D^j\hat{f}\right)(\omega)\,\overline{H_\ell(\omega)\,\hat{\psi}_0(\omega)}\right)+T_\pi\mathcal{P}\left(\left(D^j\hat{f}\right)(\omega)\,\overline{H_\ell(\omega)\,\hat{\psi}_0(\omega)}\right)$$

with respect to the orthonormal basis $\{e^{i2k\cdot}\}_{k\in\mathbb{Z}}$ for $L^2(0,\pi)$. Using $F_{j-1,\ell}$ from Equation (4.16), and

$$e^{-ik\omega} = \frac{1}{\sqrt{2}}\sqrt{2}e^{-i2k\frac{\omega}{2}},$$

it follows that

$$\begin{aligned}F_{j-1,\ell} &= \sum_{k\in\mathbb{Z}}\left\langle f, D^jT_k\psi_\ell\right\rangle e^{-ik\omega}\\ &= \frac{1}{\sqrt{2}}\sum_{k\in\mathbb{Z}}\sqrt{2}\left\langle f, D^jT_k\psi_\ell\right\rangle e^{-i2k\frac{\omega}{2}}\\ &= 2^{-\frac{1}{2}}\left(\mathcal{P}\left(\left(D^j\hat{f}\right)\left(\frac{\omega}{2}\right)\overline{H_\ell\left(\frac{\omega}{2}\right)\hat{\psi}_0\left(\frac{\omega}{2}\right)}\right)+T_\pi\mathcal{P}\left(\left(D^j\hat{f}\right)\left(\frac{\omega}{2}\right)\overline{H_\ell\left(\frac{\omega}{2}\right)\hat{\psi}_0\left(\frac{\omega}{2}\right)}\right)\right)\end{aligned}$$

From H_ℓ being a 2π-periodic function we get

$$\mathcal{P}\left(\left(D^j \hat{f}\right)\left(\frac{\omega}{2}\right)\overline{H_\ell\left(\frac{\omega}{2}\right)\hat{\psi}_0\left(\frac{\omega}{2}\right)}\right) = \overline{H_\ell\left(\frac{\omega}{2}\right)}\mathcal{P}\left(\left(D^j \hat{f}\right)\left(\frac{\omega}{2}\right)\overline{\hat{\psi}_0\left(\frac{\omega}{2}\right)}\right).$$

Using this, it suffices to show that

$$F_{j,0}(\omega) = \mathcal{P}\left(\left(D^j \hat{f}\right)(\omega)\overline{\hat{\psi}_0(\omega)}\right)$$

and the proof is done. Earlier in the proof, it was shown that

$$\left\langle f, D^j T_k \psi_0 \right\rangle = \frac{1}{2\pi}\left\langle D^j \hat{f}, e^{-ik\cdot}\hat{\psi}_0 \right\rangle.$$

Using this, Lemma 4.5 and Equation (4.16) we get

$$\begin{aligned} F_{j,0}(\omega) &= \sum_{k\in\mathbb{Z}} \left\langle f, D^j T_k \psi_0 \right\rangle e^{-ik\omega} \\ &= \sum_{k\in\mathbb{Z}} \frac{1}{2\pi}\left\langle D^j \hat{f}, e^{-ik\cdot}\hat{\psi}_0 \right\rangle e^{-ik\omega} \\ &= \mathcal{P}\left(\left(D^j \hat{f}\right)(\omega)\overline{\hat{\psi}_0(\omega)}\right). \end{aligned}$$

It can now be concluded that

$$F_{j-1,\ell}(\omega) = 2^{-\frac{1}{2}}\left(\overline{H_\ell\left(\frac{\omega}{2}\right)}F_{j,0}\left(\frac{\omega}{2}\right) + \overline{T_\pi H_\ell\left(\frac{\omega}{2}\right)}T_\pi F_{j,0}\left(\frac{\omega}{2}\right)\right).$$

■

By using the matrix H from Equation (4.9), the result from Lemma 4.7 shows that for almost every $\omega \in \mathbb{R}$

$$\begin{aligned} \begin{pmatrix} F_{j-1,0}(\omega) \\ F_{j-1,1}(\omega) \\ \vdots \\ F_{j-1,n}(\omega) \end{pmatrix} &= 2^{-\frac{1}{2}} \begin{pmatrix} \overline{H_0\left(\frac{\omega}{2}\right)}F_{j,0}\left(\frac{\omega}{2}\right) + \overline{T_\pi H_0\left(\frac{\omega}{2}\right)}T_\pi F_{j,0}\left(\frac{\omega}{2}\right) \\ \overline{H_1\left(\frac{\omega}{2}\right)}F_{j,0}\left(\frac{\omega}{2}\right) + \overline{T_\pi H_1\left(\frac{\omega}{2}\right)}T_\pi F_{j,0}\left(\frac{\omega}{2}\right) \\ \vdots \\ \overline{H_n\left(\frac{\omega}{2}\right)}F_{j,0}\left(\frac{\omega}{2}\right) + \overline{T_\pi H_n\left(\frac{\omega}{2}\right)}T_\pi F_{j,0}\left(\frac{\omega}{2}\right) \end{pmatrix} \\ &= 2^{-\frac{1}{2}} \overline{\begin{pmatrix} H_0(\omega) & T_\pi H_0(\omega) \\ H_1(\omega) & T_\pi H_1(\omega) \\ \vdots & \vdots \\ H_n(\omega) & T_\pi H_n(\omega) \end{pmatrix}} \begin{pmatrix} F_{j,0}\left(\frac{\omega}{2}\right) \\ T_\pi F_{j,0}\left(\frac{\omega}{2}\right) \end{pmatrix} \\ &= 2^{-\frac{1}{2}}\overline{H\left(\frac{\omega}{2}\right)} \begin{pmatrix} F_{j,0}\left(\frac{\omega}{2}\right) \\ T_\pi F_{j,0}\left(\frac{\omega}{2}\right) \end{pmatrix}. \end{aligned}$$

This means that

$$\sum_{\ell=0}^{n} \left|F_{j-1,\ell}(\omega)\right|^2 = 2^{-1} \left\| \overline{H\left(\frac{\omega}{2}\right)} \begin{pmatrix} F_{j,0}\left(\frac{\omega}{2}\right) \\ T_\pi F_{j,0}\left(\frac{\omega}{2}\right) \end{pmatrix} \right\|_{\mathbb{C}^{n+1}}^2. \tag{4.17}$$

The following lemmas as well as the unitary extension principle will be based on the assumption that the matrix $H(\omega)$ satisfies

$$H(\omega)^* H(\omega) = I, \quad a.e.\ \omega \in \mathbb{T}. \tag{4.18}$$

It turns out that equation (4.18) is an essential assumption and, given the general setup, the only condition we need for the unitary extension principle.

Lemma 4.8
Let $\{\psi_\ell, H_\ell\}_{\ell=0}^n$ be as defined in the general setup and assume that $H(\omega)^* H(\omega) = I$ for almost every $\omega \in \mathbb{T}$. Then, for all $j \in \mathbb{Z}$ and for all $f \in \mathcal{D}$,

$$\sum_{k\in\mathbb{Z}} \left|\left\langle f, D^j T_k \psi_0 \right\rangle\right|^2 = \sum_{\ell=0}^{n} \sum_{k\in\mathbb{Z}} \left|\left\langle f, D^{j-1} T_k \psi_\ell \right\rangle\right|^2.$$

Proof
Using Parseval's identity and Equation (4.16),

$$\sum_{\ell=0}^{n} \sum_{k\in\mathbb{Z}} \left|\left\langle f, D^{j-1} T_k \psi_\ell \right\rangle\right|^2 = \frac{1}{2\pi} \sum_{\ell=0}^{n} \int_{-\pi}^{\pi} \left|F_{j-1,\ell}(\omega)\right| d\omega. \tag{4.19}$$

The matrix $H(\omega)$ can be considered as an isometry from $\mathbb{C}^2$ to $\mathbb{C}^{n+1}$ for almost every $\omega \in \mathbb{T}$ because of the assumption $H(\omega)^* H(\omega) = I$. Using Equation (4.17) and Tonelli's theorem on Equation (4.19), it follows that

$$\begin{aligned}
\sum_{\ell=0}^{n} \sum_{k\in\mathbb{Z}} \left|\left\langle f, D^{j-1} T_k \psi_\ell \right\rangle\right|^2 &= \frac{2^{-1}}{2\pi} \int_{-\pi}^{\pi} \left\| \overline{H\left(\frac{\omega}{2}\right)} \begin{pmatrix} F_{j,0}\left(\frac{\omega}{2}\right) \\ T_\pi F_{j,0}\left(\frac{\omega}{2}\right) \end{pmatrix} \right\|_{\mathbb{C}^{n+1}}^2 d\omega \\
&= \frac{2^{-1}}{2\pi} \int_{-\pi}^{\pi} \left\| \begin{pmatrix} F_{j,0}\left(\frac{\omega}{2}\right) \\ T_\pi F_{j,0}\left(\frac{\omega}{2}\right) \end{pmatrix} \right\|_{\mathbb{C}^{2}}^2 d\omega \\
&= \frac{2^{-1}}{2\pi} \int_{-\pi}^{\pi} \left(\left|F_{j,0}\left(\frac{\omega}{2}\right)\right|^2 + \left|T_\pi F_{j,0}\left(\frac{\omega}{2}\right)\right|^2 \right) d\omega \\
&= \frac{1}{2\pi} \left(\int_{-\frac{\pi}{2}}^{\frac{\pi}{2}} \left|F_{j,0}(\omega)\right|^2 d\omega + \int_{-\frac{3\pi}{2}}^{-\frac{\pi}{2}} \left|F_{j,0}(\omega)\right|^2 d\omega \right) \\
&= \frac{1}{2\pi} \int_{-\frac{3\pi}{2}}^{\frac{\pi}{2}} \left|F_{j,0}(\omega)\right|^2 d\omega
\end{aligned}$$

Using the 2π-periodic nature of the function $F_{j,0}$ and Parseval's identity, we conclude that

$$\sum_{\ell=0}^{n}\sum_{k\in\mathbb{Z}}\left|\left\langle f,D^{j-1}T_k\psi_\ell\right\rangle\right|^2=\frac{1}{2\pi}\int_{-\pi}^{\pi}\left|F_{j,0}\left(\omega\right)\right|^2d\omega$$
$$=\sum_{k\in\mathbb{Z}}\left|\left\langle f,D^{j}T_k\psi_0\right\rangle\right|^2.$$

■

Lemma 4.9
Let $\{\psi_\ell, H_\ell\}_{\ell=0}^{n}$ be as defined in the general setup and assume that $H\left(\omega\right)^{*}H\left(\omega\right)=I$ for almost every $\omega\in\mathbb{T}$. Then the following hold.

(i) $\{T_k\psi_0\}_{k\in\mathbb{Z}}$ is a Bessel sequence with bound 2π.

(ii) If $f\in L^2\left(\mathbb{R}\right)$, then

$$\lim_{j\to-\infty}\sum_{k\in\mathbb{Z}}\left|\left\langle f,D^{j}T_k\psi_0\right\rangle\right|^2=0.$$

Proof
Let $f\in\mathcal{D}$. A consequence of Lemma 4.8 is that for any $j\in\mathbb{Z}$

$$\sum_{k\in\mathbb{Z}}\left|\left\langle f,D^{j-1}T_k\psi_0\right\rangle\right|^2\leq\sum_{k\in\mathbb{Z}}\left|\left\langle f,D^{j}T_k\psi_0\right\rangle\right|^2. \tag{4.20}$$

Let $\epsilon>0$ be given, Lemma 4.6 then states that we can find $j>0$ such that

$$\sum_{k\in\mathbb{Z}}\left|\left\langle f,D^{j}T_k\psi_0\right\rangle\right|^2\leq\left(1+\epsilon\right)2\pi\left\|f\right\|_2.$$

Using Equation (4.20) j times implies

$$\sum_{k\in\mathbb{Z}}\left|\left\langle f,T_k\psi_0\right\rangle\right|^2\leq\sum_{k\in\mathbb{Z}}\left|\left\langle f,D^{j}T_k\psi_0\right\rangle\right|^2\leq\left(1+\epsilon\right)2\pi\left\|f\right\|_2$$

and since $\epsilon>0$ was arbitrary, it follows that

$$\sum_{k\in\mathbb{Z}}\left|\left\langle f,T_k\psi_0\right\rangle\right|^2\leq2\pi\left\|f\right\|_2.$$

Because of Lemma 3.3, this holds true for all $f\in L^2\left(\mathbb{R}\right)$ and thus makes $\{T_k\psi_0\}_{k\in\mathbb{Z}}$ a Bessel sequence with Bessel bound 2π. To prove (ii), assume $f\in L^2\left(\mathbb{R}\right)$. (i) and the fact that D^j is an unitary operator implies that $\{D^j T_k \psi_0\}_{k\in\mathbb{Z}}$ is a Bessel sequence with Bessel bound 2π for all $j \in \mathbb{Z}$. Let $(a,b) \in \mathbb{R}$ be any bounded interval and write

$$f = f1_{(a,b)} + f\left(1 - 1_{(a,b)}\right).$$

Using the inequality $|x+y|^2 \leq 2\left(|x|^2 + |b|^2\right)$, $x, y \in \mathbb{C}$, we obtain

$$\begin{aligned}
\left|\left\langle f, D^j T_k \psi_0 \right\rangle\right|^2 &= \left|\left\langle f1_{(a,b)} + f\left(1 - 1_{(a,b)}\right), D^j T_k \psi_0 \right\rangle\right|^2 \\
&= \left|\left\langle f1_{(a,b)}, D^j T_k \psi_0 \right\rangle + \left\langle f\left(1 - 1_{(a,b)}\right), D^j T_k \psi_0 \right\rangle\right|^2 \\
&\leq 2\left(\left|\left\langle f1_{(a,b)}, D^j T_k \psi_0 \right\rangle\right|^2 + \left|\left\langle f\left(1 - 1_{(a,b)}\right), D^j T_k \psi_0 \right\rangle\right|^2\right).
\end{aligned}$$

This implies that

$$\begin{aligned}
\sum_{k\in\mathbb{Z}} \left|\left\langle f, D^j T_k \psi_0 \right\rangle\right|^2 &\leq 2\sum_{k\in\mathbb{Z}} \left|\left\langle f1_{(a,b)}, D^j T_k \psi_0 \right\rangle\right|^2 + 2\sum_{k\in\mathbb{Z}} \left|\left\langle f\left(1 - 1_{(a,b)}\right), D^j T_k \psi_0 \right\rangle\right|^2 \\
&\leq 2\sum_{k\in\mathbb{Z}} \left|\left\langle f1_{(a,b)}, D^j T_k \psi_0 \right\rangle\right|^2 + 2\left\|f\left(1 - 1_{(a,b)}\right)\right\|_2^2.
\end{aligned}$$

Choosing (a,b) to be a sufficiently large set, $\left\|f\left(1 - 1_{(a,b)}\right)\right\|_2^2$ becomes arbitrarily small. It is then enough to show that

$$\sum_{k\in\mathbb{Z}} \left|\left\langle f1_{(a,b)}, D^j T_k \psi_0 \right\rangle\right|^2 \to 0 \text{ as } j \to -\infty. \tag{4.21}$$

This is shown by

$$\begin{aligned}
\sum_{k\in\mathbb{Z}} \left|\left\langle f1_{(a,b)}, D^j T_k \psi_0 \right\rangle\right|^2 &= 2^j \sum_{k\in\mathbb{Z}} \left|\int_a^b f(x)\, \overline{\psi_0\left(2^j x - k\right)} dx\right|^2 \\
&\leq \|f\|_2^2\, 2^j \sum_{k\in\mathbb{Z}} \int_a^b \left|\psi_0\left(2^j x - k\right)\right|^2 dx \\
&= \|f\|_2^2 \sum_{k\in\mathbb{Z}} \int_{2^j a - k}^{2^j b - k} |\psi_0(x)|^2\, dx.
\end{aligned}$$

Using Lebesgue's dominated convergence theorem, Equation (4.21) is obtained, which concludes the proof.

■

Now the unitary extension principle is ready to be stated and proven.

Theorem 4.10 (The unitary extension principle)
Let $\{\psi_\ell, H_\ell\}_{\ell=0}^n$ be as defined in the general setup and assume that $H(\omega)^* H(\omega) = I$ for almost every $\omega \in \mathbb{T}$. The multiwavelet system $\{D^j T_k \psi_\ell\}_{j,k\in\mathbb{Z},\ell=1,\ldots,n}$ then constitutes a tight frame for $L^2(\mathbb{R})$ with frame bound equal to 2π, and

$$f = \frac{1}{2\pi} \sum_{\ell=1}^{n} \sum_{j\in\mathbb{Z}} \sum_{k\in\mathbb{Z}} \left\langle f, D^j T_k \psi_\ell \right\rangle D^j T_k \psi_\ell, \quad \forall f \in L^2(\mathbb{R}). \tag{4.22}$$

Proof
Let $\epsilon > 0$ be given, and consider a function $f \in \mathcal{D}$. Lemma 4.6 states that one can choose $J > 0$ such that for all $j > J$,

$$(1-\epsilon)\, 2\pi \|f\|_2^2 \leq \sum_{k\in\mathbb{Z}} \left| \left\langle f, D^j T_k \psi_0 \right\rangle \right|^2 \leq (1+\epsilon)\, 2\pi \|f\|_2^2 .$$

Then for any $j \in \mathbb{Z}$, Lemma 4.8 shows that

$$\begin{aligned} \sum_{k\in\mathbb{Z}} \left| \left\langle f, D^j T_k \psi_0 \right\rangle \right|^2 &= \sum_{\ell=0}^{n} \sum_{k\in\mathbb{Z}} \left| \left\langle f, D^{j-1} T_k \psi_\ell \right\rangle \right|^2 \\ &= \sum_{k\in\mathbb{Z}} \left| \left\langle f, D^{j-1} T_k \psi_0 \right\rangle \right|^2 + \sum_{\ell=1}^{n} \sum_{k\in\mathbb{Z}} \left| \left\langle f, D^{j-1} T_k \psi_\ell \right\rangle \right|^2 . \end{aligned}$$

Using this argument iterative on $\sum_{k\in\mathbb{Z}} \left|\left\langle f, D^{j-1} T_k \psi_0 \right\rangle\right|^2$, it follows that for all $m < j$,

$$\sum_{k\in\mathbb{Z}} \left| \left\langle f, D^j T_k \psi_0 \right\rangle \right|^2 = \sum_{k\in\mathbb{Z}} |\langle f, D^m T_k \psi_0 \rangle|^2 + \sum_{\ell=1}^{n} \sum_{p=m}^{j-1} \sum_{k\in\mathbb{Z}} |\langle f, D^p T_k \psi_\ell \rangle|^2 .$$

Thus it can be deduced that for all $j > J$ and $m < j$

$$(1-\epsilon)\, 2\pi \|f\|_2^2 \leq \sum_{k\in\mathbb{Z}} |\langle f, D^m T_k \psi_0 \rangle|^2 + \sum_{\ell=1}^{n} \sum_{p=m}^{j-1} \sum_{k\in\mathbb{Z}} |\langle f, D^p T_k \psi_\ell \rangle|^2 \leq (1+\epsilon)\, 2\pi \|f\|_2^2 .$$

By Lemma 4.9(ii)

$$\lim_{m\to-\infty} \sum_{k\in\mathbb{Z}} |\langle f, D^m T_k \psi_0 \rangle|^2 = 0$$

and thus, by letting $m \to -\infty$,

$$(1-\epsilon)\, 2\pi \|f\|_2^2 \leq \sum_{\ell=1}^{n} \sum_{p=-\infty}^{j-1} \sum_{k\in\mathbb{Z}} |\langle f, D^p T_k \psi_\ell \rangle|^2 \leq (1+\epsilon)\, 2\pi \|f\|_2^2 .$$

Letting $j \to \infty$

$$(1-\epsilon)\, 2\pi \, \|f\|_2^2 \leq \sum_{\ell=1}^{n} \sum_{p\in\mathbb{Z}} \sum_{k\in\mathbb{Z}} |\langle f, D^p T_k \psi_\ell \rangle|^2 \leq (1+\epsilon)\, 2\pi \, \|f\|_2^2 .$$

Because $\epsilon > 0$ was arbitrary chosen, it can be concluded that

$$\sum_{\ell=1}^{n} \sum_{p\in\mathbb{Z}} \sum_{k\in\mathbb{Z}} |\langle f, D^p T_k \psi_\ell \rangle|^2 = 2\pi \, \|f\|_2^2$$

for all $f \in \mathcal{D}$. By Lemma 3.3 it holds for all $f \in L^2(\mathbb{R})$ and Equation (4.22) is a consequences of Corollary 3.7.

■

Since the main assumption of Theorem 4.10 is

$$H(\omega)^* H(\omega) = I, \quad \text{a.e. } \omega \in \mathbb{T},$$

and $H(\omega)^* H(\omega)$ is an unitary matrix, it is possible to satisfy the main assumption by finding $H(\omega)$ such that it satisfies two equations. This is stated in the following corollary.

Corollary 4.11
Let $\{\psi_\ell, H_\ell\}_{\ell=0}^n$ be defined as in the general setup and assume that

$$\begin{cases} \sum_{\ell=0}^n |H_\ell(\omega)|^2 = 1 \\ \sum_{\ell=0}^n \overline{H_\ell(\omega)} T_\pi H_\ell(\omega) = 0 \end{cases} \tag{4.23}$$

for almost every $\omega \in \mathbb{T}$. Then all assumptions in theorem 4.10 are satisfied and the multiwavelet system $\{D^j T_k \psi_\ell\}_{j,k\in\mathbb{Z},\ell=1,\dots,n}$ constitutes a tight frame for $L^2(\mathbb{R})$ with frame bound equal to 2π.

Proof
It have to be proven that $H(\omega)^* H(\omega) = I$ for almost every $\omega \in \mathbb{T}$. This follows directly from the assumptions. ■

Using Corollary 4.11, it is possible to construct compactly supported tight multiwavelet frames based on B-splines. Remember from Theorem 4.2 that this was not possible with a single generator, but the following example shows it is with multiple generators.

Example 4.12 (Unitary extension principle on *B*-spline)
Consider the *B*-spline

$$\psi_0 = B_{2m}$$

of order $2m$ for any $m \in \mathbb{Z}^+$. Then, from known proporties of *B*-splines we obtain

$$\hat{\psi}_0(\omega) = e^{-im\omega}\left(\frac{\sin\left(\frac{\omega}{2}\right)}{\frac{\omega}{2}}\right)^{2m}.$$

It is clear that $\lim_{\omega\to 0}\hat{\psi}_0(\omega) = 1$ by L'Hôpital's rule. Furthermore, by using the trigonometric identity $\sin(2\omega) = 2\cos\omega\sin\omega$, it follows that

$$\hat{\psi}_0(2\omega) = e^{-im\omega}\cos^{2m}\left(\frac{\omega}{2}\right)\hat{\psi}_0(\omega).$$

Thus ψ_0 satisfy the conditions of the general setup with

$$H_0(\omega) = e^{-im\omega}\cos^{2m}\left(\frac{\omega}{2}\right) \in L^\infty(\mathbb{T})$$

being a 2π-periodic function. Defining

$$H_\ell(\omega) = \sqrt{\binom{2m}{\ell}}\, i^\ell e^{-im\omega}\sin^\ell\left(\frac{\omega}{2}\right)\cos^{2m-\ell}\left(\frac{\omega}{2}\right)$$

and using the binomial formula

$$(x+y)^{2m} = \sum_{\ell=0}^{2m}\binom{2m}{\ell}x^\ell y^{2m-\ell}$$

it will be shown that the conditions for Corollary 4.11 are satisfied.

$$
\begin{aligned}
\sum_{\ell=0}^{2m} |H_\ell(\omega)|^2 &= \sum_{\ell=0}^{2m} \binom{2m}{\ell} \left|i^\ell\right|^2 \left|e^{-i2m\omega}\right|^2 \sin^{2\ell}\left(\frac{\omega}{2}\right) \cos^{2(2m-\ell)}\left(\frac{\omega}{2}\right) \\
&= \sum_{\ell=0}^{2m} \binom{2m}{\ell} \left(\sin^2\left(\frac{\omega}{2}\right)\right)^\ell \left(\cos^2\left(\frac{\omega}{2}\right)\right)^{2m-\ell} \\
&= \left(\sin^2\left(\frac{\omega}{2}\right) + \cos^2\left(\frac{\omega}{2}\right)\right)^{2m} = 1, \quad \omega \in \mathbb{T}.
\end{aligned}
$$

$$
\begin{aligned}
\sum_{\ell=0}^{2m} \overline{H_\ell(\omega)} T_\pi H_\ell(\omega) &= \sum_{\ell=0}^{2m} \binom{2m}{\ell} (-i)^\ell e^{im\omega} \sin^\ell\left(\frac{\omega}{2}\right) \cos^{2m-\ell}\left(\frac{\omega}{2}\right) \cdot \\
&\qquad i^{2m-\ell} e^{-im\omega} \cos^\ell\left(\frac{\omega}{2}\right) \sin^{2m-\ell}\left(\frac{\omega}{2}\right) \\
&= \sum_{\ell=0}^{2m} \binom{2m}{\ell} (-i)^\ell i^{2m-\ell} \sin^{2m+\ell-\ell}\left(\frac{\omega}{2}\right) \cos^{2m-\ell+\ell}\left(\frac{\omega}{2}\right) \\
&= \sin^{2m}\left(\frac{\omega}{2}\right) \cos^{2m}\left(\frac{\omega}{2}\right) \sum_{\ell=0}^{2m} \binom{2m}{\ell} (-i)^\ell i^{2m-\ell} \\
&= \sin^{2m}\left(\frac{\omega}{2}\right) \cos^{2m}\left(\frac{\omega}{2}\right) ((-i)+i)^{2m} = 0.
\end{aligned}
$$

Corollary 4.11 now states that the multiwavelet $\{D^j T_k \psi_\ell\}_{j,k\in\mathbb{Z},\ell=1,\ldots,2m}$ where ψ_ℓ for $\ell = 1, \ldots, 2m$ defined by

$$
\begin{aligned}
\hat{\psi}_\ell(\omega) &= H_\ell\left(\frac{\omega}{2}\right) \hat{\psi}_0\left(\frac{\omega}{2}\right) \\
&= \sqrt{\binom{2m}{\ell}} i^\ell e^{-im\omega} \frac{\sin^{2m+\ell}\left(\frac{\omega}{4}\right) \cos^{2m-\ell}\left(\frac{\omega}{4}\right)}{\left(\frac{\omega}{4}\right)^{2m}}
\end{aligned}
$$

constitutes a tight frame with compact support for $L^2(\mathbb{R})$ with frame bound equal to 2π.

4.2 The oblique extension principle

This section is also based on the general setup in Section 4.1. The purpose of this section is to prove a more flexible version of the unitary extension principle. The reason to do this is, it is desirable that a multiwavelet frame is generated by functions $\{\psi_\ell\}_{\ell=1}^n$ that have a large number of vanishing moments. For $N \in \mathbb{N}$ it is said that a function f have N vanishing moments if

$$\int_{\mathbb{R}} x^m f(x)\ dx = 0$$

for $0 \leq m \leq N$. The reason that it is desirable that a multiwavelet frame $\{\psi_\ell\}_{\ell=1}^{n}$ have a high number of vanishing moments is because

$$\left\langle f, D^j T_k \psi \right\rangle \to 0 \text{ for } j \to \infty$$

converges faster for larger N. This is quantified in the following theorem.

Theorem 4.13
Given $N \in \mathbb{N}$, assume that the function $f \in C^N(\mathbb{R})$ and $f^{(N)} \in L^\infty(\mathbb{R})$. Assume that the function $\psi(x)$ has compact support,

$$\int_{\mathbb{R}} x^m \psi(x)\ dx = 0$$

for $0 \leq m \leq N-1$, and $\int_{\mathbb{R}} \left|D^j T_k \psi(x)\right| dx = 1$ for all $j, k \in \mathbb{Z}$. Then there exist a constant $C > 0$ depending only on N and f such that for every $j, k \in \mathbb{Z}$

$$\left|\left\langle f, D^j T_k \psi \right\rangle\right| \leq C 2^{-jN} 2^{-\frac{j}{2}}.$$

Proof
This proof follows the proof of theorem 9.5 in [8].

■

This theorem shows that the elements $\langle f, D^j T_k \psi \rangle$ only can fluctuate in the interval $\left[-C2^{-jN}2^{-\frac{j}{2}}, C2^{-jN}2^{-\frac{j}{2}}\right]$. The following result shows that the elements $\langle f, D^j T_k \psi \rangle$ also goes towards zero for $k \to \pm\infty$.

Theorem 4.14
Let $f, g \in L^2(R)$ and assume that

$$|f(x)| \leq \frac{1}{(1+|x|)^N} \quad \text{and} \quad |g(x)| \leq \frac{1}{(1+|x|)^N}. \tag{4.24}$$

Then

$$\left|\left\langle f, D^j T_k g \right\rangle\right| \leq C 2^{-\frac{j}{2}} \frac{1}{\left(1+\left|2^{-j}k\right|\right)^N}$$

where $C > 0$ and does not depend on $j, k \in \mathbb{Z}$.

Proof
Consider

$$\begin{aligned}\left|\left\langle f, D^j T_k g\right\rangle\right| &\leq \int_{\mathbb{R}} |f(x)| \left|\overline{2^{\frac{j}{2}} g\left(2^j x - k\right)}\right| dx \\ &= 2^{-\frac{j}{2}} \int_{\mathbb{R}} |f(x)| \left|\overline{g\left(x - 2^{-j} k\right)}\right| dx\end{aligned}$$

Using the assumption of f and g in Equation (4.24)

$$\left|\left\langle f, D^j T_k g\right\rangle\right| \leq \int_{\mathbb{R}} \frac{1}{\left(1+|x|\right)^N} \frac{1}{\left(1+\left|x-2^{-j}k\right|\right)^N} dx.$$

The following equality from Appendix B.1 from [4]

$$\int_{\mathbb{R}^n} \frac{2^{\mu n}}{\left(1+2^{\mu}|x-a|\right)^M} \frac{2^{\eta n}}{\left(1+2^{\eta}|x-b|\right)^N} dx \leq C_0 \frac{2^{\min(\mu,\eta) n}}{\left(1+2^{\min(\mu,\eta)}|x-b|\right)^{\min(M,N)}}$$

where $a, b \in \mathbb{R}^n, \mu, \eta \in \mathbb{R}, M, N > n$ and C_0 don't depend on a, b, μ or η is then used, such that

$$\left|\left\langle f, D^j T_k g\right\rangle\right| \leq C_0 2^{-\frac{j}{2}} \frac{1}{\left(1+\left|2^{-j}k\right|\right)^N}.$$

■

Using These two theorems will

$$\left|\left\langle f, D^j T_k \psi\right\rangle\right| \leq \left(C 2^{-jN} 2^{-\frac{j}{2}}\right)^{\frac{1}{2}} \left(C 2^{-\frac{j}{2}} \frac{1}{\left(1+\left|2^{-j}k\right|\right)^N}\right)^{\frac{1}{2}}. \tag{4.25}$$

Thus, by having a multiwavelet frame generated by functions $\{\psi_\ell\}_{\ell=1}^n$ that have a large number of vanishing moments, the elements $\langle f, D^j T_k \psi\rangle$ will naturally be sparse and, for a high enough j, negligible. If a series of functions $\{\psi_\ell\}_{\ell=1}^n$ is generated by the unitary extensions theorem, Theorem 4.10, it can then be shown that the number of vanishing moments for the function ψ_ℓ is equal to the order of zero for $H_\ell(\omega)$ at $\omega = 0$. This puts a natural restriction on the number of vanishing moments one can obtain via the unitary extension principle. A solution to this problem is called the *oblique extension principle*, and results in constructions with a potential higher number of vanishing moments.

Theorem 4.15 (The oblique extension principle)
Let $\{\psi_\ell, H_\ell\}_{\ell=0}^n$ be as defined in the general setup and assume there exist a strictly positive function $\theta \in L^\infty(\mathbb{T})$ for which

$$\lim_{\omega \to 0} \theta(\omega) = 1 \tag{4.26}$$

and such that for almost every $\omega \in \mathbb{T}$,

$$H_0(\omega)\,\overline{H_0(\omega+\nu)}\theta(2\omega) + \sum_{\ell=1}^{n} H_\ell(\omega)\,\overline{H_\ell(\omega+\nu)} = \begin{cases} \theta(\omega) & \text{if } \nu = 0 \\ 0 & \text{if } \nu = \pi. \end{cases} \tag{4.27}$$

The function $\{D^j T_k \psi_\ell\}_{j,k\in\mathbb{Z},\ell=1,\ldots,n}$ then constitute a tight frame for $L^2(\mathbb{R})$ with frame bound equal to 2π.

Proof

With the assumptions in Theorem 4.15, define the function $\widetilde{\psi}_0 \in L^2(\mathbb{R})$ by

$$\hat{\widetilde{\psi}}_0(\omega) = \sqrt{\theta(\omega)}\hat{\psi}_0(\omega). \tag{4.28}$$

Define the 2π-periodic function $\widetilde{H}_0, \ldots, \widetilde{H}_n$ by

$$\widetilde{H}_0(\omega) = \sqrt{\frac{\theta(2\omega)}{\theta(\omega)}}H_0(\omega), \quad \widetilde{H}_\ell(\omega) = \sqrt{\frac{1}{\theta(\omega)}}H_\ell(\omega), \ell = 1, \ldots, n. \tag{4.29}$$

We want to show that the unitary extension theorem can be applied to $\widetilde{\psi}_0, \widetilde{H}_0, \ldots, \widetilde{H}_n$ and thereby obtain a tight frame $\{D^j T_k \widetilde{\psi}_\ell\}_{j,k\in\mathbb{Z},\ell=1,\ldots,n}$. At last it is shows that $\widetilde{\psi}_\ell = \psi_\ell$ for $\ell = 1, \ldots, n$. First we prove that $\widetilde{\psi}_0, \widetilde{H}_0, \ldots, \widetilde{H}_n$ satisfy the conditions in the general setup. We have

$$\begin{aligned}
\hat{\widetilde{\psi}}_0(2\omega) &= \sqrt{\theta(2\omega)}\hat{\psi}_0(2\omega) \\
&= \sqrt{\theta(2\omega)}H_0(\omega)\,\hat{\psi}_0(\omega) \\
&= \sqrt{\frac{\theta(2\omega)}{\theta(\omega)}}H_0(\omega)\,\hat{\widetilde{\psi}}_0(\omega) = \widetilde{H}_0(\omega)\,\hat{\widetilde{\psi}}_0(\omega)
\end{aligned}$$

and,

$$\lim_{\omega\to 0}\hat{\widetilde{\psi}}_0(\omega) = \lim_{\omega\to 0}\left(\sqrt{\theta(\omega)}\hat{\psi}_0(\omega)\right) = 1.$$

This shows the general setup is satisfied. Define $\widetilde{\psi}_\ell$ as

$$\hat{\widetilde{\psi}}_\ell(2\omega) = \widetilde{H}_\ell(\omega)\,\hat{\widetilde{\psi}}_\ell(\omega), \ell = 1, \ldots, n. \tag{4.30}$$

Now it is enough to prove the assumptions in Corollary 4.11. Using Equation (4.27) and (4.29) with $\nu = 0$,

$$\begin{aligned}
\sum_{\ell=0}^{n}\left|\widetilde{H}_\ell(\omega)\right|^2 &= \frac{\theta(2\omega)}{\theta(\omega)}|H_0(\omega)|^2 + \sum_{\ell=1}^{n}\frac{|H_\ell(\omega)|^2}{\theta(\omega)} \\
&= \frac{1}{\theta(\omega)}\left(\theta(2\omega)|H_0(\omega)|^2 + \sum_{\ell=1}^{n}|H_\ell(\omega)|^2\right) = 1, \text{ a.e. } \omega \in \mathbb{T}.
\end{aligned}$$

Now, using that $\theta\left(2\left(\omega+\pi\right)\right)=\theta\left(2\omega\right)$ and the same equations as before but with $\nu=\pi$, we obtain

$$\begin{aligned}\sum_{\ell=0}^{n}\widetilde{H}_{\ell}\left(\omega\right)\overline{\widetilde{H}_{\ell}\left(\omega+\pi\right)} &= \frac{\theta\left(2\omega\right)}{\sqrt{\theta\left(\omega\right)\theta\left(\omega+\pi\right)}}H_{0}\left(\omega\right)\overline{\widetilde{H}_{0}\left(\omega+\pi\right)}+\\ &\qquad \frac{1}{\sqrt{\theta\left(\omega\right)\theta\left(\omega+\pi\right)}}\sum_{\ell=1}^{n}H_{\ell}\left(\omega\right)\overline{\widetilde{H}_{\ell}\left(\omega+\pi\right)}\\ &= 0,\ \text{ a.e. } \omega\in\mathbb{T}.\end{aligned}$$

It then follows from Corollary 4.11 that the functions $\{D^{j}T_{k}\psi_{\ell}\}_{j,k\in\mathbb{Z},\ell=1,\ldots,n}$ constitute a tight frame for $L^{2}\left(\mathbb{R}\right)$ with frame bound equal to 2π. Then by observing

$$\widehat{\psi}_{\ell}\left(2\omega\right)=H_{\ell}\left(\omega\right)\widehat{\psi}_{0}\left(\omega\right)=\sqrt{\theta\left(\omega\right)}\widetilde{H}_{\ell}\left(\omega\right)\frac{1}{\sqrt{\theta\left(\omega\right)}}\widehat{\widetilde{\psi}}_{0}\left(\omega\right)=\widehat{\widetilde{\psi}}_{\ell}\left(2\omega\right)$$

it is shown that $\widetilde{\psi}_{\ell}=\psi_{\ell}$ for $\ell=1,\ldots,n$.

$\blacksquare$

Choosing $\theta=1$ in Theorem 4.15, we obtain Theorem 4.10 the unitary extension principle. The extra freedom from the choice of θ makes the oblique extension principle more flexible than the unitary extension principle even though they both are able to construct the same amount of multiwavelet frames. In practice the construction of multiwavelets frames are more natural in the oblique extension principle.

Example 4.16 (unitary extension principle problem)
Let ψ_{0} be a compactly supported function satisfying the general setup for some function $H_{0}\in L^{\infty}\left(\mathbb{T}\right)$, and assume that θ and H_{ℓ} for $\ell=1,\ldots,n$ are trigonometric polynomials satisfying Theorem 4.15. Then the generated functions ψ_{ℓ} for the frame $\{D^{j}T_{k}\psi_{\ell}\}_{j,k\in\mathbb{Z},\ell=1,\ldots,n}$ have compact support. Now, in the proof for Theorem 4.15, it is shown that the same frame can be constructed from Theorem 4.10 by defining $\widetilde{\psi}_{0}\in L^{2}\left(\mathbb{R}\right)$ by Equation (4.28). The functions $\widetilde{\psi}_{\ell}$ defined from Equation (4.29) and (4.30) satisfy the conditions in the unitary extension principle , and $\widetilde{\psi}_{\ell}=\psi_{\ell}$ for all $\ell=1,\ldots,n$. However, even though the frame $\{D^{j}T_{k}\widetilde{\psi}_{\ell}\}_{j,k\in\mathbb{Z},\ell=1,\ldots,n}$ is generated by compactly supported functions, the function $\widetilde{\psi}_{0}$ is not in general a compactly supported function. So, the construction of the unitary extension principle resulting in compactly supported functions is unpredictable.

In order to use the oblique extension principle, one need to choose the function θ and $H_{1},\ldots,H_{n}$ simultaneously such that Equation (4.26) and (4.27) is satisfied. No general way have yet been shown how to do that, but an extra condition on the choice of θ will make it easier to construct frames.

Corollary 4.17
Let ψ_0 and H_0 be as in the general setup. Let $\theta \in L^\infty(\mathbb{T})$ be a strictly positive function for which $\lim_{\omega \to 0} \theta(\omega) = 1$, chosen such that the function

$$\eta(\omega) = \theta(\omega) - \theta(2\omega)\left(|H_0(\omega)|^2 + |H_0(\omega+\pi)|^2\right) \tag{4.31}$$

is positive. Fix $n \geq 2$ and let $\{G_\ell\}_{\ell=2}^n$ be 2π-periodic trigonometric polynomials for which

$$\sum_{\ell=2}^{n} |G_\ell(\omega)|^2 = 1, \text{ and } \sum_{\ell=2}^{n} G_\ell(\omega)\overline{G_\ell(\omega+\pi)} = 0, \, \omega \in \mathbb{R}. \tag{4.32}$$

Let ρ, σ be 2π-periodic functions such that

$$|\rho(\omega)|^2 = \theta(\omega), \quad |\sigma(\omega)|^2 = \eta(\omega).$$

Define then the 2π-periodic function $\{H_\ell\}_{\ell=1}^n$ by

$$H_1(\omega) = e^{i\omega}\rho(2\omega)\overline{H_0(\omega+\pi)}, \quad H_\ell(\omega) = G_\ell(\omega)\sigma(\omega), \, \ell = 2, \ldots, n.$$

The functions $\{\psi_\ell\}_{\ell=1}^n$ given by equation (4.8) then generate a tight frame $\{D^j T_k \psi_\ell\}_{j,k\in\mathbb{Z},\ell=1,\ldots,n}$ for $L^2(\mathbb{R})$.

Proof
It needs to be shown that the function θ and H_ℓ for $\ell = 0, 1, \ldots, n$ satisfies Equation (4.27). First for $\nu = 0$,

$$\begin{aligned}
&|H_0(\omega)|^2\theta(2\omega) + \sum_{\ell=1}^{\infty} |H_0(\omega)|^2 \\
&= |H_0(\omega)|^2\theta(2\omega) + |H_1(\omega+\pi)|^2|\rho(2\omega)|^2 + |\sigma(\omega)|^2\sum_{\ell=2}^{n}|G_\ell(\omega)| \\
&= |H_0(\omega)|^2\theta(2\omega) + |H_1(\omega+\pi)|^2\theta(2\omega) + \mu(\omega) = \theta(\omega).
\end{aligned}$$

Similary for $\nu = \pi$,

$$
\begin{aligned}
&H_0(\omega)\overline{H_0(\omega+\pi)}\theta(2\omega) + \sum_{\ell=1}^{n} H_{\ell=1}^{n} H_\ell(\omega)\overline{H_\ell(\omega+\pi)} \\
&= H_0(\omega)\overline{H_0(\omega+\pi)}\theta(2\omega) + \rho(2\omega)\overline{\rho(2(\omega+\pi))}e^{i\omega}e^{-i(\omega+\pi)}H_0(\omega)\overline{H_0(\omega+\pi)} + \\
&\qquad \sigma(\omega)\overline{\sigma(\omega+\pi)}\sum_{\ell=2} G_\ell(\omega)\overline{G_\ell(\omega+\pi)} \\
&= H_0(\omega)\overline{H_0(\omega+\pi)}\theta(2\omega) - \theta(2\omega)H_0(\omega)\overline{H_0(\omega+\pi)} = 0
\end{aligned}
$$

■

The oblique extension principle is very useful to construct multiwavelet frames based on B-splines.

Theorem 4.18
Let B_{2m} denote the B-spline of order $2m$ with two-scale symbol $H_0(\omega) = e^{-im\omega}\cos^{2m}\left(\frac{\omega}{2}\right)$. Then for each positive integer $M \leq 2m$, there exist a trigonometric polynomial θ of the form

$$\theta(\omega) = 1 + \sum_{j=1}^{M-1} c_j \sin^{2j}\left(\frac{\omega}{2}\right), \tag{4.33}$$

for which the following hold.

(i) $c_j \geq 0$ for all $j = 1, \ldots, M-1$, i.e., $\theta(\omega) > 0$ for all $\omega \in \mathbb{R}$.

(ii) The functions η in Equation (4.31) is positive.

(iii) The generators in the tight multiwavelet frames constructed via the oblique extension principle and its corollaries have M vanishing moments.

The coefficients c_j, $j = 1, \ldots, M-1$ can be determined via the requirement that

$$\left(1 + \sum_{j=1}^{\infty} \frac{(2j-1)!}{(2j)!\,(2j+1)} y^j\right)^{4m} = 1 + \sum_{j=1}^{M-1} c_j y^j + O\left(|y|^M\right) \text{ as } y \to 0.$$

Proof
This proof can be found in [2]. ■

Constructing tight multiwavelet frames using B-splines by Theorem 4.18, the amount of vanishing moments of ψ_ℓ is not bounded by the amount of zeroes of $H_\ell(\omega)$ at $\omega = 0$ but by M.

Chapter 5

Wavelet Transformation

Now that frames, more specifically wavelet frames, have been introduced, as well as the oblique extension principle, it is time to figure out how to use them in practise. One way is by discrete wavelet transformation. This transformation creates a decomposition of a discrete signal. Since this is a discrete transformation the theory must be converted to a discrete format. This will first be explained by considering the orthonormal wavelets setup and then, later on, generalized to wavelet frames. Recall that functions $f \in V_L$ can be represented by the scaling function basis $\left\{2^{\frac{L}{2}}\varphi\left(2^L x-k\right)\right\}_{k\in\mathbb{Z}}$ such that

$$f(x)=\sum_{k\in\mathbb{Z}} b[k]\varphi\left(2^L x-k\right)$$

for some sequence of coefficients $b[k]\in\ell^2(\mathbb{R})$. In the case where $\left\{2^{\frac{L}{2}}\varphi\left(2^L x-k\right)\right\}_{k\in\mathbb{Z}}$ is an orthonormal basis for V_L, we have

$$\begin{aligned} b[n] &= 2^{\frac{L}{2}}\left\langle f, 2^{\frac{L}{2}}\varphi\left(2^L x-n\right)\right\rangle \\ &= \int_{-\infty}^{\infty} f(x)2^L\overline{\varphi\left(2^L x-n\right)}dx. \end{aligned}$$

Using that $\int_{\mathbb{R}}\varphi(x)\,dx=1$, we have $2^{-\frac{L}{2}}=\int_{-\infty}^{\infty}2^{\frac{L}{2}}\overline{\varphi\left(2^L x-n\right)}dx$ such that

$$b[n]=\frac{\int_{-\infty}^{\infty} f(x)2^{\frac{L}{2}}\overline{\varphi\left(2^L x-n\right)}dx}{\int_{-\infty}^{\infty}2^{\frac{L}{2}}\overline{\varphi\left(2^L x-n\right)}dx}.$$

This is similar to calculate a weighted average for the function $f(x)$. By defining $2^L=N^{-1}$ and letting Ω be a neighborhood of Nn over a domain proportional to N such that

$$\frac{\int_{\Omega} f(x)2^{\frac{L}{2}}\overline{\varphi\left(2^L x-n\right)}dx}{\int_{\Omega}2^{\frac{L}{2}}\overline{\varphi\left(2^L x-n\right)}dx}=f(Nn).$$

This means that the sampled function value $f(Nn)$ is an approximation of $b[n]$. Thus when handling signals such as $f \in V_L$, it is enough to work with the sampled version $f(Nn)$ as a replacement for $b[n]$. Before explaining how the decomposition of the sampled signal $f \in V_L$ works, some definitions must be made and some information given.

Definition 5.1
Let $f \in L^2(\mathbb{R})$. Define

$$a_j[n] = \left\langle f, 2^{\frac{j}{2}}\varphi\left(2^j x - n\right)\right\rangle \text{ and } d_j[n] = \left\langle f, 2^{\frac{j}{2}}\psi\left(2^j x - n\right)\right\rangle$$

where $j, n \in \mathbb{Z}$.

Let $2^L = N^{-1}$, then

$$b[n] = N^{-\frac{1}{2}} a_L[n] \approx f(Nn).$$

From [6], it is known, by a scaling of $\sqrt{2}$, that

$$a_0[k] = \frac{1}{\sqrt{2}}\left\langle \varphi\left(\frac{1}{2}\cdot\right), \varphi(\cdot - k)\right\rangle \tag{5.1}$$

$$= h[k] \tag{5.2}$$

which is the low-pass filter coefficients with respective high-pass filter coefficients noted as $g[k]$. The idea is now to create a decomposition of the approximated sampled signal, $a_L[n]$, of $f \in V_L$. Since $V_L = V_{L-1} \bigoplus W_{L-1}$, the function f can be written as

$$f(x) = \sum_{k\in\mathbb{Z}} a_{L-1}[k]\varphi_{L-1,k}(x) + \sum_{k\in\mathbb{Z}} d_{L-1}[k]\psi_{L-1,k}(x) \tag{5.3}$$

where

$$\sum_{k\in\mathbb{Z}} a_{L-1}[k]\varphi_{L-1,k}(x) \in V_{L-1} \quad \text{and} \quad \sum_{k\in\mathbb{Z}} d_{L-1}[k]\psi_{L-1,k}(x) \in W_{L-1}.$$

The challenge now is to figure out how to calculate $a_{L-1}[k]$ and $d_{L-1}[k]$ by only knowing $a_L[k]$. Before showing how to calculate those quantities, a lemma must be considered.

Lemma 5.2
Let φ be the scaling function for an MRA that generates an orthogonal wavelet $\{\psi_{j,k}\}_{j,k\in\mathbb{Z}}$. Then

$$\left\langle \varphi_{j-1,p}, \varphi_{j,k} \right\rangle = h[k-2p] \quad \text{and} \quad \left\langle \psi_{j-1,p}, \psi_{j,k} \right\rangle = g[k-2p] \tag{5.4}$$

for $k, p \in \mathbb{Z}$.

Proof
Consider

$$\left\langle \varphi_{j-1,p}, \varphi_{j,k} \right\rangle = \int_{\mathbb{R}} 2^{\frac{j-1}{2}} \varphi\left(2^{j-1}t - p\right) 2^{\frac{j}{2}} \overline{\varphi\left(2^{j}t - k\right)}\, dt.$$

Using substitution, with $t = 2^{-j}(u + 2p)$, we obtain

$$\begin{aligned} \left\langle \varphi_{j-1,p}, \varphi_{j,k} \right\rangle &= \int_{\mathbb{R}} 2^{-\frac{1}{2}} \varphi\left(2^{-1}(u+2p) - p\right) \overline{\varphi\left(u - k + 2p\right)}\, du \\ &= \int_{\mathbb{R}} 2^{-\frac{1}{2}} \varphi\left(\frac{u}{2}\right) \overline{\varphi\left(u - (k-2p)\right)}\, du = h[k-2p]. \end{aligned}$$

A similar calculation yields

$$\left\langle \psi_{j-1,p}, \psi_{j,k} \right\rangle = g[k-2p].$$

$\blacksquare$

Proposition 5.3
Let φ be the scaling function for an MRA that generates an orthogonal wavelet basis $\{\psi_{j,k}\}_{j,k\in\mathbb{Z}}$ and let $a_j[n]$ and $d_j[n]$ be defined as in Definition 5.1. Then

$$a_{j-1}[p] = \sum_{n\in\mathbb{Z}} h[n-2p]a_j[n] \quad \text{and} \quad d_{j-1}[p] = \sum_{n\in\mathbb{Z}} g[n-2p]a_j[n].$$

Proof
Consider

$$\begin{aligned} a_{j-1}[p] &= \left\langle f, \varphi_{j-1,p} \right\rangle \\ &= \int_{\mathbb{R}} f(x)\, \overline{\varphi_{j-1,p}(x)} dx \\ &= \int_{\mathbb{R}} \sum_{n\in\mathbb{Z}} a_j[n] \varphi_{j,n}(x)\, \overline{\varphi_{j-1,p}(x)} dx. \end{aligned}$$

Then using Fubini's theorem

$$\begin{aligned} a_{j-1}[p] &= \sum_{n\in\mathbb{Z}} a_j[n] \int_{\mathbb{R}} \varphi_{j,n}(x)\, \overline{\varphi_{j-1,p}(x)} dx \\ &= \sum_{n\in\mathbb{Z}} a_j[n] \left\langle \varphi_{j-1,p}, \varphi_{j,n} \right\rangle = \sum_{n\in\mathbb{Z}} a_j[n] h[n-2p]. \end{aligned}$$

A similar calculation can be made to obtain

$$d_{j-1}[p] = \sum_{n\in\mathbb{Z}} a_j[n] g[n-2p].$$

■

Example 5.4 (Haar wavelet transform)
The discrete transformation will be demonstrated by doing a wavelet transformation with the Haar wavelet. The Haar wavelet is constructed from the low-pass filter

$$m_0(\omega) = \frac{1}{2} + \frac{1}{2} e^{i\omega}.$$

The low-pass filter coefficients, from this low-pass filter, is $h = \left(\frac{1}{2}, \frac{1}{2}\right)$. applying this filter, by convolution, to a sampled signal x, a new signal, y, is constructed

$$y[n] = \frac{1}{2} x[n] + \frac{1}{2} x[n+1].$$

This can be described as a matrix vector product, $y = H_{low} x$, where

$$H_{low} = \begin{bmatrix} \ddots & & & & & & & & \\ \cdots & 0 & \frac{1}{2} & \frac{1}{2} & 0 & 0 & 0 & 0 & \cdots \\ \cdots & 0 & 0 & \frac{1}{2} & \frac{1}{2} & 0 & 0 & 0 & \cdots \\ \cdots & 0 & 0 & 0 & \frac{1}{2} & \frac{1}{2} & 0 & 0 & \cdots \\ \cdots & 0 & 0 & 0 & 0 & \frac{1}{2} & \frac{1}{2} & 0 & \cdots \\ & & & & & & & & \ddots \end{bmatrix}.$$

The same can be done for the high-pass filter from the Haar wavelet, such that

$z = H_{high}x$, where

$$H_{high} = \begin{bmatrix} \ddots & & & & & & & & \\ \cdots & 0 & -\frac{1}{2} & \frac{1}{2} & 0 & 0 & 0 & 0 & \cdots \\ \cdots & 0 & 0 & -\frac{1}{2} & \frac{1}{2} & 0 & 0 & 0 & \cdots \\ \cdots & 0 & 0 & 0 & -\frac{1}{2} & \frac{1}{2} & 0 & 0 & \cdots \\ \cdots & 0 & 0 & 0 & 0 & -\frac{1}{2} & \frac{1}{2} & 0 & \cdots \\ & & & & & & & & \ddots \end{bmatrix}.$$

This matrix vector products can be represented as convolutions such that

$$y[p] = \sum_{m=-\infty}^{\infty} x[m]h[m-p] \quad \text{and} \quad z[p] = \sum_{m=-\infty}^{\infty} x[m]g[m-p] \tag{5.5}$$

where $h = \begin{bmatrix}\cdots & 0 & \frac{1}{2} & \frac{1}{2} & 0 & \ldots\end{bmatrix}$ and $g = \begin{bmatrix}\cdots & 0 & -\frac{1}{2} & \frac{1}{2} & 0 & \ldots\end{bmatrix}$. By defining

$$H = \begin{bmatrix} H_{low} \\ H_{high} \end{bmatrix} \tag{5.6}$$

Then

$$\begin{bmatrix} \vdots \\ y_{-1} \\ y_0 \\ y_1 \\ \vdots \\ z_{-1} \\ z_0 \\ z1 \\ \vdots \end{bmatrix} = H \begin{bmatrix} \vdots \\ x_{-2} \\ x_{-1} \\ x_0 \\ x_1 \\ x_2 \\ \vdots \end{bmatrix}.$$

The vector y and z is respectively the low-pass and high-pass decomposition of the signal x and it is possible to reconstruct the signal x by only knowing the vectors y and z. In terms of x, y and z

$$
\begin{aligned}
&\vdots \\
y_1 - z_1 &= \frac{x_1 + x_0}{2} - \frac{x_1 - x_0}{2} = x_0 \\
y_1 + z_1 &= \frac{x_1 + x_0}{2} + \frac{x_1 - x_0}{2} = x_1 \\
y_2 - z_2 &= \frac{x_2 + x_1}{2} - \frac{x_2 - x_1}{2} = x_1 \\
y_2 + z_2 &= \frac{x_2 + x_1}{2} + \frac{x_2 - x_1}{2} = x_2 \\
y_3 - z_3 &= \frac{x_3 + x_2}{2} - \frac{x_3 - x_2}{2} = x_2 \\
y_3 + z_3 &= \frac{x_3 + x_2}{2} + \frac{x_3 - x_2}{2} = x_3 \\
&\vdots
\end{aligned}
$$

As observed, it is only necessary to have the odd entries of the vectors y and z to reconstruct the signal x. Using this knowledge on Equation (5.5), it is only necessary to calculate

$$
y[p] = \sum_{m=-\infty}^{\infty} x[m]h[m-2p] \quad \text{and} \quad z[p] = \sum_{m=-\infty}^{\infty} x[m]g[m-2p] \tag{5.7}
$$

such that every even row in H is skipped. This is called *downsampling* and more specifically, downsampling by a factor of 2, in this case.

Using Equation (5.3) and Proposition 5.3, it is possible for the samplet signal $b[n]$ to be decomposed into $a_{j-1}[p]$ and $d_{j-1}[p]$. This is done by convolving the sampled signal with the low-pass and high-pass coefficients and downsampling it by a factor of 2. After decomposition of a_j to a_{j-1} and d_{j-1}, it is possible to reconstruct a_j by convolution.

Proposition 5.5
With the same assumptions as in Proposition 5.3. Then

$$
a_j[p] = \sum_{n\in\mathbb{Z}} h[p-2n]a_{j-1}[n] + \sum_{n\in\mathbb{Z}} g[p-2n]d_{j-1}[n]. \tag{5.8}
$$

Proof

Since $V_j = V_{j-1} \bigoplus W_{j-1}$, the union of the bases $\{\psi_{j-1,n}\}_{n\in\mathbb{Z}}$ and $\{\varphi_{j-1,n}\}_{n\in\mathbb{Z}}$ will be an orthonormal basis of V_j. This means that

$$\varphi_{j,p} = \sum_{n\in\mathbb{Z}} \langle \varphi_{j,p}, \varphi_{j-1,n} \rangle \varphi_{j-1,n} + \sum_{n\in\mathbb{Z}} \langle \varphi_{j,p}, \psi_{j-1,n} \rangle \psi_{j-1,n}.$$

And thus, by using Lemma 5.2

$$\begin{aligned}
a_j[p] &= \langle f, \varphi_{j,p} \rangle \\
&= \left\langle f, \sum_{n\in\mathbb{Z}} \langle \varphi_{j,p}, \varphi_{j-1,n} \rangle \varphi_{j-1,n} + \sum_{n\in\mathbb{Z}} \langle \varphi_{j,p}, \psi_{j-1,n} \rangle \psi_{j-1,n} \right\rangle \\
&= \sum_{n\in\mathbb{Z}} \langle \varphi_{j,p}, \varphi_{j-1,n} \rangle \langle f, \varphi_{j-1,n} \rangle + \sum_{n\in\mathbb{Z}} \langle \varphi_{j,p}, \psi_{j-1,n} \rangle \langle f, \psi_{j-1,n} \rangle \\
&= \sum_{n\in\mathbb{Z}} h[p-2n] a_{j-1}[n] + \sum_{n\in\mathbb{Z}} g[p-2n] d_{j-1}[n]
\end{aligned}$$

■

5.1 Wavelet Transformation Algorithm

The algorithm of the transformation will be explained, now that the deconstruction and reconstruction of signals $b[n]$ have been explained. To easier explain the algorithm the following notation is necessary.

$$x_{zeros}[n] = \begin{cases} x\left[\frac{n}{2}\right] & \text{for } n = 0 \bmod 2 \\ 0 & \text{for } n = 1 \bmod 2 \end{cases} \tag{5.9}$$

The notation x_{zeros} interleave x with zeros.

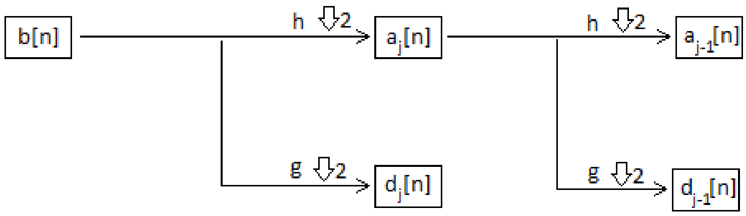

Figure 5.1: Decomposition

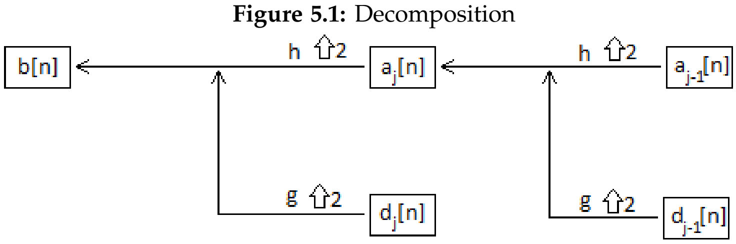

Figure 5.2: Reconstruction

Algorithm 1: Wavelet Deconstruction

Result: $\left(a_{j-k}, \left[d_j, d_{j-1}, \ldots, d_{j-k}\right]\right)$
$b[n]$ = sampled signal;
$h[n]$ = low-pass coefficients;
$g[n]$ = high-pass coefficients;
highPassList = [ ];
k = deconstruct amount;
$a_{j+1}[n] = b[n]$;
$i = 0$;
while $i \leq k$ **do**
  Convolution between $a_{j+1-i}[n]$ and $h[n]$;
  $\widetilde{a}_{j-i}[n] = \left(a_{j+1-i} * h\right)[n]$;
  Downsampling $\widetilde{a}_{j-i}$ by a factor 2;
  $a_{j-i}[p] = \widetilde{a}_{j-i}[2p]$;
  Repeat with g instead of h;
  $\widetilde{d}_{j-i}[n] = \left(a_{j+1-i} * g\right)[n]$;
  $d_{j-i}[p] = \widetilde{d}_{j-i}[2p]$;
  Insert $d_{j-i}[p]$ into highPassList;
  $i = i + 1$;
end

Algorithm 2: Wavelet Reconstruction

Result: a_{j+1}
$a_j[n]$ = the j'th deconstructed low-pass coefficients;
$d_j[n]$ = the j'th deconstructed high-pass coefficients;
$h[n]$ = low-pass coefficients;
$g[n]$ = high-pass coefficients;
Upsampling a_j and d_j by a factor 2 as in equation (5.9)
$a_{j+1}[n] = \left(a_{zeros,j} * h\right)[n] + \left(d_{zeros,j} * g\right)[n]$;

As seen in Figure 5.1, Algorithm 1 have been used on $b[n]$ with $k = 2$. Figure 5.2 shows that Algorithm 2 have been used twice, first on the pair $\left(a_{j-1}, d_{j-1}\right)$ to reconstruct a_j and then on the pair $\left(a_j, d_j\right)$ to finally reconstruct $b[n]$. An important thing to consider is, at what frequency intervals the wavelet transformation filters the signal. This can be considered by considering the Nyquist frequency.

Definition 5.6 (Nyquist frequency)
Let $x_a(x)$ be an analog signal. Then the sequence of samples $x[n]$ is obtained from the analog signal according the the relation

$$x[n] = x_a(nT).$$

> T is called the sampling period and its reciprocal $f_T = \frac{1}{T}$ is called the Nyquist frequency[7].

Every instance of the orthonormal wavelet decomposition splits the frequency interval of the signal in half with respect to the Nyquist frequency, f_T. For example, the first instance of the wavelet decomposition splits the frequency interval $[0, f_T]$ up in the intervals $\left[0, \frac{f_T}{2}\right]$ and $\left[\frac{f_T}{2}, f_T\right]$. The second instance splits the frequency interval $\left[0, \frac{f_T}{2}\right]$ into the intervals $\left[0, \frac{f_T}{4}\right]$ and $\left[\frac{f_T}{4}, \frac{f_T}{2}\right]$. Thus every instance of the decomposition splits the low-frequency interval into two.

5.2 Wavelet Frame Transformation

The deconstruction and reconstruction for the wavelet transformation have been explained, but as it have been stated in Chapter 4 Wavelet Frames, constructing an orthonormal wavelet basis can be troublesome. But like wavelet frames is similar to orthonormal wavelets, a similar transformation can be made, called the discrete wavelet frame transformation. biggest differences from the orthonormal wavelet transformation and wavelet frame transformation is, the orthonormal wavelet is generated by an orthonormal basis and is generated from only one ψ. The wavelet frame basis is not necessary orthonormal and is generated by multiple different ψ_ℓ. This section is based on [5]. It can be assumed that the wavelet frame scaling function ψ_0 generates an orthonormal basis for $L_2(\mathbb{R})$, thus $b[n]$ can be used to represent the sampled function $f \in V_L$ as in the orthonormal wavelet transformation. From the general setup in Section 4.1, it is known that

$$\frac{1}{\sqrt{2}}\psi_\ell\left(\frac{x}{2}\right) = \sum_{n\in\mathbb{Z}} a_{0,\ell}[n]\,\psi_0(x-n)$$

where

$$a_{0,\ell} = \frac{1}{\sqrt{2}}\left\langle \psi_\ell\left(\frac{x}{2}\right), \psi_0(x-n)\right\rangle.$$

Thus instead of Definition 5.1, a corresponding definition for wavelet frames is

Definition 5.7
Let $f \in L^2(\mathbb{R})$. Define

$$a_j[n] = \left\langle f, 2^{\frac{j}{2}}\psi_0\left(2^j x - n\right)\right\rangle \text{ and } d_{j,\ell}[n] = \left\langle f, 2^{\frac{j}{2}}\psi_\ell\left(2^j x - n\right)\right\rangle$$

where $j, n \in \mathbb{Z}$.

Since the scaling function ψ_0 has been assumed to be orthonormal, $a_j[n]$ from Definition 5.1 is equal in structure to $a_j[n]$ in Definition 5.7.

Proposition 5.8
Let ψ_0 be defined by Equation (4.7). Let $a_j[n]$ and $d_{j,\ell}[n]$ be defined as in Definition 5.7. Then

$$a_{j-1}[p] = \sum_{n\in\mathbb{Z}} a_{0,0}[n-2p]a_j[n] \quad \text{and} \quad d_{j-1,\ell}[p] = \sum_{n\in\mathbb{Z}} a_{0,\ell}[n-2p]a_j[n].$$

Proof
Consider

$$\begin{aligned}
d_{j-1,\ell}[p] &= \int_{\mathbb{R}} f(x)\, 2^{\frac{j-1}{2}} \psi_\ell \left(2^{j-1}x - p\right) dx \\
&= \int_{\mathbb{R}} f(x)\, 2^{\frac{j-1}{2}} 2^{\frac{1}{2}} \sum_{n\in\mathbb{Z}} a_{0,\ell}[n]\, \psi_0 \left(2\left(2^{j-1}x - p\right) - n\right) dx \\
&= \int_{\mathbb{R}} f(x)\, 2^{\frac{j}{2}} \sum_{n\in\mathbb{Z}} a_{0,\ell}[n]\, \psi_0 \left(2^{j}x - 2p - n\right) dx.
\end{aligned}$$

Using Fubini's theorem

$$\begin{aligned}
d_{j-1,\ell}[p] &= \sum_{n\in\mathbb{Z}} a_{0,\ell}[n] \int_{\mathbb{R}} f(x)\, 2^{\frac{j}{2}} \psi_0 \left(2^{j}x - (2p+n)\right) \\
&= \sum_{n\in\mathbb{Z}} a_{0,\ell}[n] \left\langle f(x), 2^{\frac{j}{2}} \psi_0 \left(2^{j}x - (2p+n)\right)\right\rangle \\
&= \sum_{n\in\mathbb{Z}} a_{0,\ell}[n]\, a_j[2p+n] \\
&= \sum_{n\in\mathbb{Z}} a_{0,\ell}[n-2p]\, a_j[n].
\end{aligned}$$

■

The reconstruction with wavelet frames is a bit more complicated then for orthonormal wavelets since the wavelet frames does not have an orthonormal structure. To explain this reconstruction more easily some notation is needed. Define for suitable sequences u, v

$$[\mathcal{S}_u v][n] = \sum_{k\in\mathbb{Z}} v[k]\, u[n-2k] \tag{5.10}$$

$$[\mathcal{T}_u v][n] = 2\sum_{k\in\mathbb{Z}} v[k]\, \overline{u[k-2n]} \tag{5.11}$$

with corresponding Fourier series

$$\begin{aligned}
\widehat{[\mathcal{S}_u v]}(\omega) &= \sum_{n\in\mathbb{Z}} \sum_{k\in\mathbb{Z}} v[k]\, u[n-2k]\, e^{-in\omega} \\
&= \sum_{p\in\mathbb{Z}} \sum_{k\in\mathbb{Z}} v[k]\, u[p]\, e^{-i(p+2k)\omega} \\
&= \sum_{p\in\mathbb{Z}} u[p]\, e^{-ip\omega} \sum_{k\in\mathbb{Z}} v[k]\, e^{-ik2\omega} \\
&= \hat{u}(\omega)\, \hat{v}(2\omega)
\end{aligned} \tag{5.12}$$

$$\begin{aligned}
\widehat{[\mathcal{T}_u v]}(\omega) &= 2\sum_{n\in\mathbb{Z}}\sum_{k\in\mathbb{Z}} v[k]\,\overline{u[k-2n]}e^{-in\omega} \\
&= 2\sum_{p\in\mathbb{Z}}\sum_{k\in\mathbb{Z}} v[k]\,\overline{u[p]}e^{-i\frac{1}{2}(k-p)\omega} \\
&= 2\sum_{p\in\mathbb{Z}} \overline{u[p]}e^{ix\frac{\omega}{2}} \sum_{k\in\mathbb{Z}} v[k]\,e^{-ik\frac{\omega}{2}} \\
&= \sum_{p\in\mathbb{Z}} \overline{u[p]\,e^{-ip\frac{\omega}{2}}} \sum_{k\in\mathbb{Z}} v[k]\,e^{-ik\frac{\omega}{2}} + \\
&\quad \sum_{p\in\mathbb{Z}} \overline{u[p]\,e^{-ip\left(\frac{\omega}{2}+\pi\right)}} \sum_{k\in\mathbb{Z}} v[k]\,e^{-ik\left(\frac{\omega}{2}+\pi\right)} \\
&= \overline{\hat{u}\left(\frac{\omega}{2}\right)}\hat{v}\left(\frac{\omega}{2}\right) + \overline{\hat{u}\left(\frac{\omega}{2}+\pi\right)}\hat{v}\left(\frac{\omega}{2}+\pi\right).
\end{aligned} \tag{5.13}$$

Now the perfect reconstruction can be stated for wavelet frames.

Proposition 5.9
With the same assumption as in Proposition 5.8. Then

$$a_j[p] = 2\left(\sum_{n\in\mathbb{Z}} a_{0,0}[p-2n]a_{j-1}[n] + \sum_{\ell=1}^{n}\sum_{n\in\mathbb{Z}} a_{0,\ell}[p-2n]d_{j-1,\ell}[n]\right). \tag{5.14}$$

Proof
Consider

$$\tilde{a}_j[p] = 2\left(\sum_{n\in\mathbb{Z}} a_{0,0}[p-2n]a_{j-1}[n] + \sum_{\ell=1}^{n}\sum_{n\in\mathbb{Z}} a_{0,\ell}[p-2n]d_{j-1,\ell}[n]\right).$$

By choosing $u = a_{0,\ell}$, the definitions in Equation (5.10) and (5.11), give

$$\left[\mathcal{S}_{a_{0,\ell}}\left[\mathcal{T}_{a_{0,\ell}} v\right]\right][p] = 2\sum_{n\in\mathbb{Z}} a_{0,\ell}[p-2n]\sum_{i\in\mathbb{Z}} v[p]a_{0,\ell}[i-2n]$$

for $\ell = 0,\ldots,n$. By choosing $v = a_j$ and using Proposition 5.8, we have

$$\tilde{a}_j[p] = \left[\mathcal{S}_{a_{0,0}}\left[\mathcal{T}_{a_{0,0}} a_j\right]\right][p] + \sum_{\ell=1}^{n}\left[\mathcal{S}_{a_{0,\ell}}\left[\mathcal{T}_{a_{0,\ell}} a_j\right]\right][p]. \tag{5.15}$$

Taking the Fourier series on both sides of Equation (5.15), using Equation (5.12) and (5.13), gives

$$\begin{aligned}
\hat{\tilde{a}}_j(\omega) &= H_0(\omega)\left(\overline{H_0(\omega)}\hat{a}_j(\omega) + \overline{H_0(\omega+\pi)}\hat{a}_j(\omega+\pi)\right) + \\
&\quad \sum_{\ell=1}^{n} H_\ell(\omega)\left(\overline{H_\ell(\omega)}\hat{a}_j(\omega) + \overline{H_\ell(\omega+\pi)}\hat{a}_j(\omega+\pi)\right) \\
&= \hat{a}_j(\omega)\left(H_0(\omega)\,\overline{H_0(\omega)} + \sum_{\ell=1}^{n} H_\ell(\omega)\,\overline{H_\ell(\omega)}\right) + \\
&\quad \hat{a}_j(\omega+\pi)\left(H_0(\omega)\,\overline{H_0(\omega+\pi)} + \sum_{\ell=1}^{n} H_\ell(\omega)\,\overline{H_\ell(\omega+\pi)}\right).
\end{aligned}$$

Since H_0 and H_ℓ for $\ell = 1, \ldots, n$ is constructed from Theorem 4.15, we have

$$H_0(\omega)\,\overline{H_0(\omega)} + \sum_{\ell=1}^{n} H_\ell(\omega)\,\overline{H_\ell(\omega)} = 1 \text{ and}$$
$$H_0(\omega)\,\overline{H_0(\omega+\pi)} + \sum_{\ell=1}^{n} H_\ell(\omega)\,\overline{H_\ell(\omega+\pi)} = 0$$

and thus

$$\hat{\tilde{a}}_j(\omega) = \hat{a}_j(\omega). \tag{5.16}$$

From the injectivity of the Fourier series, we conclude that

$$\tilde{a}_j[n] = a_j[n].$$

A perfect reconstruction have thus been achieved.

■

The algorithm for wavelet frame deconstruction and reconstruction is very similar to the algorithms for orthonormal wavelets. There are only more repetition and a scaling for the reconstruction as can be seen in Algorithm 3 and 4.

Algorithm 3: Wavelet Frame Deconstruction

Result: $\left(a_{j-k}, \left[\left(d_{j,1}, \ldots, d_{j,n}\right), \left(d_{j-1,1}, \ldots, d_{j-1,n}\right), \ldots, \left(d_{j-k,1}, \ldots, d_{j-k,n}\right)\right]\right)$

$b[n] =$ sampled signal;

$h[n] =$ low-pass coefficients;

$g_\ell[n] =$ the ℓ'th high-pass coefficients;

highPassList$_\ell = [\ ]$;

$k =$ deconstruct amount;

$a_{j+1}[n] = b[n]$;

$i = 0$;

while $i \leq k$ **do**

  Convolution between $a_{j+1-i}[n]$ and $h[n]$;

  $\widetilde{a}_{j-i}[n] = \left(a_{j+1-i} * h\right)[n]$;

  Downsampling $\widetilde{a}_{j-i}$ by a factor 2;

  $a_{j-i}[p] = \widetilde{a}_{j-i}[2p]$;

  $\ell = 1$;

  while $\ell \leq n$ **do**

    Repeat with g_ℓ instead of h;

    $\widetilde{d}_{j-i,\ell}[n] = \left(a_{j+1-i} * g_\ell\right)[n]$;

    $d_{j-i,\ell}[p] = \widetilde{d}_{j-i,\ell}[2p]$;

    Insert $d_{j-i,\ell}[p]$ into highPassList$_\ell$;

    $\ell = \ell + 1$

  end

  $i = i + 1$;

end

Algorithm 4: Wavelet Frame Reconstruction

Result: a_{j+1}

$a_j[n] =$ the j'th deconstructed low-pass coefficients;

$d_{j,\ell}[n] =$ the ℓ'th element of the j'th deconstructed high-pass coefficients list;

$h[n] =$ low-pass coefficients;

$g_\ell[n] =$ the ℓ'th high-pass coefficients;

Upsampling a_j and $d_{j,\ell}$ by a factor 2 as in equation (5.9)

$a_{j+1}[n] = 2\left(\left(a_{zeros,j} * h\right)[n] + \sum_{\ell=1}^{n}\left(d_{zeros,j,\ell} * g_\ell\right)[n]\right)$;

As known from wavelets frames, the corresponding filter coefficients can be very inconvenient to calculate. By using B-splines to construct a wavelet frame structure, the filter coefficients is very convenient to calculate. The calculation of these coefficients is shown in Example 5.10.

Example 5.10 (Wavelet frames high-pass and low-pass filter coefficients from B-splines) From Example 4.12, it is known that the B-spline

$$\psi_0 = B_{2m}$$

has the corresponding low-pass filter

$$\begin{aligned} H_0(\omega) &= e^{-im\omega}\cos^{2m}\left(\frac{\omega}{2}\right) \in L^\infty(\mathbb{T}) \\ &= \frac{1}{2^{2m}} e^{-im\omega} \sum_{k=0}^{2m} \binom{2m}{k} e^{i\frac{\omega}{2}k} e^{-i\frac{\omega}{2}(2m-k)} \\ &= \sum_{k=0}^{2m} \frac{1}{2^{2m}} \binom{2m}{k} e^{-i\omega(2m-k)} \end{aligned}$$

and corresponding high-pass filters

$$\begin{aligned} H_\ell(\omega) &= \sqrt{\binom{2m}{\ell}} i^\ell e^{-im\omega} \sin^\ell\left(\frac{\omega}{2}\right)\cos^{2m-\ell}\left(\frac{\omega}{2}\right) \\ &= \sqrt{\binom{2m}{\ell}} \frac{1}{2^{2m}} e^{-im\omega} \sum_{k=0}^{\ell} (-1)^{\ell-k}\binom{\ell}{k} e^{i\omega k} e^{-i\frac{\omega}{2}(\ell)} \sum_{j=0}^{2m-\ell}\binom{2m-\ell}{j} e^{i\omega j} e^{-i\frac{\omega}{2}(2m-\ell)} \\ &= \sqrt{\binom{2m}{\ell}} \frac{1}{2^{2m}} e^{-i2m\omega} e^{-i\omega\ell} \sum_{k=0}^{\ell}\sum_{j=0}^{2m-\ell} (-1)^{\ell-k}\binom{\ell}{k}\binom{2m-\ell}{j} e^{i\omega(k+j)} \\ &= \sqrt{\binom{2m}{\ell}} \frac{1}{2^{2m}} \sum_{k=0}^{\ell}\sum_{j=0}^{2m-\ell} (-1)^{\ell-k}\binom{\ell}{k}\binom{2m-\ell}{j} e^{-i\omega((2m+\ell)-(k+j))}. \end{aligned}$$

This gives a very explicit expression for the low-pass and high-pass filter coefficients.

Chapter 6

Discussion

In Chapter 5, the discrete orthonormal wavelet and wavelet frame transformation were explained. In this chapter, the two discrete transformations will be compared based on examples of its application. This discussion starts with a quick overview over the two transformations, followed by a demonstration of noise reduction on multiple signals.

6.1 Overview

As a reminder, some important information of the orthonormal wavelet transformation and wavelet frame transformation will be stated.

6.1.1 Orthonormal Wavelet

The orthonormal wavelet transformation is based on orthonormal wavelets with compact support. These wavelets are constructed from a MRA which is a series of subspaces $\{V_j\}_{j\in\mathbb{Z}}$ defined in Definition 2.1. A signal $f \in V_j$ is sampled to the sequence $b\,[n]$ as stated in the beginning of Chapter 5. When the wavelet transformation is applied, the sequence b is decomposed into two signals, a_{j-1} and d_{j-1}. The subspaces V_{j-1} and W_{j-1}, where $a_{j-1} \in V_{j-1}$ and $d_{j-1} \in W_{j-1}$, only have $\{0\}$ in common, meaning $V_j = V_{j-1} \bigoplus W_{j-1}$. Because of this the decomposition is very predictable. One consequence of this is the predictable split in the frequency interval of the signal when decomposed from the orthonormal wavelet transformation. Every sequential use of the orthonormal wavelet transformation splits the frequency interval in half.

6.1.2 Wavelet Frames

Just like orthonormal wavelets, wavelet frames are based on a MRA except that the scaling function for the MRA only generates a Riesz basis, not an orthogonal basis. Thus, for the wavelet frame to create an surjective transformation it must, in general, be overdetermined. This makes the wavelet frame a multiwavelet system with multiple generator functions ψ_ℓ. The predictability of the decomposition thus becomes more complicated. Since the transformation is not injective the decomposition can be different for the same signal and thus W_j cannot be defined, other than

$$\overline{\bigcup_{j\in\mathbb{Z}} W_j} = L^2\left(\mathbb{R}\right).$$

6.2 Accessibility

The construction of an orthonormal wavelet and a wavelet frame are different. In this section it will be summarized how they are constructed and how they are different.

6.2.1 Orthonormal Wavelet

To construct an orthonormal wavelets with compact support, a 2π-periodic low-pass filter function $m_0 \in L^2\left(-\pi, \pi\right)$ must be found that satisfies the following:

(i) m_0 must be a trigonometric polynomial,

(ii) $m_0 \in C^1\left(-\pi, \pi\right)$ is a 2π-periodic function,

(iii) $|m_0\left(\omega\right)|^2 + |m_0\left(\omega+\pi\right)|^2 = 1$,

(iv) $|m_0\left(0\right)| = 1$,

(v) $m_0\left(\omega\right) \neq 0 \quad \text{for} \quad \omega \in \left[-\frac{1}{2}\pi, \frac{1}{2}\pi\right]$.

This means that

$$m_0\left(\omega\right) = \sum_{k=-N}^{N} a_k e^{-ik\omega},$$

and thus, a finite amount of coefficients a_k must be found such that m_0 satisfy the right conditions. These coefficients are the low-pass filter coefficients used in the discrete orthonormal wavelet transformation algorithm.

6.2.2 Wavelet Frames

The construction of a multiwavelet system can be deduced directly from the scaling function ψ_0 and the multiple high-pass filters $H_1, \ldots, H_\ell$ from the following relation

$$\hat{\psi}_\ell\left(2\omega\right) = H_\ell\left(\omega\right)\hat{\psi}_0\left(\omega\right).$$

The requirements for $H_0, \ldots, H_\ell$ is

(i) $H_\ell \in L^\infty(\mathbb{T})$ is a 2π-periodic tr for $\ell = 0, \dots, n$,

(ii) $\hat{\psi}_0(2\omega) = H_0(\omega)\,\hat{\psi}_0(\omega)$

(iii) $\begin{cases} \sum_{\ell=0}^{n} |H_\ell(\omega)|^2 = 1 \\ \sum_{\ell=0}^{n} \overline{H_\ell(\omega)} T_\pi H_\ell(\omega) = 0 \end{cases}.$

These conditions enables the use of the unitary extension principle. By using more advanced, but not more strict, conditions the oblique extension principle can be used in place of the unitary extension principle. Since

$$H_\ell(\omega) = \sum_{k\in\mathbb{Z}} c_{k,\ell} e^{-ik\omega}$$

the low-pass and high-pass filter coefficients are defined as $\{c_{k,\ell}\}_{\in\mathbb{Z}}$, low-pass for $\ell = 0$ and high-pass for $\ell = 1, \dots n$.

6.3 Comparison

The algorithm used for applying the orthonormal wavelets and wavelet frame transformation are very similar. The only difference is the number of high-pass filter repetitions in the decompositions and reconstruction algorithm and the reconstruction equation. Thus the wavelet frame transformation algorithm tends to take longer than the orthonormal wavelet transformation.
The construction criteria for the orthonormal wavelet transformation is stricter than the construction criteria for the wavelet frame transformation. This means wavelet frames are easier to construct, but the wavelet frame transformation is non-injective unlike the orthonormal wavelet transformation. This trade off is relatively important depending what kind of study one wishes to do with the decomposition.
Since the wavelet frame transformation decomposes into multiple high-pass decompositions, the redundancy of the wavelet frame transformation is higher than the orthonormal wavelet transformation. This increase in redundancy makes the wavelet frame transformation very effective for noise reduction, as we will see, but very ineffective for compression. The increase in redundancy creates more coefficients with overlapping information. Since the information is overlapping, the change of individual coefficient will affect the original signal less compared to the one to one transformation the orthonormal wavelet transformation results in. Thus setting coefficients to zero in the high-pass filter decompositions becomes more effective at reducing noise for the wavelet frame transformation than the orthonormal wavelet transformation. At the same time, since the increase in coefficients from the increased redundancy makes the resulting transformation larger for the wavelet frame transformation, it supports the idea that compression is ineffective.

In the case of noise reduction, it is possible to be more flexible with the study on the high-pass decompositions. The trait off for this flexibility is the lack of prediction of information in the multiple high-pass decompositions. In contrast, the orthonormal wavelet transformation is very predictable because of the orthogonal nature of the transformation. Thus, if one searches for a clear structure in a known frequency interval this predictability can be very useful.
In the following section, Section 6.4, some examples will be shown such that this comparison becomes more apparent.

6.4 Examples of Algorithm

In this section some examples of the wavelet frame transformation and orthonormal wavelet transformation will be presented. In order to ensure consistency the filters will stay the same for the two transformations respectively.
For the orthonormal wavelet the low-pass and high-pass filters will be Daubechie wavelets of degree 4, such that the amount of filter coefficients are 8 coefficients per filter. The wavelet frame filter coefficients are calculated by the use of Example 5.10. Selecting $m = 4$ gives the resulting filter coefficients:

- $a_{0,0} = \left[\frac{1}{256}, \frac{1}{32}, \frac{7}{64}, \frac{7}{32}, \frac{35}{128}, \frac{7}{32}, \frac{7}{64}, \frac{1}{32}, \frac{1}{256}\right]$,
- $a_{0,1} = \left[\frac{\sqrt{2}}{128}, \frac{3\sqrt{2}}{64}, \frac{7\sqrt{2}}{64}, \frac{7\sqrt{2}}{64}, 0, -\frac{7\sqrt{2}}{64}, -\frac{7\sqrt{2}}{64}, -\frac{3\sqrt{2}}{64}, -\frac{\sqrt{2}}{128}\right]$,
- $a_{0,2} = \left[\frac{\sqrt{7}}{128}, \frac{\sqrt{7}}{32}, \frac{\sqrt{7}}{32}, -\frac{\sqrt{7}}{32}, -\frac{5\sqrt{7}}{64}, -\frac{\sqrt{7}}{32}, \frac{\sqrt{7}}{32}, \frac{\sqrt{7}}{32}, \frac{\sqrt{7}}{128}\right]$,
- $a_{0,3} = \left[\frac{\sqrt{14}}{128}, \frac{\sqrt{14}}{64}, -\frac{\sqrt{14}}{64}, -\frac{3\sqrt{14}}{64}, 0, \frac{3\sqrt{14}}{64}, \frac{\sqrt{14}}{64}, -\frac{\sqrt{14}}{64}, -\frac{\sqrt{14}}{128}\right]$,
- $a_{0,4} = \left[\frac{\sqrt{70}}{256}, 0, -\frac{\sqrt{70}}{64}, 0, \frac{3\sqrt{70}}{128}, 0, -\frac{\sqrt{70}}{64}, 0, \frac{\sqrt{70}}{256}\right]$,
- $a_{0,5} = \left[\frac{\sqrt{14}}{128}, -\frac{\sqrt{14}}{64}, -\frac{\sqrt{14}}{64}, \frac{3\sqrt{14}}{64}, 0, -\frac{3\sqrt{14}}{64}, \frac{\sqrt{14}}{64}, \frac{\sqrt{14}}{64}, -\frac{\sqrt{14}}{128}\right]$,
- $a_{0,6} = \left[\frac{\sqrt{7}}{128}, -\frac{\sqrt{7}}{32}, \frac{\sqrt{7}}{32}, \frac{\sqrt{7}}{32}, -\frac{5\sqrt{7}}{64}, \frac{\sqrt{7}}{32}, \frac{\sqrt{7}}{32}, -\frac{\sqrt{7}}{32}, \frac{\sqrt{7}}{128}\right]$,
- $a_{0,7} = \left[\frac{\sqrt{2}}{128}, -\frac{3\sqrt{2}}{64}, \frac{7\sqrt{2}}{64}, -\frac{7\sqrt{2}}{64}, 0, \frac{7\sqrt{2}}{64}, -\frac{7\sqrt{2}}{64}, \frac{3\sqrt{2}}{64}, -\frac{\sqrt{2}}{128}\right]$, 4
- $a_{0,8} = \left[\frac{1}{256}, -\frac{1}{32}, \frac{7}{64}, -\frac{7}{32}, \frac{35}{128}, -\frac{7}{32}, \frac{7}{64}, -\frac{1}{32}, \frac{1}{256}\right]$.

6.4.1 Noise Reduction

The performance of the wavelet frame transformation and orthonormal wavelet transformation will be compared when reducing noise from multiple audio signals in this subsection. This is done by presenting the signals and ending with an

overall discussion comparing the two transformations based on the results. All the different signals will be numerated, Signal_1, Signal_2, and so on.
Every one of these signals have different versions such as an original signal version, a noisy signal version and so on. These versions will be presented when the signal is introduced. Every signal have an audio file connected to it though the represented URL seen in each respective figures. The noise reduction program, every plot and audio file for every signal can also be found within the folder accessed by the URL `https://bit.ly/3cSQKIg`.
The comparison for the signal analysis will be done by calculating the energy, peak signal-to-noise ratio, PSNR, and listening to the resulting noise reduced audio files. The energy of a signal can be calculated by the L_2-norm and the PSNR is defined as

$$PSNR(S_1, S_2) = 20\log_{10}(MAX) - 10\log_{10}(MSE(S_1, S_2)) \tag{6.1}$$

where S_1, S_2 are two signals to be compared, $MSE(S_1, S_2)$ is the mean square error between S_1 and S_2 and MAX is the maximum possible value of the signal. Every signal is sampled with a resolution of 32 bit, thus

$$MAX = 2^{32} - 1.$$

The higher the PSNR, the more the two signals are alike, coefficient to coefficient, since the mean square error tends to zero if the signals are alike. For a controlled study of the noise reduction, Gaussian noise will be added to the original signal and result in a noisy signal version of the original signal.
The procedure for noise reduction on the noisy signal will be done by bounding the coefficients by an absolute bound, B_{abs}. This bound is set upon chosen high-pass filter decompositions. If a high-pass filter decomposition coefficient, $d_j[n]$, have absolute value lower then the absolute bound then it is set to zero. This generates a new decomposition, $\widetilde{d_j}[n]$, defined as

$$\widetilde{d_j}[n] = \begin{cases} d_j[n] & \text{for } |d_j[n]| \geq B_{abs} \\ 0 & \text{for } |d_j[n]| < B_{abs} \end{cases}$$

which is used in place of d_j in the reconstruction. When this new decomposition is used in the orthonormal wavelet transformation and wavelet frame transformation algorithm shown in Algorithm 2 and 4 respectively, we call it the *orthonormal wavelet reconstruction* and *wavelet frame reconstruction*. The choice of B_{abs} and which high-pass filter decompositions B_{abs} is used upon will be represented by a table for each of the signals. Table 6.1 is one of such tables.
Ten different audio signal will now be introduced. Each introduction is followed by the same procedure of having Gaussian noise added and then noise reduced.

Plots of the noisy signal and the noise reduced signals will be presentes with URL links to there audio files. When all the signals have been presented, two tables with energy and PSNR calculations will be presented. To better understand this procedure, lets go though the first signal.

Signal$_1$ - Voice

Signal$_1$ is an audio signal of a voice recording with intervals of pauses in between sentences. This signal can be seen in Figure 6.1.

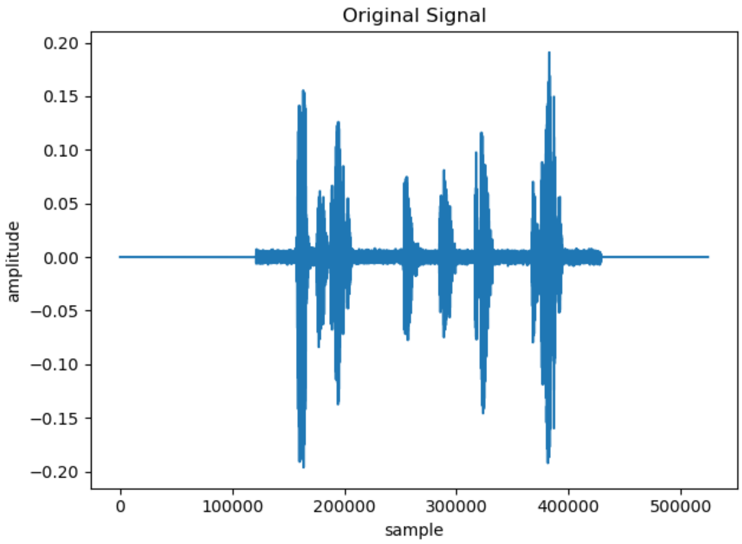

Figure 6.1: The original signal of Signal$_1$, `https://bit.ly/2X54byi`, with energy $\left\|S_{1,original}\right\|_2 = 9.09$.

The noise reduction values can be seen in Table 6.1. The absolute bound and choice of high-pass filter decompositions the bound is used on can be different between the orthonormal wavelet transformation and wavelet frame transformation. In the case of Signal$_1$ only the absolute bound is different as shown in Table 6.1.

Signal_1	Noise reduction values
Gaussion noise	standard deviation = 0.006
Absolute bound (Orthonormal wavelet)	0.0085
Chosen high-pass filters decompositions	First 4
Absolute bound (Wavelet frame)	0.008
Chosen high-pass filters decompositions	First 4

Table 6.1: The noise reduction values for both the orthonormal wavelet reconstruction and wavelet frame reconstruction used on Signal_1

As known, the wavelet frame transformation results in multiple high-pass filter decompositions for every iteration in the wavelet frame reconstruction. Thus when reading **Chosen high-pass filters decompositions** in Table 6.1, it says **First 4**. This should be read as every high-pass decomposition for the first 4 chosen iteration of the wavelet frame reconstruction. The standard deviation is chosen such that the difference of energy of the noisy signal and the original signal isn't very big. If the energy is too large, effective noise reduction can't be expected. The noisy signal can be seen compared to the original signal in Figure 6.2.

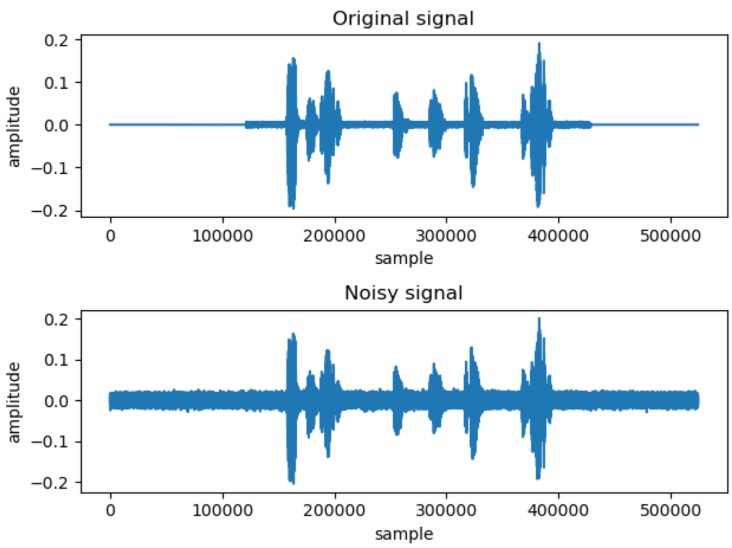

Figure 6.2: The original signal of Signal_1, `https://bit.ly/2X54byi`, compared side to side with its noisy signal, `https://bit.ly/2T8cjgi`.

The orthonormal wavelet reconstruction and wavelet frame reconstruction can be seen compared to the noisy signal in Figure 6.3 and 6.4 respectively.

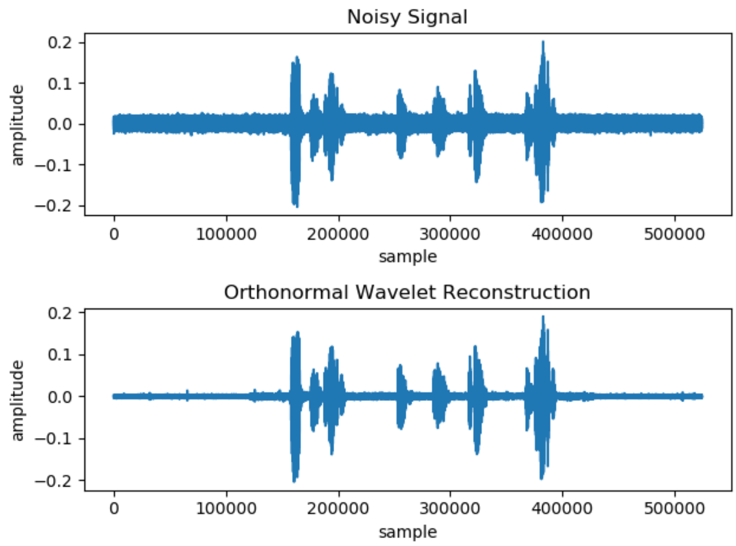

Figure 6.3: the noisy signal of Signal_1, `https://bit.ly/2T8cjgi`, compared with its orthonormal wavelet reconstruction, `https://bit.ly/3bBQ1tz`.

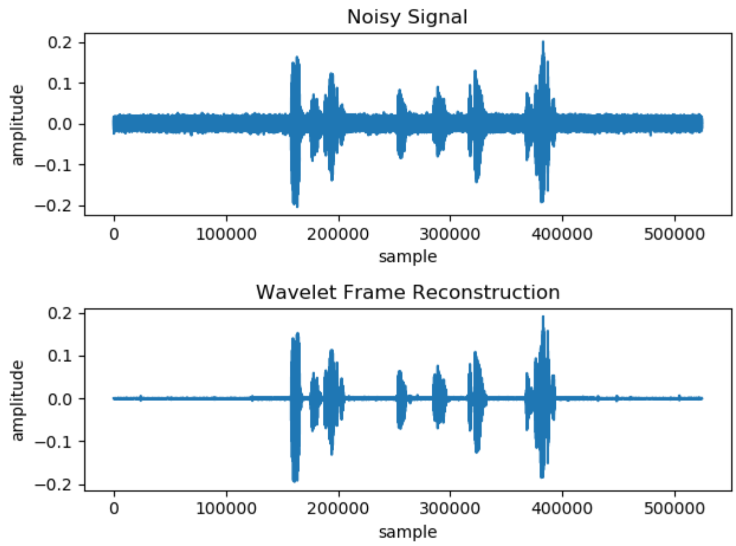

Figure 6.4: the noisy signal of Signal_1, `https://bit.ly/2T8cjgi`, compared with its wavelet frame reconstruction, `https://bit.ly/3buRWQt`.

The rest of the signals will now be introduced and the results of the study will be discussed at the end.

Signal$_2$ - Acoustic Guitar

Signal$_2$ is an audio signal of an acoustic guitar playing a chord progression. Since chords have a combination of notes of different frequencies, Signal$_2$ becomes more complicated then Signal$_1$. Signal$_2$ can be seen in Figure 6.5.

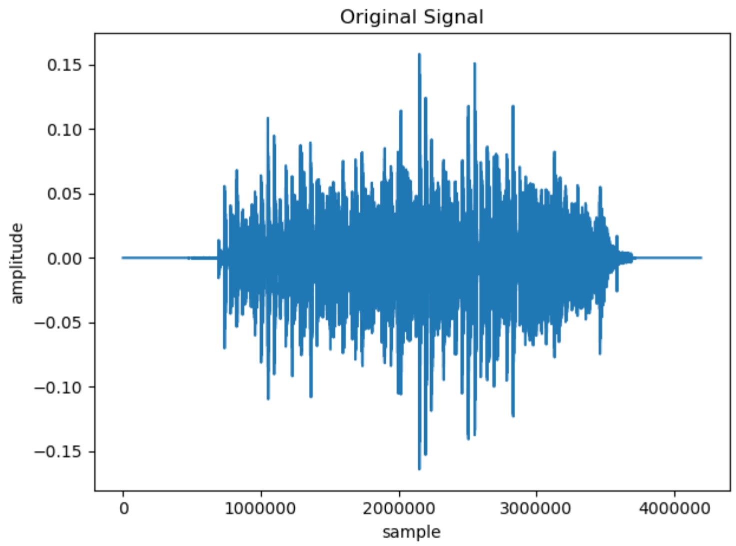

Figure 6.5: The original signal of Signal$_2$, `https://bit.ly/2Z8YS3g`, with energy $\left\|S_{2,original}\right\|_2 = 23.28$.

The noise reduction values for Signal$_2$ can be seen in Table 6.2.

Signal$_2$	Noise reduction values
Gaussion noise	standard deviation $= 0.002$
Absolute bound (Orthonormal wavelet)	0.00075
Chosen high-pass filters decompositions	First 8
Absolute bound (Wavelet frame)	0.00075
Chosen high-pass filters decompositions	First 8

Table 6.2: The noise reduction values for both the orthonormal wavelet reconstruction and wavelet frame reconstruction used on Signal$_2$

The orthonormal wavelet reconstruction and wavelet frame reconstruction can be seen compared to the noisy signal in Figure 6.6 and 6.7 respectively.

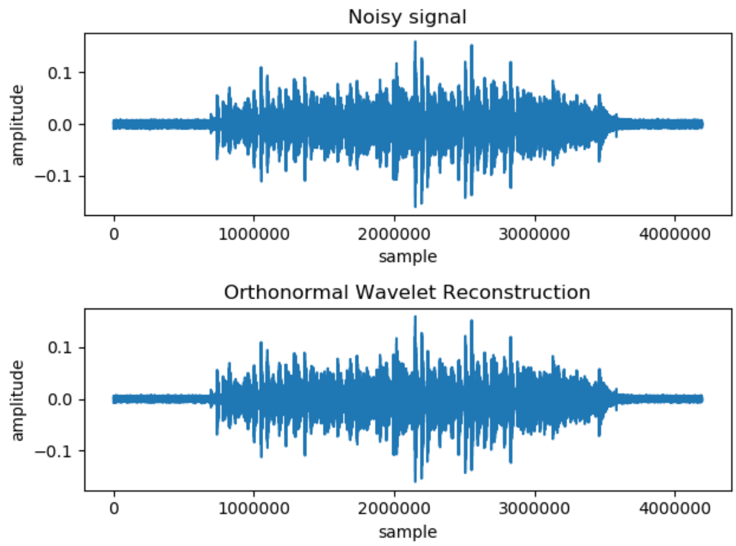

Figure 6.6: the noisy signal of Signal_2, `https://bit.ly/2y5qfjD`, compared with its orthonormal wavelet reconstruction, `https://bit.ly/363PTSE`.

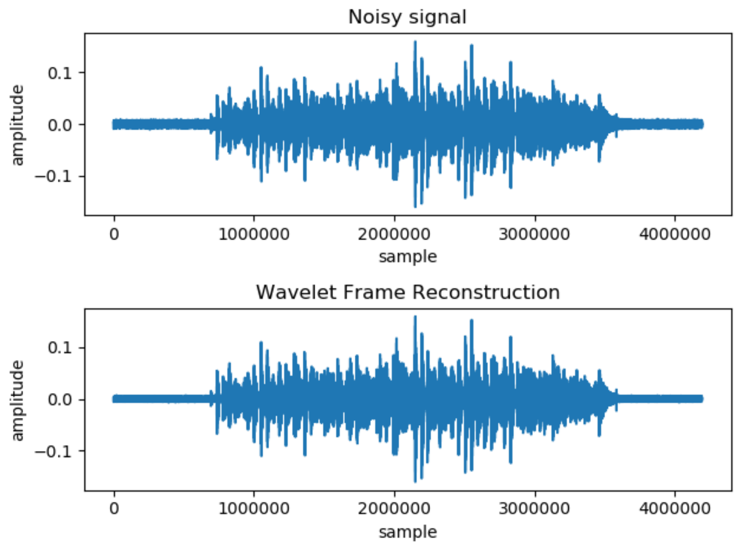

Figure 6.7: the noisy signal of Signal_2, `https://bit.ly/2y5qfjD`, compared with its wavelet frame reconstruction, `https://bit.ly/2T8bB2C`.

Every signal from now on is samples of music from different genres.

Signal$_3$ - Electronic Dance

Signal$_3$ is an audio signal of electronic dance music. This signal have different combinations of amplitudes and frequencies. High frequencies with relatively low amplitude are more susceptible to be filtered out with the noise when noise reducing and thus make the orthonormal wavelet reconstruction and wavelet frame reconstruction less effective. Signal$_3$ can be seen in Figure 6.8

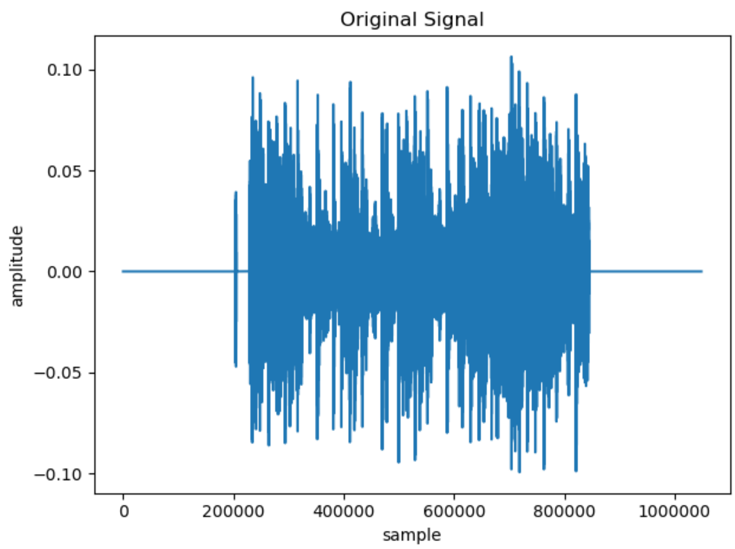

Figure 6.8: The original signal of Signal$_3$, `https://bit.ly/2T57292`, with energy $\left\|S_{3,original}\right\|_2 =$ 23.28.

The noise reduction values for Signal$_3$ can be seen in Table 6.3.

Signal$_3$	Noise reduction values
Gaussion noise	standard deviation $= 0.004$
Absolute bound (Orthonormal wavelet)	0.004
Chosen high-pass filters decompositions	First 4
Absolute bound (Wavelet frame)	0.004
Chosen high-pass filters decompositions	First 4

Table 6.3: The noise reduction values for both the orthonormal wavelet reconstruction and wavelet frame reconstruction used on Signal$_3$

The orthonormal wavelet reconstruction and wavelet frame reconstruction can be seen compared to the noisy signal in Figure 6.9 and 6.10 respectively.

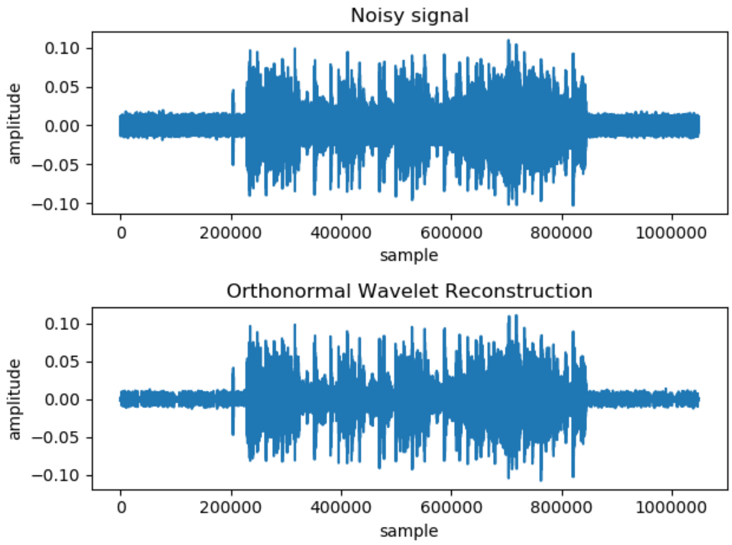

Figure 6.9: the noisy signal of Signal_3, `https://bit.ly/3614ttU`, compared with its orthonormal wavelet reconstruction, `https://bit.ly/3dMHGEU`.

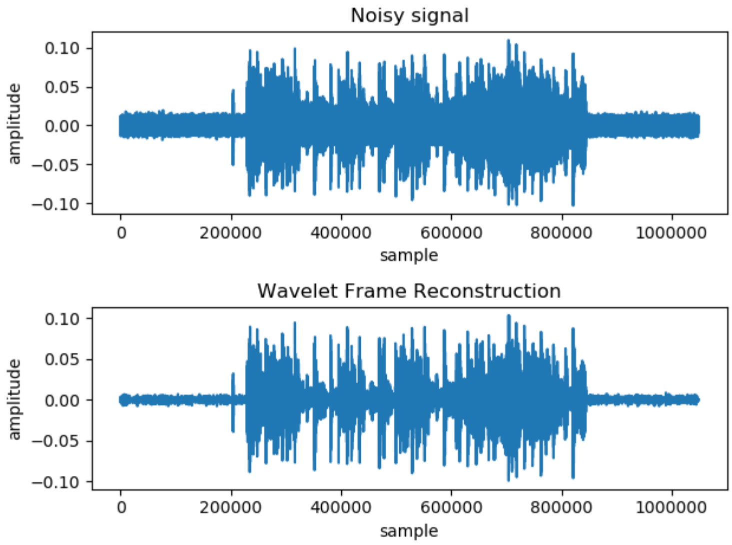

Figure 6.10: the noisy signal of Signal_3, `https://bit.ly/3614ttU`, compared with its wavelet frame reconstruction, `https://bit.ly/2Z59Jv1`.

Signal_4 - Funk

Signal_4 is an audio signal of funk music. This signal have a very distorted opening. This signal is used to test whether or not the orthonormal wavelet reconstruction and wavelet frame reconstruction can differentiate between noise and part of the signal that look like noise, but is in fact a part of the original signal. Signal_4 can be seen in Figure 6.11.

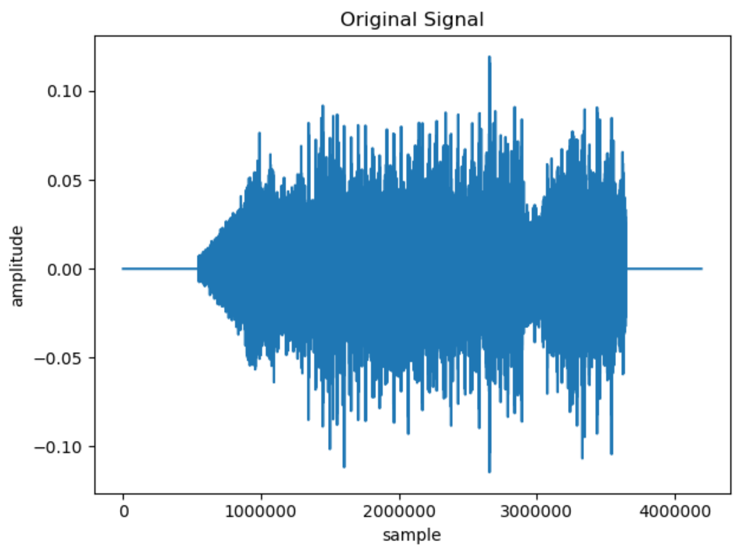

Figure 6.11: The original signal of Signal_4, `https://bit.ly/2T57292`, with energy $\left\|S_{4,original}\right\|_2 = 21.92$.

The noise reduction values for Signal_4 can be seen in Table 6.4.

Signal_4	Noise reduction values
Gaussion noise	standard deviation $= 0.004$
Absolute bound (Orthonormal wavelet)	0.0025
Chosen high-pass filters decompositions	First 3
Absolute bound (Wavelet frame)	0.0025
Chosen high-pass filters decompositions	First 2

Table 6.4: The noise reduction values for both the orthonormal wavelet reconstruction and wavelet frame reconstruction used on Signal_4

The orthonormal wavelet reconstruction and wavelet frame reconstruction can be seen compared to the noisy signal in Figure 6.12 and 6.13 respectively.

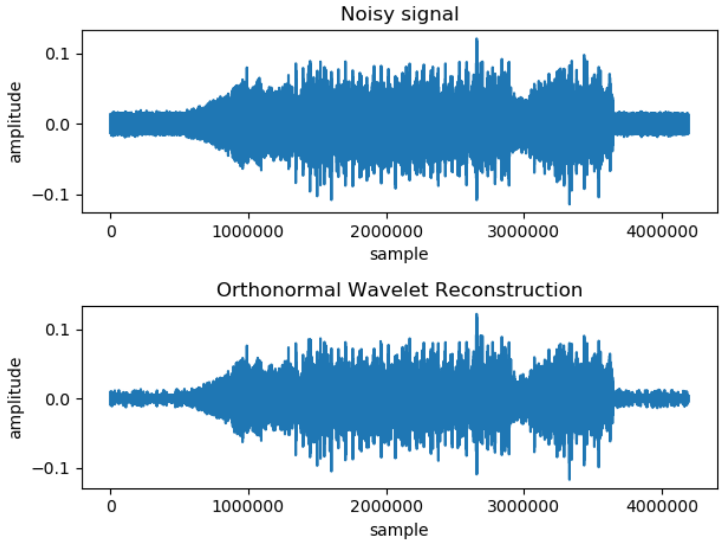

Figure 6.12: the noisy signal of Signal_4, `https://bit.ly/3cMkF4Y`, compared with its orthonormal wavelet reconstruction, `https://bit.ly/2Zoz2Zc`.

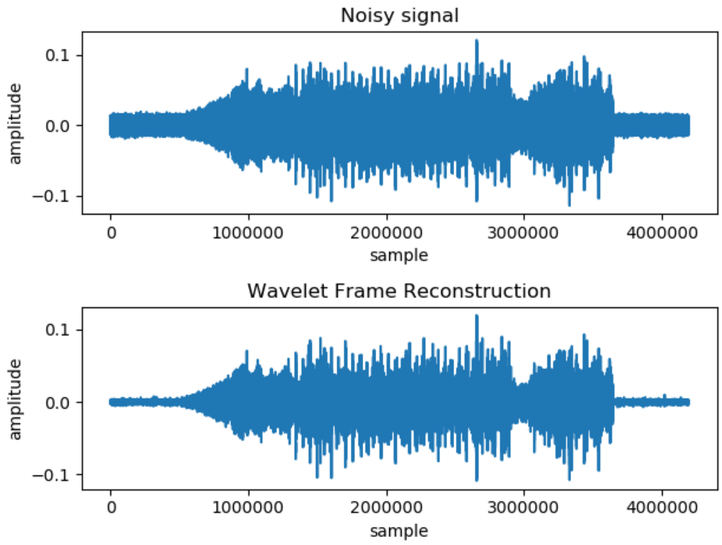

Figure 6.13: the noisy signal of Signal_4, `https://bit.ly/3cMkF4Y`, compared with its wavelet frame reconstruction, `https://bit.ly/2WNLAI4`.

Signal$_5$ - Soul

Signal$_5$ is an audio signal of soul music. This piece of music includes brass and Woodwind instruments and can be seen in Figure 6.14.

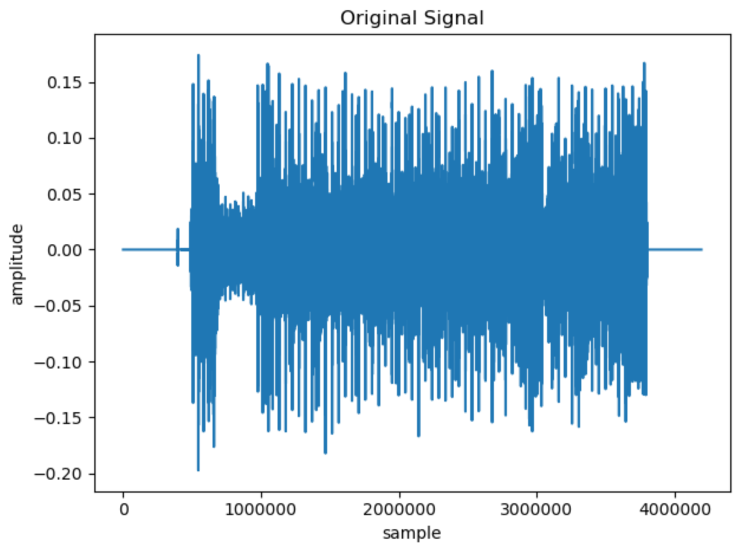

Figure 6.14: The original signal of Signal$_5$, `https://bit.ly/2T57292`, with energy $\left\|S_{5,original}\right\|_2 =$ 34.48.

The noise reduction values for Signal$_5$ can be seen in Table 6.5.

Signal$_5$	Noise reduction values
Gaussion noise	standard deviation $= 0.005$
Absolute bound (Orthonormal wavelet)	0.00225
Chosen high-pass filters decompositions	First 3
Absolute bound (Wavelet frame)	0.002
Chosen high-pass filters decompositions	First 3

Table 6.5: The noise reduction values for both the orthonormal wavelet reconstruction and wavelet frame reconstruction used on Signal$_5$

The orthonormal wavelet reconstruction and wavelet frame reconstruction can be seen compared to the noisy signal in Figure 6.15 and 6.16 respectively.

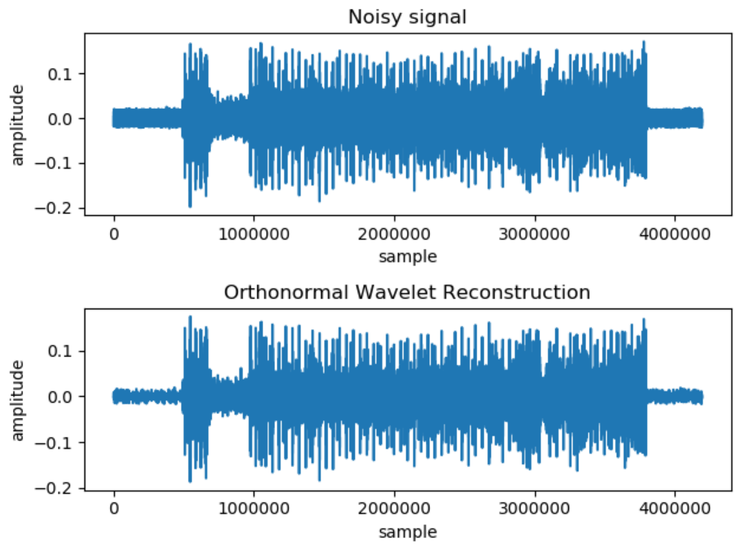

Figure 6.15: the noisy signal of Signal_5, `https://bit.ly/2LGaEKy`, compared with its orthonormal wavelet reconstruction, `https://bit.ly/2Zn6FLa`.

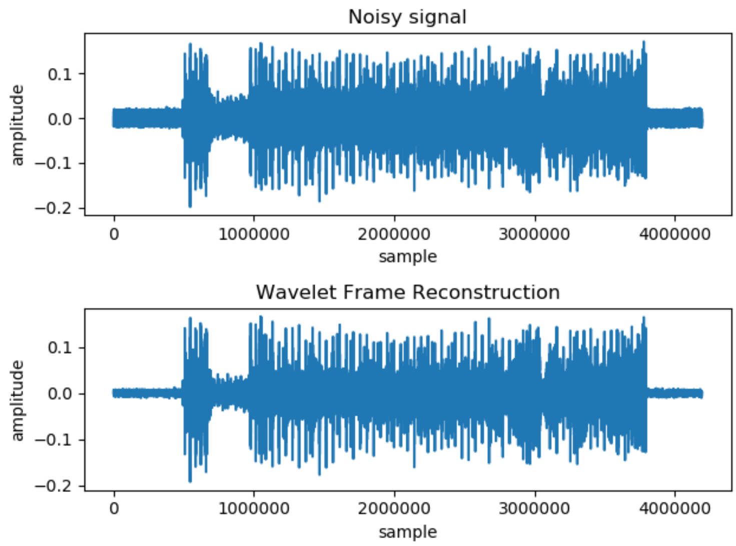

Figure 6.16: the noisy signal of Signal_5, `https://bit.ly/2LGaEKy`, compared with its wavelet frame reconstruction, `https://bit.ly/3gdukDR`.

Signal_6 - Disco

Signal_6 is an audio signal of disco music and can be seen in Figure 6.17.

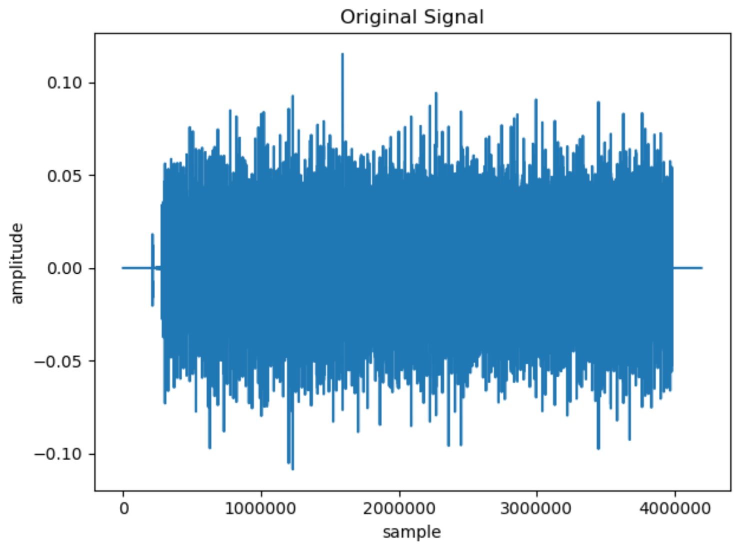

Figure 6.17: The original signal of Signal$_6$, `https://bit.ly/2WMtTs5`, with energy $\left\|S_{6,original}\right\|_2 = 24.62$.

The noise reduction values for Signal$_6$ can be seen in Table 6.6.

Signal$_6$	Noise reduction values
Gaussion noise	standard deviation = 0.005
Absolute bound (Orthonormal wavelet)	0.0025
Chosen high-pass filters decompositions	First 4
Absolute bound (Wavelet frame)	0.0025
Chosen high-pass filters decompositions	First 3

Table 6.6: The noise reduction values for both the orthonormal wavelet reconstruction and wavelet frame reconstruction used on Signal$_6$

The orthonormal wavelet reconstruction and wavelet frame reconstruction can be seen compared to the noisy signal in Figure 6.18 and 6.19 respectively.

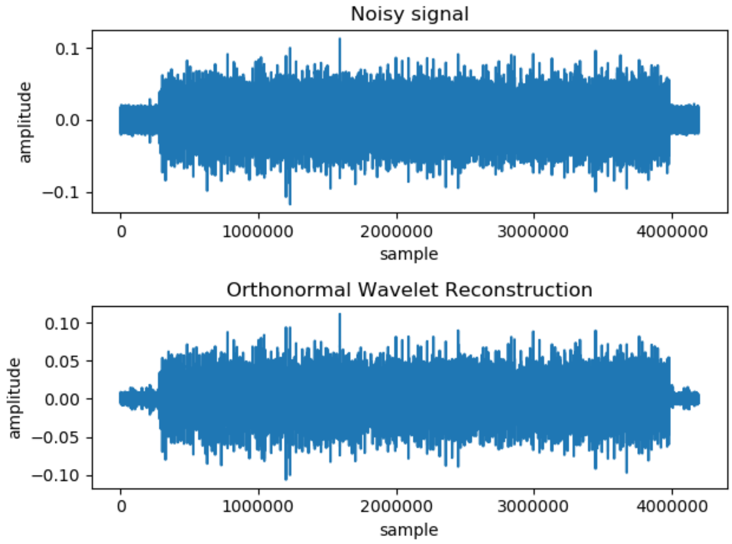

Figure 6.18: the noisy signal of Signal_6, `https://bit.ly/3e7X4Ml`, compared with its orthonormal wavelet reconstruction, `https://bit.ly/3bNjVuU`.

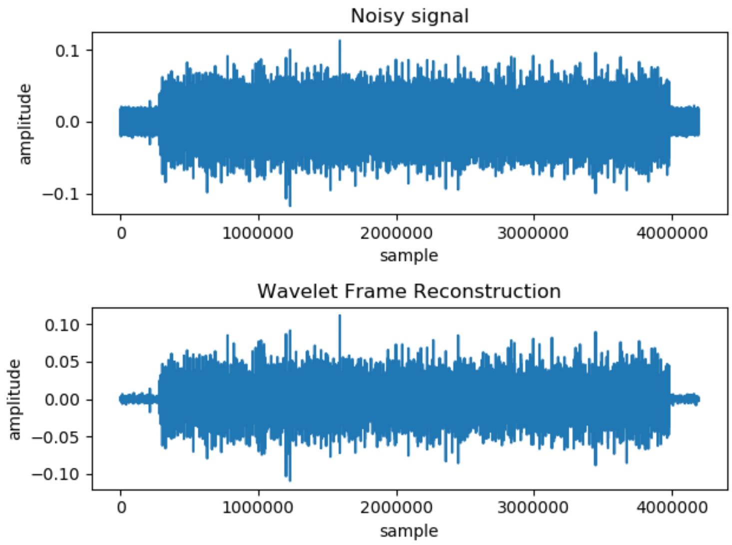

Figure 6.19: the noisy signal of Signal_6, `https://bit.ly/3e7X4Ml`, compared with its wavelet frame reconstruction, `https://bit.ly/36fHbRb`.

Signal_7 - Classical Piano

Signal_7 is an audio signal of classical piano. The audio is a lot more simple since there only is a melody and bass chords. The signal can be seen in Figure 6.20

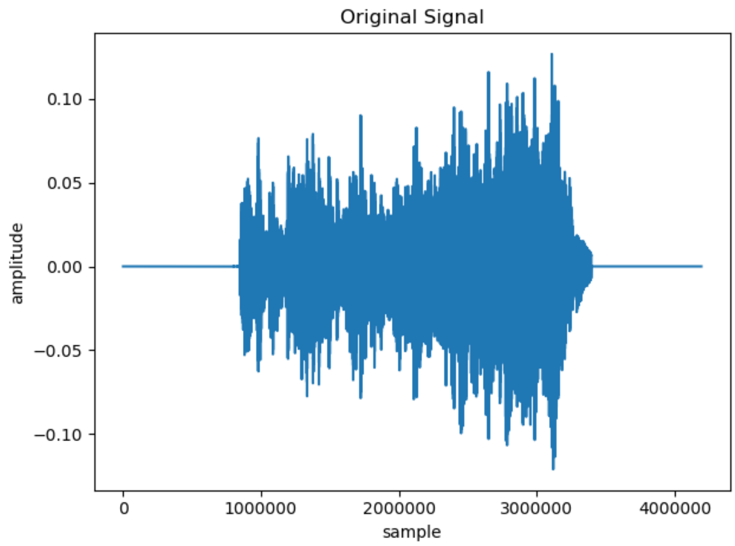

Figure 6.20: The original signal of Signal$_7$, `https://bit.ly/3bMW3Yy`, with energy $\left\|S_{7,original}\right\|_2 = 29.92$.

The noise reduction values for Signal$_7$ can be seen in Table 6.7.

Signal$_7$	Noise reduction values
Gaussion noise	standard deviation $= 0.005$
Absolute bound (Orthonormal wavelet)	0.0045
Chosen high-pass filters decompositions	First 4
Absolute bound (Wavelet frame)	0.003
Chosen high-pass filters decompositions	First 2

Table 6.7: The noise reduction values for both the orthonormal wavelet reconstruction and wavelet frame reconstruction used on Signal$_7$

The orthonormal wavelet reconstruction and wavelet frame reconstruction can be seen compared to the noisy signal in Figure 6.21 and 6.22 respectively.

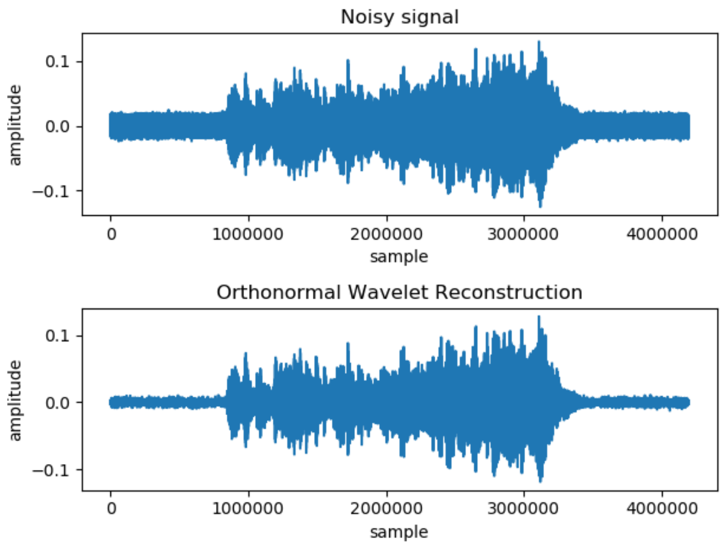

Figure 6.21: the noisy signal of Signal$_7$, `https://bit.ly/2AMb3ch`, compared with its orthonormal wavelet reconstruction, `https://bit.ly/3e2cmC7`.

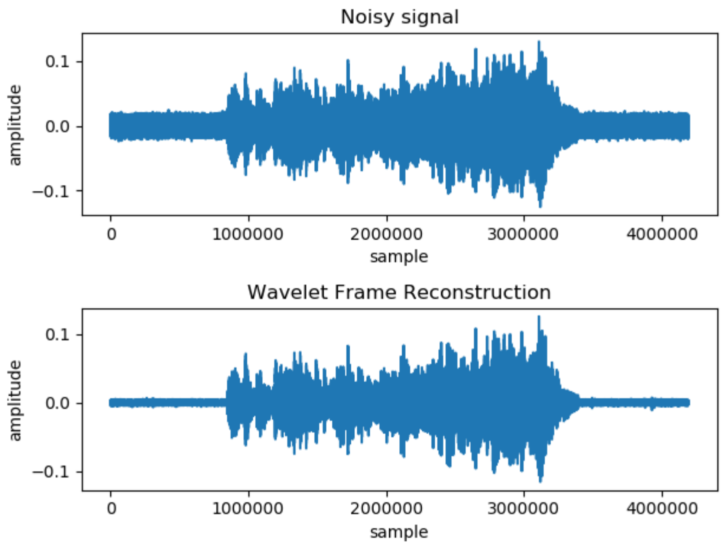

Figure 6.22: the noisy signal of Signal$_7$, `https://bit.ly/2AMb3ch`, compared with its wavelet frame reconstruction, `https://bit.ly/2Tlu8Iw`.

Signal$_8$ - Electronic Korean Pop

Signal$_8$ is an audio signal of electronic Korean pop music. It resembles Signal$_3$, but the style and tempo is different. This signal can be seen in Figure 6.23.

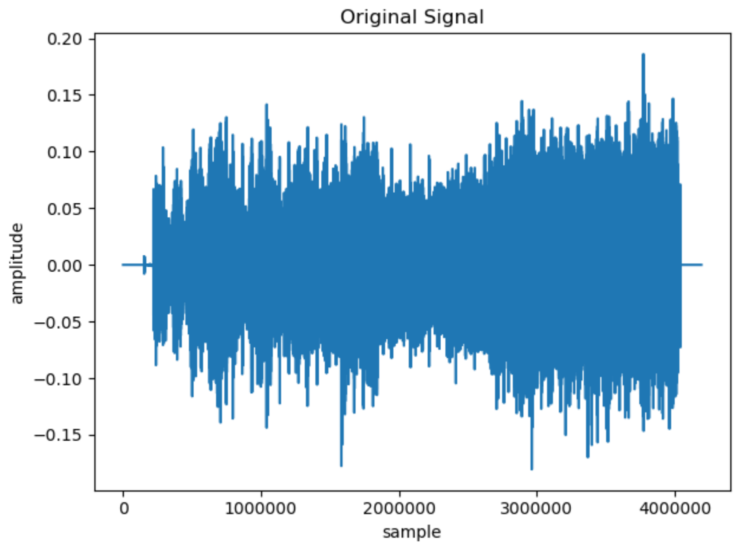

Figure 6.23: The original signal of Signal$_8$, `https://bit.ly/36hB9zw`, with energy $\left\| S_{8,original} \right\|_2 = 44.31$.

The noise reduction values for Signal$_8$ can be seen in Table 6.8.

Signal$_8$	Noise reduction values
Gaussion noise	standard deviation $= 0.008$
Absolute bound (Orthonormal wavelet)	0.003
Chosen high-pass filters decompositions	First 4
Absolute bound (Wavelet frame)	0.001
Chosen high-pass filters decompositions	First 6

Table 6.8: The noise reduction values for both the orthonormal wavelet reconstruction and wavelet frame reconstruction used on Signal$_8$

The orthonormal wavelet reconstruction and wavelet frame reconstruction can be seen compared to the noisy signal in Figure 6.24 and 6.25 respectively.

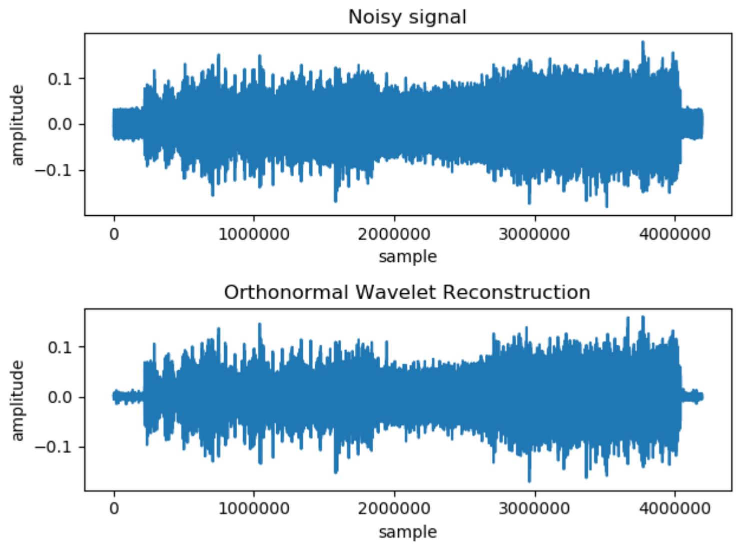

Figure 6.24: the noisy signal of Signal_8, `https://bit.ly/3e1JhGR`, compared with its orthonormal wavelet reconstruction, `https://bit.ly/2WMaMhQ`.

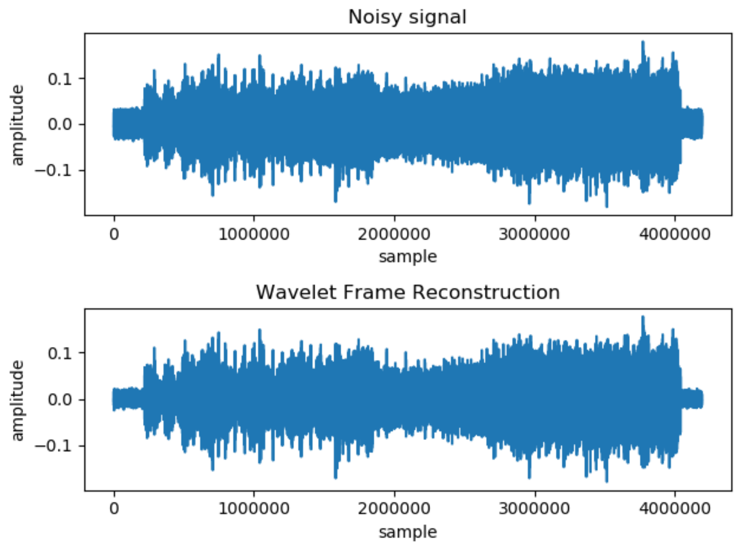

Figure 6.25: the noisy signal of Signal_8, `https://bit.ly/3e1JhGR`, compared with its wavelet frame reconstruction, `https://bit.ly/2WL4dfI`.

Signal_9 - Electronic Pop

Signal_9 is another audio signal of electronic pop music, but the pace of this song is a lot slower then the other. This signal can be seen in Figure 6.26.

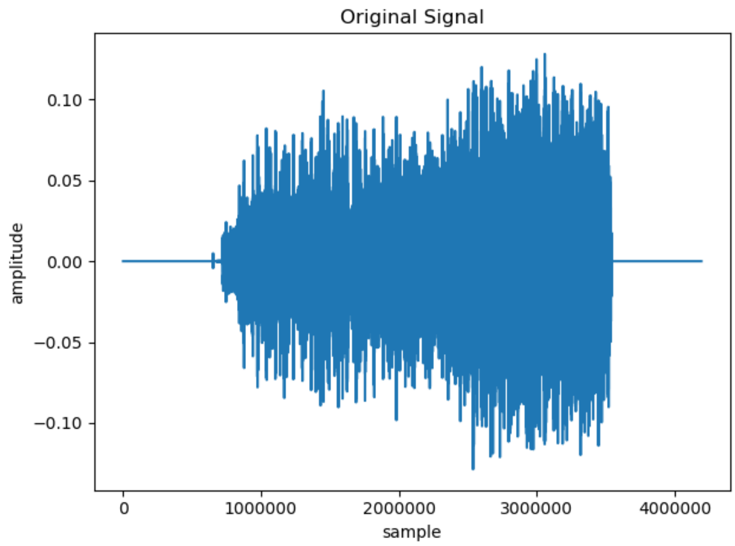

Figure 6.26: The original signal of Signal_9, `https://bit.ly/3bNl3i8`, with energy $\left\| S_{9,original} \right\|_2 = 31.58$.

The noise reduction values for Signal_9 can be seen in Table 6.9.

Signal_9	Noise reduction values
Gaussion noise	standard deviation $= 0.005$
Absolute bound (Orthonormal wavelet)	0.002
Chosen high-pass filters decompositions	First 4
Absolute bound (Wavelet frame)	0.001
Chosen high-pass filters decompositions	First 6

Table 6.9: The noise reduction values for both the orthonormal wavelet reconstruction and wavelet frame reconstruction used on Signal_9

The orthonormal wavelet reconstruction and wavelet frame reconstruction can be seen compared to the noisy signal in Figure 6.27 and 6.28 respectively.

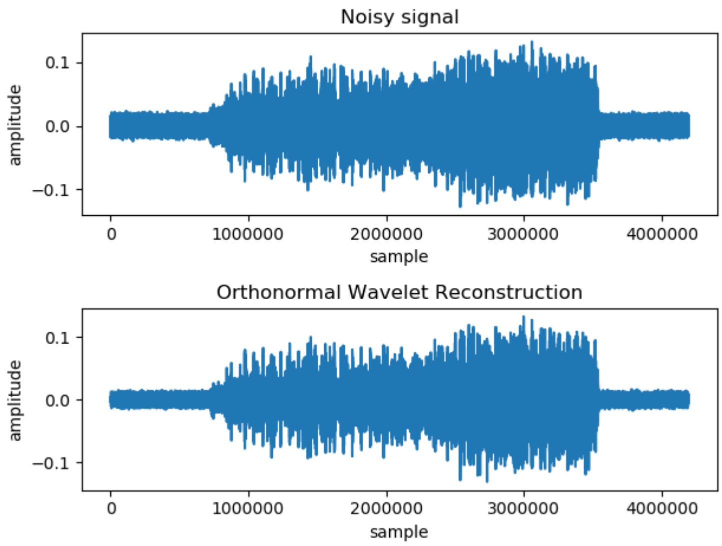

Figure 6.27: the noisy signal of Signal$_9$, `https://bit.ly/3bKvZNH`, compared with its orthonormal wavelet reconstruction, `https://bit.ly/3cPpQB4`.

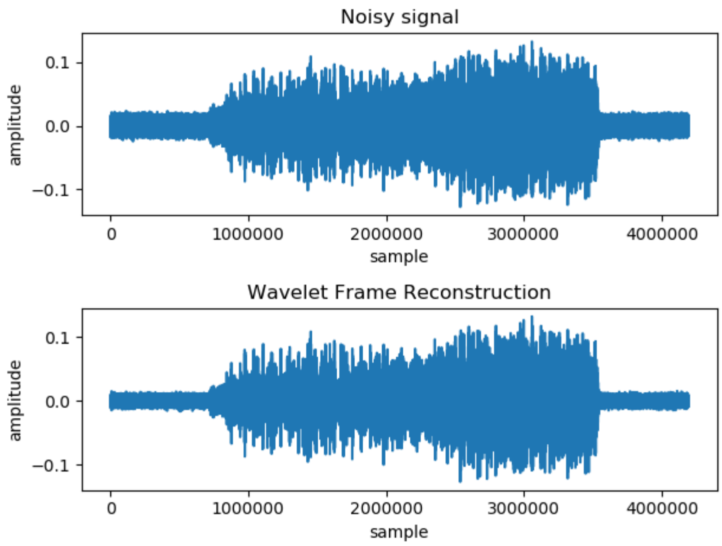

Figure 6.28: the noisy signal of Signal$_9$, `https://bit.ly/3bKvZNH`, compared with its wavelet frame reconstruction, `https://bit.ly/3efDBJN`.

Signal$_{10}$ - Metal

Signal$_{10}$ is an audio signal of metal music. This signal have very low frequency high amplitude sound from the electric guitar, bass and drums. This signal can be seen in Figure 6.29.

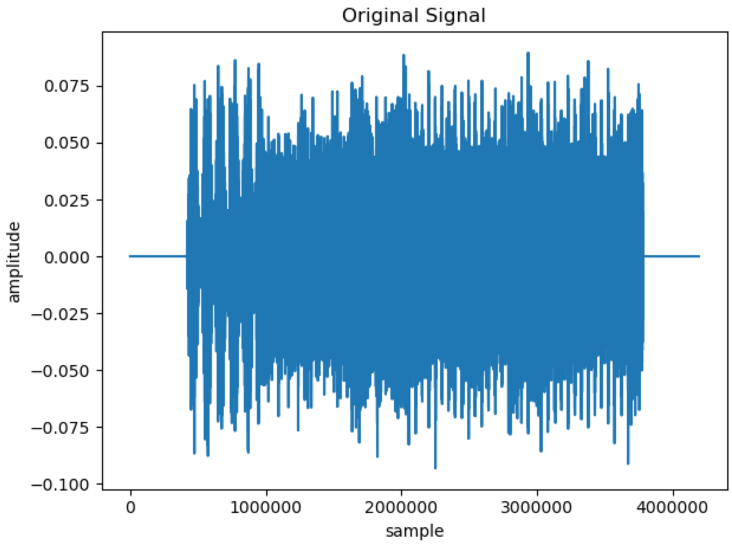

Figure 6.29: The original signal of Signal$_{10}$, `https://bit.ly/2TpH2Fz`, with energy $\left\|S_{10,original}\right\|_2 = 25.38$.

The noise reduction values for Signal$_{10}$ can be seen in Table 6.10.

Signal$_{10}$	Noise reduction values
Gaussion noise	standard deviation $= 0.005$
Absolute bound (Orthonormal wavelet)	0.002
Chosen high-pass filters decompositions	First 6
Absolute bound (Wavelet frame)	0.0015
Chosen high-pass filters decompositions	First 6

Table 6.10: The noise reduction values for both the orthonormal wavelet reconstruction and wavelet frame reconstruction used on Signal$_{10}$

The orthonormal wavelet reconstruction and wavelet frame reconstruction can be seen compared to the noisy signal in Figure 6.30 and 6.31 respectively.

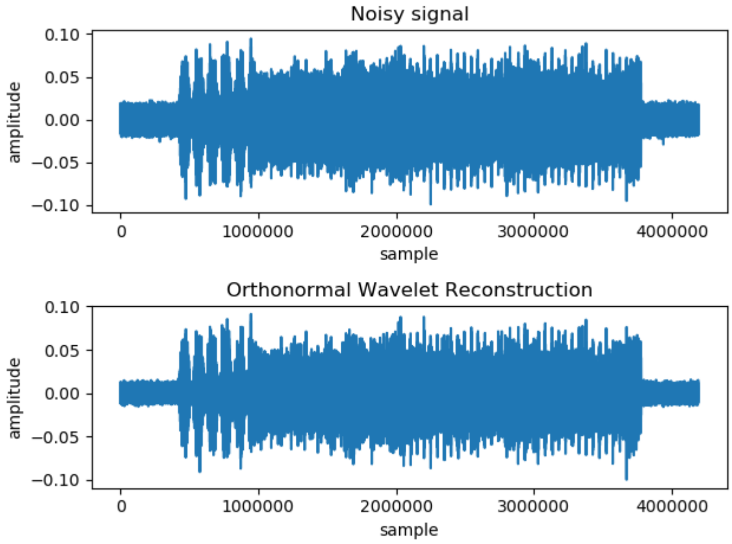

Figure 6.30: the noisy signal of Signal$_{10}$, `https://bit.ly/3e0ZrAq`, compared with its orthonormal wavelet reconstruction, `https://bit.ly/2zQk9Eu`.

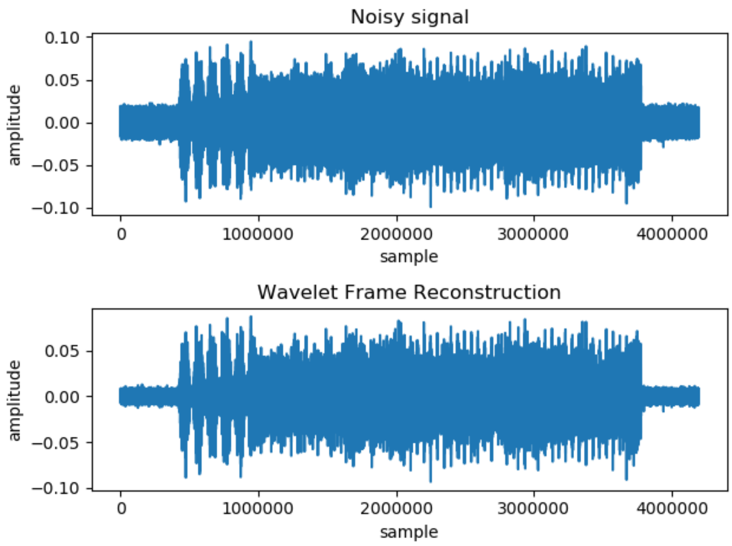

Figure 6.31: the noisy signal of Signal$_{10}$, `https://bit.ly/3e0ZrAq`, compared with its wavelet frame reconstruction, `https://bit.ly/3cPKyAG`.

6.4.2 Results

The energy and PSNR results can be seen in Table 6.11 and 6.12 respectively

	L_2 norm Original Signal	L_2 norm Noisy Signal	L_2 norm Orthonormal wavelet reconstruction	L_2 norm Wavelet frame reconstruction
Signal_1	9.09	10.08	9.06	8.53
Signal_2	23.28	23.63	23.43	23.01
Signal_3	12.55	13.20	12.16	10.47
Signal_4	21.92	23.40	21.54	19.21
Signal_5	34.48	35.97	33.89	31.31
Signal_6	24.62	26.67	24.11	21.85
Signal_7	29.92	31.62	29.94	28.60
Signal_8	44.31	47.25	40.00	41.56
Signal_9	31.58	33.19	30.63	30.45
Signal_{10}	25.38	27.37	24.07	21.91

Table 6.11: L_2 norm calculations for every signal

The idea of these calculations is to see how close the orthonormal wavelet reconstruction and wavelet frame reconstruction is to the original signal. The PSNR compares signals coefficient to coefficient. The problem with this is that the amplitude of a signal can decrease throughout the reconstruction algorithm. This means the PSNR won't be as high as we might expect, but it will still be better then the PSNR between the noisy signal and the original signal. This is why the energy is important to consider as well. Lower energy implies less noise, but to low energy is bad, since it implies more then necessary information have been removed with the noise. If the energy of the reconstructions is lower then the noisy signal but not much lower than the original signal, then one can expect a reduction in noise. If the energy and the PSNR happens to be favorable, then one is able to conclude that the noise reduction was a success.

As can be seen in Table 6.11, the wavelet frame reconstruction yields in a lower energy then the orthonormal wavelet reconstruction. Both have lower energy then the noisy signal.

	PSNR Noisy signal	PSNR Orthonormal wavelet reconstruction	PSNR wavelet frame reconstruction
$Signal_1$	237.10	244.07	243.53
$Signal_2$	246.64	247.64	248.45
$Signal_3$	240.62	240.85	239.31
$Signal_4$	240.61	242.79	241.71
$Signal_5$	238.68	239.73	239.12
$Signal_6$	238.68	241.19	240.79
$Signal_7$	238.69	247.73	247.69
$Signal_8$	234.60	232.52	235.77
$Signal_9$	240.62	240.85	239.31
$Signal_{10}$	238.68	238.46	239.36

Table 6.12: The PSNR calculation between all the signals versions and there respectively original signal version

The PSNR results, seen in Table 6.12, shows a tendency for the orthonormal wavelet transformation to have the highest PSNR comparison value to the original signal. $Signal_2$, $Signal_8$ and $Signal_{10}$ shows the wavelet frame reconstruction to have highest PSNR. In the general case both transformations will result in a reconstruction whose PSNR are higher and energy that are lower than that of the noisy signal. This makes both successful for noise reduction. But which transformation is better? To answer this the audio must be taken into consideration.

Listening to the audio of the reconstructions, it is clear that the wavelet frame reconstruction results in a better noise reduction then the orhtonormal wavelet reconstruction. The orthonormal wavelet reconstruction does result in a cleaner reconstruction when relatively high frequencies are involved, but this is at the cost of noise reduction. The difference in how clean the reconstruction becomes is not large enough, compared to the difference in noise reduction, to conclude that the orthonormal wavelet transformation is superior to the wavelet frame transformation. With the extra flexibility the wavelet frame transformation gives, it is clear that this transformation results in the superior transformation for noise reduction. If more time was available for this project, repeated examples could be made where more advanced handling of the wavelet frame transformation decomposition could be done to see the effect it have on the reconstruction. This could be for every chosen iteration of the wavelet frame reconstruction, only some of the decompositions will have the absolute bound set upon it. And different absolute bounds could be set for different decompositions depending on the iteration.

Chapter 7

Conclusion

In this project, a new method for decomposing a signal that contains the wavelet structure, but are less troublesome and taxing to construct then orthonormal wavelets, have been found. This new method is called wavelet frames. It have been proven that the wavelet frame transformation results in a perfect reconstruction of a decomposed signal. The wavelet frame transformation was applied in the discrete wavelet frame transformation algorithm, Algorithm 3 and 4, and compared to the discrete orthonormal wavelet transformation algorithm, Algorithm 1 and 2. The comparison was done by noise reducing a set of audio signals by using the wavelet frame reconstruction and orthonormal wavelet reconstruction. The result of the comparison states that the wavelet frame transformation is more effective at noise reduction, but the orthonormal wavelet transformation give, in general, a more stable but less effective noise reduction.

Bibliography

[1] Wenjie He Charles K. Chui and Joachim Stöckler. "Compactly supported tight and sibling frames with maximum vanishing moments." In: *Applied and Computational Harmonic Analysis* 13 (2002), pp. 224–262.

[2] Wenjie He Charles K. Chui and Joachim Stöckler. "Framelets: MRA-based constructions of wavelet frames." In: *Applied and Computational Harmonic Analysis* 14 (2003), pp. 1–46.

[3] Ole Christensen. *Frames and bases, an introductory course*. Birkhäuser, 2008.

[4] L. Grafakos. *Modern Fourier analysis*. Springer, 2014.

[5] Bin han. *Framelets and Wavelets*. Birkhâuser, 2017.

[6] Peter Løfqvist Henriksen. *Wavelets*. `https://drive.google.com/file/d/1Hk_k3xzv7DjrCqAxMrr-_p8bGPeqMJQ1/view?usp=sharing`. 2019.

[7] K. Deergha Rao. *Digital Signal Processing*. Springer, 2018.

[8] David F. Walnut. *An Introduction to Wavelet Analysis*. Birkhäuser, 2002.